Investigation of Chalcopyrite and Pyrite Flotation in High Salinity Water

by

Mingbo Zhang

A thesis submitted in partial fulfillment of the requirements for the degree of

Master of Science
in
Chemical Engineering

Department of Chemical and Materials Engineering
University of Alberta

Abstract

In this study, the flotation behaviors of chalcopyrite and pyrite single and mixed minerals in Milli-Q water, NaCl solution, and sea water were investigated. The performance of different collectors was evaluated. Collectorless flotation was also studied under potentiostatic control to explore the flotation behavior of chalcopyrite, pyrite and their mixture, which provides an insight and opportunity for the development of new technology from high salinity water to effectively separate chalcopyrite and pyrite.

The surface properties and mechanism of pyrite flotation were investigated by a range of different techniques such as SEM, EDX, ToF-SIMS, and zeta potential measurement. The research showed substantial slime coating on chalcopyrite and pyrite surface in sea water at high pH in the presence of collector. In conclusion, this study improves our fundamental understanding of sulfide mineral flotation in sea water and provides basic knowledge on how to depress pyrite flotation in sea water in order to produce high-grade concentrates of valuable minerals such as chalcopyrite.

Acknowledgement

I would like to thank my supervisors, Dr. Qingxia (Chad) Liu and Dr. Hongbo Zeng for their guidance and great support throughout my two years MSc study. Dr. Liu taught me a lot of valuable knowledge of mineral processing and gave me many instructions regarding my research. Dr. Zeng taught me a lot of surface and colloid science which is quite important to my research.

I would like to thank Dr. Zhenghe Xu for his permission to use the UV-Vis spectroscopy and contact angle goniometer in his lab. I would also like to thank Dr. Qi Liu for his permission to use the Pulverisette 2 mechanized agate mortar/pestle grinder in his lab. I would also like to thank Dr. Dimitre Karpuzov, Dr. Shihong Xu, Dr. Anquang He at ACSES for their help in XPS, SEM and ToF-SIMS, Mr. Shiraz Merali for XRD, XRF and AAS measurement and Mr. Jason Dibbs for his help in glassware making.

The financial supports from NSERC, Teck Resources Ltd., Vale Base Metals Technical Excellence Centre, and C^5MPT are greatly appreciated. I would also like to thank Ms. Zhaohui Qiu and Dr. Hesheng Yu for their advice and instruction to my research. I would also like to thank Mr. Jiahao Xia, Ms. Chongdan Luo, Mr. Junchen Yan and Ms. Celine Mah for their great help in my experiment.

Finally, I would like to thank my father, my mother and my girlfriend for the support and faith they give to me.

Table of Contents

List of Tables

List of Figures

List of Symbols

Wt.	Weight, g
a	Weight percentage of mineral, %
E	Half–cell potential, V
E^0	Standard half–cell potential, V
R	Ideal gas constant, 8.314 $J\cdot mol^{-1}\cdot K^{-1}$
T	Absolute temperature (Kelvin = ^{o}C + 273), K
F	Faraday constant, 96500 C mol^{-1}
a	Chemical activity for the relevant species
e	Elementary charge, C
ζ_V	Zeta potential distribution of valuable mineral, mV
ζ_G	Zeta potential distribution of gangue mineral, mV
eV	Electronvolt
R_e	Resistance of the electrolyte, Ω
R_p	Resistance of the pore, Ω
R_t	Resistance of the charge transfer, Ω
C_c	Capacitance of the coating layer, μF
C_d	Capacitance of the double-layer, μF
L	Inductance of adsorption-layer, H
P_c	Collision probability between bubbles and particles, %
P_a	Adhesion probability of particles after collision, %
P_d	Probability that subsequent detachment would occur, %
D_p	Diameters of particles, mm
D_b	Diameters of bubbles, mm

List of Abbreviations

PAX	Potassium amyl xanthate
iPOPECTU	N-isopropoxypropyl-N’-ethoxycarbonyl thiourea
XRF	X-Ray fluorescence
XPS	X-Ray photoelectron spectroscopy
ESCA	Electron spectroscopy for chemical analysis
SEM	Scanning electron microscopy
EDS	Energy dispersive X-Ray spectroscopy
ToF-SIMS	Time-of-Flight secondary ion mass spectrometry
EDL	Electrical double layer
AAS	Atomic absorption spectroscopy
EIS	Electrochemical impedance spectroscopy
FRA	Frequency response analyzer
AC	Alternating current
CV	Cyclic voltammetry
LSV	Linear sweep voltammetry
sccm	Standard cubic centimeters per minute
rpm	Revolutions per minute
SBX	Sodium butyl xanthate
Cp	Chalcopyrite
Py	Pyrite
HCl	Hydrochloric acid
$HClO_4$	Perchloric acid
H_2SO_4	Sulfuric acid
NaCl	Sodium chloride
DSA	Drop shape analyzer
SHE	Standard hydrogen electrode
UV-Vis	Ultraviolet-visible
MTC	Monothiocarbonate
Eh	Redox potential

Chapter 1 Introduction

1.1 Principles of froth flotation

Froth flotation, which is a process to separate valuable mineral particles from the gangue minerals by using the difference of surface wettability, is an important process in mining and mineral processing industry. The ground raw minerals are mixed with water to form slurry. Through the use of different reagents, the valuable minerals in the slurry are usually made hydrophobic and the gangue minerals are made hydrophilic. The hydrophobic mineral particles then attach to the air bubbles coming from the bottom of the flotation tank and rise to the surface of the pulp forming froths. The floated mineral, which is called concentrates, is removed from the pulp. The mineral, which is non-floatable and still left in the tank, is called tailings or tails.

1.2 Overview of the froth flotation of sulfide minerals

Sulfide minerals are the largest group of minerals for base metals resources. Most sulfide minerals are semiconductors of electrons, which can receive and release electrons to develop a rest potential in a solution. As a result, the surface of some sulfide minerals like orpiment, realgar and stibnite is very active and exhibit natural floatability.

The main metals in sulfide minerals are Pb, Cu, Sb, As, Ag, Bi, Fe, Co, and Ni. Only three to five compounds each are formed by Zn, Cd, Mn, Ge, Sn, Tl, Mo, and Hg, but among them are some industrially important minerals like sphalerite (ZnS), molybdenite (MoS_2), and cinnabar (HgS). Simple sulfide minerals include acanthite (Ag_2S), matraite (ZnS), covellite (CuS) and galena (PbS). There are also persulfide types of minerals, including pyrite (FeS_2) and molybdenite (MoS_2). There are also more complex sulfides including boulangerite ($Pb_5Sb_4S_{11}$), pyrargyrite (Ag_3SbS_3) and enargite (Cu_3AsS_4), and chalcopyrite ($CuFeS_2$).

1.2.1 Copper sulfides

Copper sulfides are one of important sulfide minerals with the formula of Cu_xS_y. In the mining industry, some minerals which compose of both copper and iron with the formula of $Cu_xFe_yS_Z$, are also referred to as "copper sulfides". Some of the copper sulfides are really economically valuable. Chalcopyrite ($CuFeS_2$) and chalcocite (Cu_2S) are the two most important copper sulfide minerals. Bornite (Cu_5FeS_4) and enargite (Cu_3AsS_4) are rare resources for copper sulfides.

Commonly, porphyry copper deposits contain only small amount of copper (0.4 % to 1 %), but the volume of the ore makes its economic value remarkable. The most part in the ore is silicates (Si_xO_y). Pyrite (FeS_2) content may largely vary in the ore, with moderate pyrite content being in the range of

5 - 15 % of the total ore. Copper ore may also contain iron sulfides such as pyrrhotite ($Fe_{(0.8-1)}S$)) and marcasite (FeS_2). In general, iron sulfides are the main gangue mineral for copper sulfides.

1.2.2 Flotation reagents

Flotation reagents are of vital importance for flotation to effectively separate the desired mineral from gangue mineral. The overall pH of the pulp is controlled with pH modifiers to make the froth flotation effective at a certain pH range. In addition, the froth structure can be improved by the use of frothers, which are surface active reagents to aid in the formation of froth. The flotation reagents can be roughly divided into collectors, frothers, modifiers, activators and depressants. Collectors are organic chemicals that make the target mineral surface hydrophobic to improve the attachment of the mineral particles to bubbles, which allow the particles to be recovered in the froth product. Frothers are used to stabilize the bubble and to produce stable froth in flotation system. Both activators and depressants, which are often referred to as the regulators of flotation, are added to adsorb on target mineral surfaces. Activators normally adsorb on the surface of minerals to facilitate the interaction between mineral surface and the collector. A depressant is a chemical that can either prevent a collector from adsorbing onto a certain mineral, or make the surface of a given mineral hydrophilic in the presence of collectors.

1.2.3 Collector

The main function of a collector chemical is to selectively form a hydrophobic layer on the surface of the desired minerals for the attachment onto air bubbles. Collectors can be divided into two distinct groups: non-ionizing and ionizing groups. Non-ionizing collectors are generally neutral and hydrophobic and in a liquid form. On the contrary, ionizing type of collectors are able to dissociate in water to function as surface active agents. Ionizing group is further divided in anionic and cationic collectors. (Bulatovic, 2007)

Anionic collector can be hydrolyzed in water so that it can form negative collector ion in water, which is the polar group. Anionic collector can carry negatively charged functional groups on divalent sulfur, as an example in the case of xanthates or dithiophosphates. In addition, anionic collector can carry negatively charged functional groups on carboxyl group or sulfate group. (Bulatovic, 2007)

The main element of cationic collectors is, in general, the nitrogen group that functions as cationic site (hydrophilic). Hydrocarbons group are functioning as hydrophobic site. Most of the cationic collectors are amines, which are organic derivatives of ammonia. Characteristics of amine collectors are determined by hydrocarbon chain length and functional groups. Cationic collectors are reactive to a negatively charged mineral surface. (Hukki, 1964; Bulatovic, 2007)

Thiol collectors such as xanthates, dithiophosphates, thiocarbamates and mercaptans are chemicals, which are conventionally used to float the sulfide minerals. These chemicals are heteropolar and contain a polar part and non-polar part. Sulfur group in thio collectors is hydrophilic, and has affinity to sulfide minerals. (Hukki, 1964; Fuerstenau & Urbina, 1987)

1.3 Composition of flotation water

Mineral processing consumes a great amount of water, which represents 80 % - 85 % of the volume in mineral pulp. The quality of the process water in the flotation plays an important role in mineral flotation.

The shortage of freshwater resources has been a major challenge for the minerals processing industry, especially for the minerals flotation process, in which a great amount of water is needed. For countries facing water shortage, mining industry might compete the freshwater resources with other users/industries. In fact, about 96 % - 97 % of the earth's water is sea water, and only 0.5 % - 0.8 % of the earth's total water is fresh water. The impact of sea water on flotation performance has gained more and more attention due to the shortage of fresh water. Its salinity is about 35 ‰, and its pH is approximately 8.2. The high salinity is caused by dissolved salt. Sodium and chloride concentrations contribute most of the total salinity, as is shown in Table 1.1. The chemical composition and total salinity of sea water vary slightly among different locations in the world. The organic compounds, temperature, turbidity and suspended solids may also vary greatly among different locations. There are also some techniques to prepare artificial sea water for the related research. Artificial sea water rather than natural sea water was reported to minimize biological effects and to provide a reproducible solution of known composition. In this research, the formula and method we used were come from the “Preparation of artificial sea water” (Kester et al., 1967). The composition of the artificial sea water is presented in Table 1.1.

Table 1.1 Composition of artificial sea water

Contribution of various ions	Concentration in ‰	Concentration in ppm	Concentration in mol/L
Chloride (Cl^-)	19.353	19353	0.546
Sodium (Na^+)	10.765	10765	0.458
Sulfate (SO_4^{2-})	2.711	2711	0.028
Magnesium (Mg^{2+})	1.295	1295	0.053
Calcium (Ca^{2+})	0.414	414	0.010
Potassium (K^+)	0.387	387	0.010
Bicarbonate (HCO_3^-)	0.142	142	0.002
Bromide (Br^-)	0.066	66	0.001
Strontium (Sr^{2+})	0.008	8	9.13E-05
Boric acid (H_3BO_3)	0.026	26	4.21E-04
Fluoride (F^-)	0.001	1	2.63E-05
Total	35.168	35168	1.109

1.4 The use of sea water as process water in froth flotation

It has been reported that the floatability of natural hydrophobic minerals is significantly improved in concentrated electrolyte solutions.

Certain salts can improve particle-particle (coagulation/flocculation) and particle-bubble (flotation) interactions. As reported in literatures, salinity could be a positive factor for particle/bubble attachment during minerals flotation. Yoon (1982) and Paulson and Pugh (1996) proposed that reduced bubble sizes and increased bubble population in electrolyte solutions can increase the efficiency of bubble-particle collision and attachment. Fuerstenau et al. (1983) and Yoon and Sabey (1989) attributed the increased bubble-particle attachment to the reduction of zeta potential of both bubbles and particles, resulting from the compression of electrical double-layer in the presence of electrolytes. Another possible mechanism proposed is that the water-structure breaker types of inorganic electrolytes destabilize the hydrated layers surrounding mineral particles, enhancing the bubble-particle attachment (Klassen & Mokrousov, 1963). Castro and Laskowski (2011) proposed that because hydrophobic surfaces and bubbles usually carry the same charge, the attachment of the hydrophobic particles to bubbles is opposed by an electrical double layer repulsive force. With increasing ionic strength such a repulsive force is reduced and flotation of hydrophobic solids is enhanced. Bubble coalescence is also prevented at such salt concentrations, reducing the bubble size. Besides, electrolytes can prevent bubble from coalescence (Castro et al., 2010), both of which are positive factors for minerals flotation.

Even though the sea water flotation has a lot of advantages which could improve the flotation efficiency, there still exist some problems and challenges. The challenges in using sea water is its complex chemistry because it contains not only simple electrolytes but also some secondary ions in addition to NaCl with a possible depressing effect to target minerals, which may interfere with the flotation of some sulfide minerals. As a result, the flotation behavior of some sulfide minerals in sea water is very different from that in NaCl solutions. The salinity of sea water is typically 35 ‰, with important secondary ions such as, sulfate ions (2.711 ‰), magnesium ions (1.295 ‰), calcium ions (0.414 ‰), bicarbonate ions (0.142 ‰), borate ions (0.026 ‰), etc, which also have great influence on the flotation process. They may influence the surface chemistry and the floatability of some minerals. Some of these secondary ions can form colloidal precipitates in alkaline solutions at pH > 10, probably forming a slime coating on the mineral surfaces. For example, calcium and magnesium ions could form colloidal hydroxides, carbonates and sulfates precipitates. These precipitates might depress the flotation of some minerals like molybdenite.

Besides, the buffering effect of sea water significantly increases the lime consumption for adjusting pH to alkaline conditions. Sea water has a natural pH of around 7.8 - 8.2, which depends on salinity and concentration of the carbonate/bicarbonate ions (HCO_3^-/CO_3^{2-}) and boric acid/borate ions ($B(OH)_3 / B(OH)_4^-$). These ions are responsible for the buffering effect of sea water.

1.5 Objectives

The objective of this project is to explore the flotation behaviors of chalcopyrite and pyrite in high salinity water. The research will investigate the flotation of single and mixed minerals in Milli-Q water, NaCl solution, and sea water, and the influence of slime coating on flotation recoveries. High recoveries for chalcopyrite and strong pyrite depression should be achieved. The flotation performance of different collectors will be investigated, and the flotation experiments will be conducted using both Hallimond tube and electrochemical cell. The effects of pH, Eh, and electrolyte on flotation recovery will be studied. The flotation response was correlated with surface species in relation to surface hydrophobicity. The flotation results will be compared in order to achieve better recovery and selectivity. This research will improve our fundamental understanding of sulfide mineral flotation in sea water for the development of new technologies on sulfide mineral flotation in sea water.

1.6 References

Bulatovic, S. M. (2007). *Handbook of flotation reagents: chemistry, theory and practice: Volume 1: flotation of sulfide ores*. Elsevier.

Castro, S., & Laskowski, J. S. (2011). Froth flotation in saline water. *Kona*, *29*(4), 2011.

Castro, S., Venegas, I., Landero, A., & Laskowski, J. S. (2010). Frothing in seawater flotation systems. In *Proc. 25th International Mineral Processing Congress. Brisbane* (Vol. 4039, p. 4047).

Fuerstenau, D. W., Rosenbaum, J. M., & Laskowski, J. (1983). Effect of surface functional groups on the flotation of coal. *Colloids and Surfaces*, *8*(2), 153-173.

Fuerstenau, D. W., & Urbina, R. H. (1987). Flotation fundamentals. *Reagents in Mineral Technology. Marcel Dekker, New York*, 1-38.

Hukki, R. T. (1964). *Mineraalien hienonnus ja rikastus*. Teknillisten tieteiden akatemia= Akademin för tekniska vetenskaper.

Kester, D. R., Duedall, I. W., Connors, D. N., & Pytkowicz, R. M. (1967). PREPARATION OF ARTIFICIAL SEAWATER. *Limnology and Oceanography*, *12*(1), 176-179.

Klassen, V. I., & Mokrousov, V. A. (1963). *An introduction to the theory of flotation*. Butterworths.

Paulson, O., & Pugh, R. J. (1996). Flotation of inherently hydrophobic particles in aqueous solutions of inorganic electrolytes. *Langmuir*, *12*(20), 4808-4813.

Yoon, R. H. (1982). Flotation of coal using micro-bubbles and inorganic salts. *Min. Congr. J.;(United States)*, *68* (12).

Yoon, R. H., & Sabey, J. B. (1982). *Coal flotation in inorganic salt solutions* (No. VPI/CER-1-Bulletin). Virginia Polytechnic Inst. and State Univ., Blacksburg (USA). Virginia Center for Coal and Energy Research.

Chapter 2 Materials and Experimental Techniques

2.1 Materials and reagents

2.1.1 Mineral ores

High purity chalcopyrite and pyrite were purchased from Boreal Science. Each mineral was first crushed by a jaw crusher (RETSCH, Germany) into small pieces. Then the high purity minerals were hand-picked and further crushed and pulverized using a Pulverisette 2 mechanized agate mortar/pestle grinder (FRITSCH, Germany). The mineral particles with the size fractions between 38 μm and 75 μm were screened out for use in the flotation tests. The minerals were ultrasonic cleaned with deionized water until the supernatant is clean. The clean minerals were dried in vacuum drying oven. In order to minimize the mineral oxidation, the mineral particles were saved in plastics sample bag with 1.5 g in each bag and vacuum-sealed in a large bag.

X-ray diffraction analysis of the clean chalcopyrite and pyrite samples showed that there were no other impurities except a small amount of wurtzite. Chemical analysis of the two mineral samples indicated that chalcopyrite contained 29.87 % copper, indicating the purity of chalcopyrite is 85.9 % and that pyrite contain 43.80 % iron, indicating the purity of pyrite is

93.9 %.

2.1.2 Artificial sea water

During the experiment, we used artificial sea water rather than natural sea water to provide stable and reproducible solution and minimize the biological effects. To avoid precipitation of Ca^{2+}, Mg^{2+} and Sr^{2+} when preparing the artificial sea water, we made the sea water in two containers separately and then combine them. In one container, we added 71.778 g NaCl (58.44 g/mol), 12.024 g Na_2SO_4 (142.04 g/mol), 2.031 g KCl (74.55 g/mol), 0.588 g $NaHCO_3$ (84.01 g/mol), 0.294 g KBr (119.00 g/mol), 0.078 g H_3BO_3 (61.83 g/mol), 0.009 g NaF (41.99 g/mol) and 2004 ml Milli-Q water. In another container, we added 32.53 g $MgCl_2{\cdot}6H_2O$, 4.56 g $CaCl_2{\cdot}2H_2O$, 0.08 g $SrCl_2{\cdot}6H_2O$ and 871.8 g Milli-Q water. The composition of the artificial sea water is listed in the Table 1.1.

2.1.3 Collectors

Three collectors were used in the experiments. Potassium amyl xanthate (PAX) was obtained from Prospec Chemical Ltd, Canada. Isopropyl ethyl thionocarbamate was obtained from Charles Tennant & Company (Canada) Ltd. The molecular structure of N-isopropoxypropyl-N'-ethoxycarbonyl thiourea (iPOPECTU) is given in

Figure 2.1. It was prepared by a one-pot synthesis process (Liu et al., 2015). The synthesized product used in this study is with the purity greater than 95 %.

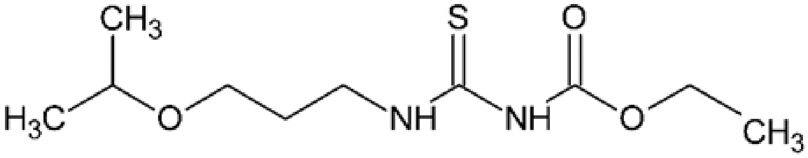

Figure 2.1 Molecular structure of N-isopropoxypropyl-N'-ethoxycarbonyl thiourea (iPOPECTU)

2.2 Characterization techniques

2.2.1 X-Ray fluorescence (XRF)

X-ray fluorescence is the emitted x-rays produced from a materials that have been excited by striking high energy x-rays or radioactive source. This technology provides one of the simplest, most accurate and economic analytical methods for the chemical composition of many different materials. This technique is non-destructive for sample, which requires a small amount of samples. It is suitable for solid, liquid and powdered samples. We used AMETEK EDAX (Energy Dispersive) XRF ORBIS PC in this experiment.

2.2.2 UV-Vis spectroscopy

Ultraviolet–visible spectroscopy absorption is the measurement of the attenuation of a beam of light after it passes through or reflects from a sample in the ultraviolet-visible spectral region. It measures the intensity of light passing through a sample (I), and compares with the initial intensity before it passes through the sample (I_0). The ratio I/I_0 is called the transmittance, and is usually expressed as a percentage (%T). The basic parts of an ultraviolet–visible spectrophotometer are a holder for the sample, a light source, a diffraction grating in a monochromator and a detector of light. We used Shimadzu UV-3600 in this experiment.

2.2.3 X-ray photoelectron spectroscopy (XPS)

X-ray photoelectron spectroscopy (XPS) is a popular surface chemical analysis technique of a sample. It is also known as ESCA (Electron Spectroscopy for Chemical Analysis). XPS spectra are obtained by irradiating a material with x-rays while measuring the kinetic energy and number of electrons that escape from the surface of 0 to 10 nm in depth of the sample. It is widely used to determine what elements are present on the surface of the sample. The AXIS 165 X-ray photoelectron spectrometer (Kratos Analytical) was used in this study.

2.2.4 Scanning electron microscopy (SEM)

A scanning electron microscope (SEM) scans a focused electron beam over a surface to create a high-resolution image of the sample. The electrons in the beam interact with the sample, producing various signals that can be used to obtain the surface topography and composition. It is widely used in laboratory to investigate the microstructure and chemistry of a lot of organic and inorganic materials. SEM usually connects with EDS (Energy Dispersive X-Ray Spectroscopy), which is used for the elemental analysis and chemical characterization of the sample. The JAMP-9500F equipped with electron guns for Secondary Electron Microscopy was used in this study.

2.2.5 Time of flight secondary ion mass spectrometry (ToF-SIMS)

Time-of-Flight Secondary Ion Mass Spectrometry (ToF-SIMS) provides elemental and chemical state, and molecular information from surfaces of solid materials. The average depth of this analysis is approximately 1 nm. ToF-SIMS is accomplished by exciting a samples surface with a finely focused ion beam, which causes secondary ions and ion clusters to be emitted from the samples surface. A time-of-flight analyzer is used to measure the exact mass of the emitted ions and clusters. From the exact mass and intensity of the SIMS peak, the identity of an element or molecular fragments can be determined. The ToF-SIMS images were obtained on a ToF-SIMS IV spectrometer (ION-TOF GmbH) in this study.

2.2.6 Contact angle measurements

The contact angle is the angle, usually measured through the liquid, where a liquid/vapor interface contacts a solid surface. It quantifies the wettability of a solid surface by a liquid via the Young’s equation. A given system of solid, liquid, and vapor at a given temperature and pressure has a unique equilibrium contact angle. There are many methods to measure the contact angle like the static sessile drop method, the Dynamic Wilhelmy method, Washburn's capillary rise method. The static sessile drop method was used in this study and the Theta Optical Tensiometer (T200 Biolin Sci) was used to measure the contact angle.

2.2.7 Zeta potential measurements

Zeta potential is the electric potential at the location of the slipping plane of the electrical double layer (EDL). It is caused by the net electrical charge contained within the region bounded by the slipping plane. It is widely used for quantification of the magnitude of the surface charge or surface potential. The zeta potential is a key indicator of the stability of dispersions of colloidal particle. The magnitude of the zeta potential indicates the degree of electrostatic repulsion between adjacent, similarly charged particles in dispersion. The Zetasizer Nano (Nano ZS) is used to measure the zeta potential in this study.

2.2.8 Atomic absorption spectrometer

Atomic absorption spectroscopy (AAS) is a spectroanalytical technique to quantitatively determine the chemical elements using the absorption of optical radiation by free atoms in the gaseous state. The technique uses the absorption spectrometry to assess the concentration of the substance in a sample. It requires standards with known analyte content to establish the relation between the measured absorbance and the substance concentration. A Varian SpectrAA-220FS (Varian, USA) atomic absorption spectrometer (AAS) was used to do this analysis.

2.2.9 Electrochemical impedance spectroscopy

Electrochemical impedance spectroscopy (EIS) is a powerful technique that can be used to provide information about the properties of electrochemical process. It measures dielectric properties of a medium as a function of frequency and employs the simple concept of resistance/capacitance by impedance. Among other factors, EIS is an experimental technique that can be used to separate and quantify different sources of voltage loss. During an impedance measurement, a frequency response analyzer (FRA) is used to impose a small amplitude AC signal to the electrochemical cell. The AC voltage and current response of the cell is analyzed by the FRA to determine the resistive, capacitive and inductive behavior (impedance) of the cell at a certain frequency. By applying physically-sound equivalent circuit models wherein physiochemical processes occurring within the fuel cell are represented by a network of resistors, capacitors and inductors. The meaningful qualitative and quantitative information could be extracted based on the sources of impedance. EIS is useful for research and manufacturing of new materials and electrode structures. The EIS measurements were conducted by using a 1255B Frequency Response Analyzer from Solartron Analytical.

2.2.10 Cyclic voltammetry

Cyclic voltammetry is an electrochemical technique which measures the current in an electrochemical cell under conditions where voltage is in excess of that predicted by the Nernst equation. Cyclic voltammetry is performed by cycling the potential of a working electrode, and measuring the resulting current. The current at the working electrode is plotted versus the applied voltage to give the cyclic voltammogram. A three-electrode system is used as a standard cyclic voltammetry analysis, which includes reference electrode, working electrode, and counter electrode. An electrolyte is added to the cell to ensure sufficient conductivity. In linear sweep voltammetry (LSV), a fixed potential range is employed. In the case of cyclic voltammetry, the voltage is swept between two values at a fixed rate, however, when the voltage reaches to the maximum, the scan is reversed and the voltage is swept back to the minimum. This technique is an important and widely used electroanalytical technique in many areas. The CHI600E electrochemical analyzer/workstation (CH Instruments, Inc., Austin) was used to do the analysis.

2.2.11 Micro-flotation

A home-built micro-flotation cell was used in this study (Figure 2.2). The bottom part of this cell has a magnetic stir bar on the top of a sintered glass frit with pore size 1.6 μm to agitate the flotation pulp in the cell. The narrow throat connecting the flotation tube to the collection tube allows only one bubble to pass from the bottom part when no frother added, which greatly minimizes the water carried to the froth and minimizes the mechanical entrainment. The flotation gas (nitrogen) comes from a cylinder to the flow meter and then connects to the bottom part of the tube.

In a flotation test, 1.5 g mineral particles with size range between 38 to 75 μm were mixed with 150 ml process water and agitated in a beaker to fully mix the particles with the process water. The pH is adjusted using sodium hydroxide or hydrochloric acid with different concentrations to the desired value and the collector is then added. The pulp is conditioned for 5 min in the beaker. The conditioned pulp was then transferred to the flotation cell and floated for 5 min with high purity nitrogen at a flow rate of 30 sccm. The concentrates and tails were collected and filtered after the flotation. The filter paper together with mineral particles was dried at 70 ℃ overnight. The samples were then weighted and the flotation recovery was calculated by the following equation:

$$Recovery(\%) = \frac{Weight\ of\ concentrate}{Weight\ of\ concentrate + Weight\ of\ tail}$$

For the mixed minerals flotation, the mixed minerals were analyzed with XRF. The recovery of the mineral is calculated by the characteristics elements contain in the mineral in concentrates and feed.

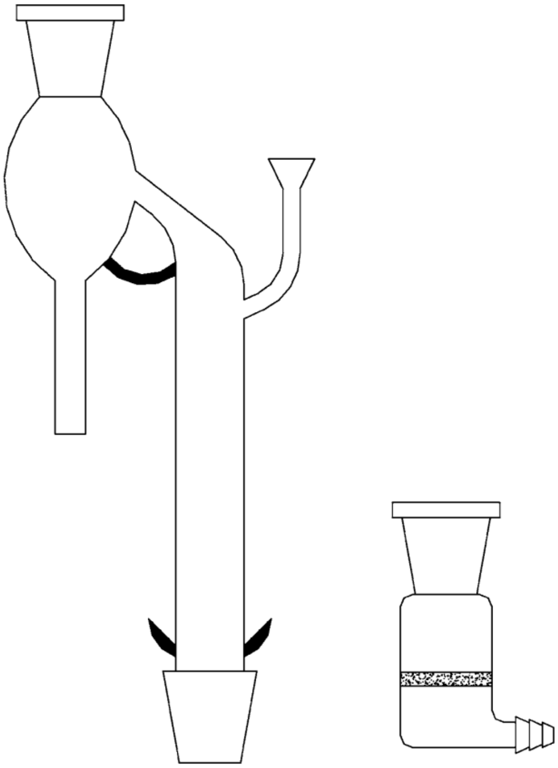

Figure 2.2 Schematics of the flotation cell

For the electrochemical flotation, a modified Hallimond flotation tube with a three electrodes system was used (Figure 2.3). The reference electrode was calomel electrode. The counter electrode was platinum foil. The working electrode was a cylinder made by platinum mesh. The three electrodes system was controlled by a potentiostat instrument. The mineral particles was stirred in the flotation cell and kept interacting with the platinum mesh to attain a desired potential.

Process water was pretreated before each flotation experiment. The water was purged with high purity nitrogen for 1 h. 1.5 g mineral particles were then transferred to the flotation cell by the de-oxygen process water. The water was then added to just about the same position with the upper nitrogen inlet. The upper nitrogen inlet was then purged with high purity nitrogen to exhaust the air trap in the cell and prevent the oxidation of the mineral in the pulp. The stir bar at the bottom of the cell was adjusted to make mineral particles efficiently contact with the platinum mesh. The mineral particles were conditioned at a set potential for 30 min. When the conditioning is over, the upper nitrogen was shut down and the lower nitrogen was purged into the cell with the flow rate of 30 sccm. The speed of the stir bar was set at 700 rpm to make the flotation experiment effective.

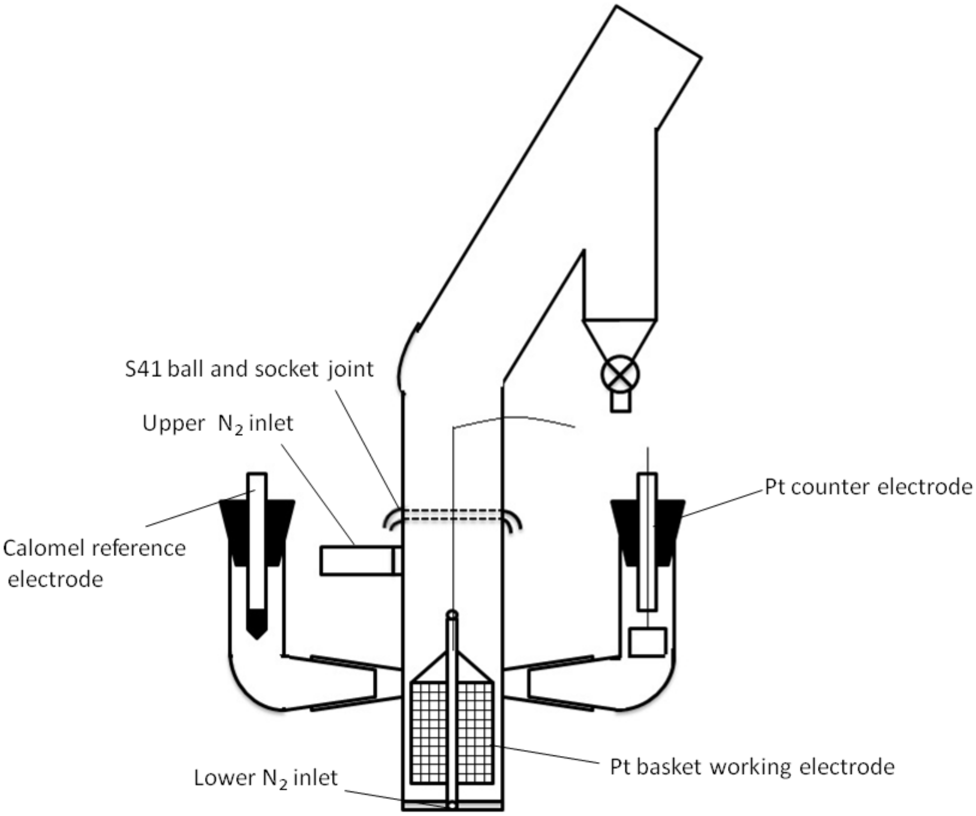

Figure 2.3 Schematics of the modified Hallimond flotation tube

Chapter 3 The Effect of High Salinity Water on the Flotation Performance of Chalcopyrite and Pyrite with Different Collectors

3.1 Introduction

Pyrite (FeS_2) is the most abundant sulfide minerals, which is usually considered as less-valuable and undesired gangue mineral when associated with other base-metal minerals, such as copper, lead and nickel. The excessive presence of pyrite in the concentrates is not acceptable. Chalcopyrite ($CuFeS_2$) is one of the most important copper sulfide minerals with abundant content of copper. The key challenges in the successful selective flotation of chalcopyrite result from the relative abundance of pyrite in the ore that may contaminate the concentrates of chalcopyrite. The objective of the flotation of chalcopyrite is to achieve good separation from pyrite. Therefore, it is essential to depress iron sulfides to produce high-grade concentrates of valuable minerals (Boulton, Fornasiero, & Ralston, 2001; Ball & Rickard, 1976; Shen, Fornasiero, & Ralston, 1998; Xiaojun & Kelebek, 2000). To a certain extent, the successful separation of chalcopyrite from pyrite is determined by the floatability of the pyrite. It's also very important to explore the collectors which have strong affinity with chalcopyrite but little affinity with pyrite. For sulfide minerals, sulfydryl compounds are usually used as collectors, such as xanthate, thionocarbamate or dithiophosphate (Ackerman et al., 1987). The high ionic concentration of recycled water and sea water requires more stable and more powerful complexing molecules to achieve a smart molecular architecture on the mineral surface for flotation. Since the discovery of xanthate for sulfide mineral flotation in early 1920s, other collector molecules such as thiocarbamate, thionocarbamate, dithiophosphate, and mercaptobenzothiazole were developed for the sulfide mineral flotation to improve the recovery and selectivity (Fairthorne, Fornasiero, & Ralston, 1997; Nagaraj, Basilio, & Yoon, 1989; Mielczarski & Yoon, 1989). More recently, it was reported that the copper recovery and grade were improved when N-isopropoxypropyl-N'-ethoxycarbonyl thiourea (iPOPECTU) was used as a collector as compared with sodium butyl xanthate (SBX) (Liu et al., 2015; Yuan & Zhong, 2012). Using iPOPECTU as a collector, the copper recovery and grade were 4.54 % and 0.95 % higher than using SBX, respectively. It is believed that iPOPECTU is a better collector for copper flotation due to the selectivity of binding (head) group with copper atoms on the surface and the longer and flexible chain length of the hydrophobic tail $(CH_3)_2$-O-CH_2-CH_2-CH_2-. In this study, the performance of three collectors, namely potassium amyl xanthate (PAX), thionocarbamate and

N-isopropoxypropyl-N'-ethoxycarbonyl thiourea (iPOPECTU), were investigated for the flotation of pyrite in high salinity water to improve our fundamental understanding of mineral flotation in sea water.

3.2 Materials and experimental methods

3.2.1 Materials

High purity pyrite and chalcopyrite, purchased from Boreal Science, was crushed and pulverized to obtain the size fractions between 38 μm and 75 μm for the flotation test. The particles smaller than 38 μm were for the zeta potential distribution measurements. The minerals were ultrasonically cleaned with deionized water at least three times to wash away the impurities and dried in a vacuum drying oven at room temperature. X-ray diffraction analysis of the clean chalcopyrite and pyrite samples showed that there were no other impurities. Chemical analysis of the two mineral samples indicated that chalcopyrite contained 29.87 % copper, indicating the purity of chalcopyrite is 85.9 % and that pyrite contain 43.80 % iron, indication the purity of pyrite is 93.9 %.

Three collectors were used in the experiments. Potassium amyl xanthate (PAX) was obtained from Prospec Chemical Ltd, Canada. Isopropyl ethyl thionocarbamate was obtained from Charles Tennant & Company (Canada) Ltd. N-isopropoxypropyl-N'-ethoxycarbonyl thiourea (iPOPECTU) was prepared in house by a one-pot synthesis process (Liu et al., 2015). The synthesized product used in this study is with the purity greater than 95 %. The molecular structures of the collectors are given in Table 3.1. Collector solutions were made using fresh Milli-Q water (18.2 MΩ·cm resistivity) purified by a millipore purification system.

Table 3.1 Molecular structure of xanthate, thionocarbamate and iPOPECTU (Liu et al., 2015)

Xanthate	Thionocarbamate	iPOPECTU
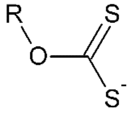	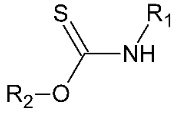	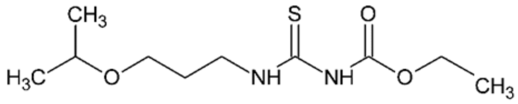

We used artificial sea water rather than natural sea water to provide a stable and reproducible solution and minimize the biological effects in the experiment. The composition was provided in previous study (Kester, Duedall, Connors, & Pytkowicz, 1967). The composition of the artificial sea water is listed in Table 1.1. The concentration of the NaCl solution used in the experiment was 0.4 M.

3.2.2 Experimental methods

3.2.2.1 Flotation tests

The flotation test was conducted using a modified Hallimond flotation tube (Siwek, Zembala, & Pomianowski, 1981). 1.5 g chalcopyrite or pyrite particles, with the size ranging from 38 μm to 75 μm, were mixed with 150 ml of process water (Milli-Q water, NaCl solution or artificial sea water) at a desired pH with the collector concentration of 0 or 1×10^{-5} M. After five minutes of the conditioning in the desired solution, the pulp was transferred to the flotation tube. The flotation test was conducted for five minutes with 30 standard cubic centimeters per minute (sccm) nitrogen flow rate and 700 revolutions per minute (rpm) of the stir bar. Both the concentrates and tailings were collected, filtered, and dried overnight at 70 ℃. The recoveries were calculated by the mass ratio of concentrate to the total of concentrates and tailings. Each flotation test was repeated at least three times to confirm that the results were responsible and reliable. The average flotation recoveries and standard deviations were reported.

For the flotation of mixed mineral, 0.75 g chalcopyrite and 0.75 g pyrite was conditioned in a 150 ml of process water (Milli-Q water, NaCl solution or artificial sea water) at a desired pH with the collector concentrations of 0 or 1×10^{-5} M for 5 min. The flotation test was also conducted for 5 minutes with 30 standard cubic centimeters per minute (sccm) nitrogen flow rate and 700 revolutions per minute (rpm) of the stir bar. Both the concentrates and tailings were collected, filtered, and dried overnight at 70 ℃. The concentrate and tailing were analyzed by XRF. The recoveries were calculated by the mass and weight percentage of each mineral in concentrates and tailings respectively.

$$Cp\ Recovery(\%) = \frac{Wt.of\ concentrate \times a1\%}{Wt.of\ concentrate \times a1\% + Wt.of\ tail \times a2\%}$$

$$Py\ Recovery(\%) = \frac{Wt.of\ concentrate \times b1\%}{Wt.of\ concentrate \times b1\% + Wt.of\ tail \times b2\%}$$

Where a1 % and a2 % are the weight percentage of mineral of chalcopyrite in concentrates and tailings respectively, and b1 % and b2 % are the weight percentages of mineral of pyrite in concentrates and tailings respectively.

3.2.2.2 Contact angle measurements

High purity chunk pyrite samples were used for contact angle measurements. The samples were wet-polished by a series of polishing papers down to 1000 grade. The freshly polished samples were washed by immersing them into pH 2 HCl solution, sonicated for 10 min, rinsed with Milli-Q water, and then immersed immediately in 150 mL of the desired testing solution. The samples were conditioned in different solutions at different pHs with 1×10^{-5} M collector for five minutes. The samples were then rinsed with sufficient Milli-Q water and blow-dried with high purity nitrogen before loading into a Drop Shape Analyzer (DSA 10 from KRUSS USA) equipped with a CCD camera. The contact angles on the pure pyrite sample without any conditioning were also measured. The sessile drop technique was used to determine the contact angle. A 10 μL Milli-Q water drop was placed on the surface of the treated sample, and a real-time video of the drop was recorded. The image of the water drop was analyzed using the vendor-provided instrument software. Measurements were conducted on at least three different sites of the mineral surface. The average and standard deviations calculated from the measurements are reported.

3.3 Results and discussion

3.3.1 Flotation of single pure mineral

The flotation recoveries of chalcopyrite and pyrite in different process water without the addition of collectors at different pHs are shown in Figure 3.1 and Figure 3.2, respectively. Figure 3.1 shows that the flotation recoveries increases by 10 % in NaCl solution and sea water as compared to that in Milli-Q water at pH lower than 8. But when the pH is higher than 10, the flotation recoveries was greatly decreased in Milli-Q water and sea water. For the flotation in Milli-Q water, the decrease of recovery at high pH may be caused by the formation of hydrophilic iron hydroxide on the surface of chalcopyrite. For the decrease in sea water may be caused by the formation of magnesium and calcium hydroxide precipitates onto the surface of chalcopyrite, which will be elucidated in later section. Figure 3.2 shows that the flotation recoveries of pyrite were the lowest in Milli-Q water, but much higher in NaCl solution and sea water. The flotation recovery is lower in sea water compared to that in NaCl solution, which may be caused by the magnesium and calcium containing in sea water forming $MgOH^+$ and $CaOH^+$ on the surface of pyrite and decreased the surface wettability. Again, the decrease of flotation recoveries at high pH may be caused by the iron hydroxide forming on the surface of pyrite and magnesium and calcium hydroxide forming in sea water.

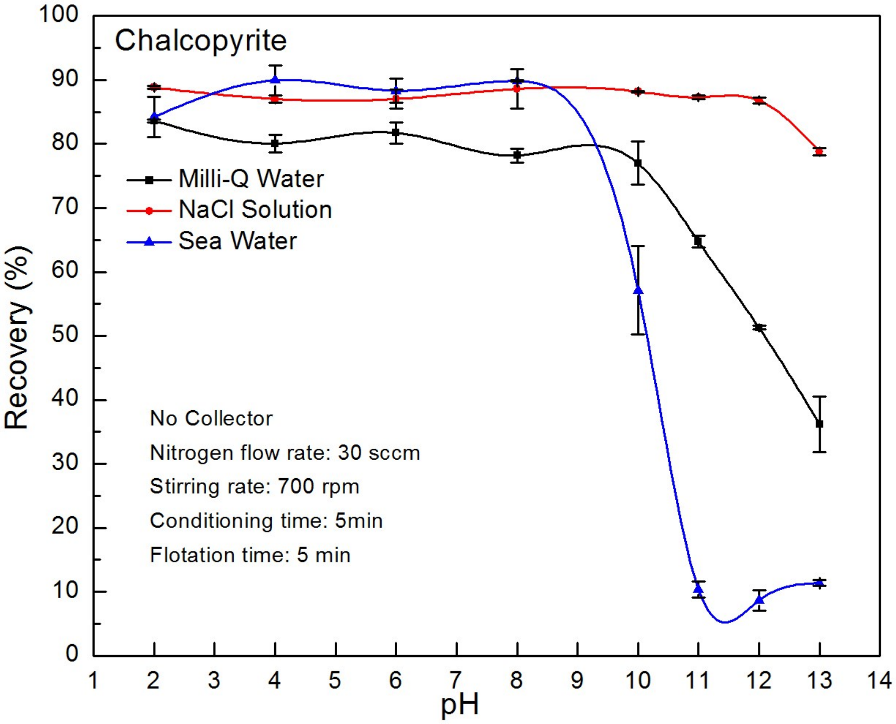

Figure 3.1 Flotation response of chalcopyrite as a function of pH in the absence of collector in different process water

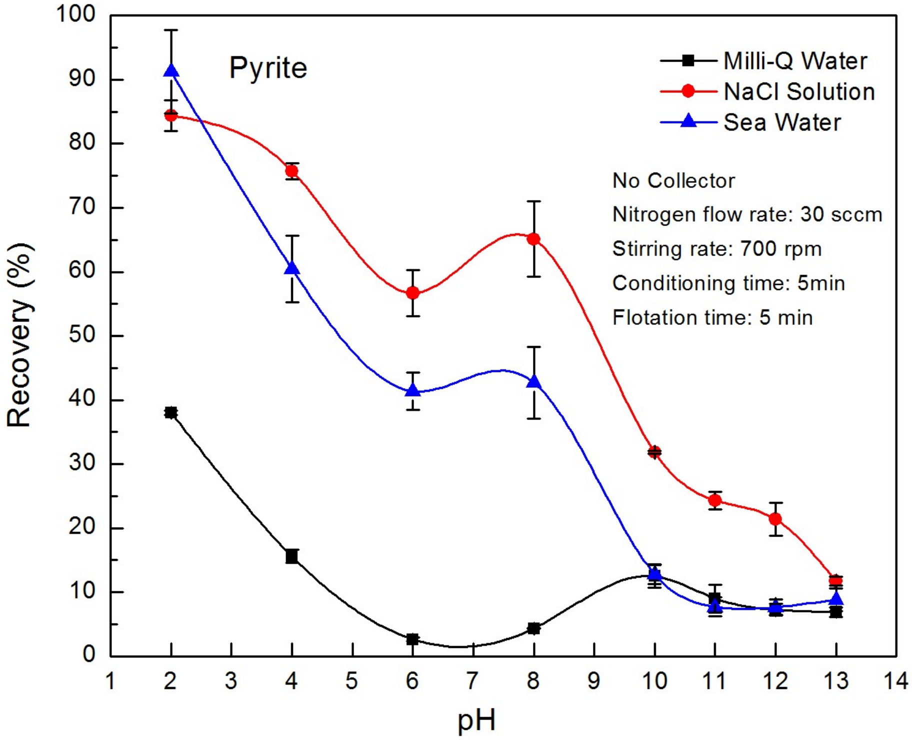

Figure 3.2 Flotation response of pyrite as a function of pH in the absence of collector in different process water

The flotation recoveries of chalcopyrite in Milli-Q water, NaCl solution and sea water with the addition of collectors at different pHs are shown in Figure 3.3, Figure 3.4 and Figure 3.5, respectively. Figure 3.3 shows that the flotation recovery of chalcopyrite was improved by the addition of collectors. The performance of the three collectors is almost the same in Milli-Q water with PAX has the highest flotation recovery. The flotation recovery didn’t drop with the addition of collector at high pH, which was caused by the surface adsorption of collector.

Figure 3.3 and Figure 3.4 show that the flotation of chalcopyrite was improved in NaCl solution compared to that in Milli-Q water. In Milli-Q water, the flotation recoveries of chalcopyrite in three different collectors were between 80 % - 90 %. But the recoveries were higher than 90 % in NaCl solution. The flotation recoveries is highest with the addition of thionocarbamate when pH less than 6 and is highest with the addition of PAX when pH is higher than 6.

Figure 3.5 shows that the flotation recovery of chalcopyrite was greatly dropped when the pH is higher than 9. This is caused by the magnesium and calcium forming the hydrophilic hydroxides precipitates coating on the surface of chalcopyrite which largely depressed the flotation. Liu and Zhang (2000) reported that calcium ions and calcium hydroxide precipitates caused strong depression of the chalcopyrite and the recovery dropped to nearly zero at pH 12, which indicated their adverse effects on the flotation of chalcopyrite. Castro and Laskowski (2011) also reported that copper sulfide minerals, such as, chalcocite and chalcopyrite float well in sea water in the pH range of 8.0 - 9.5, however, the flotation recovery abruptly decreases at pH higher than 10.The detailed mechanism will be further proved in the following chapter. Figure 3.5 also shows that the performance of chalcopyrite is the best with the addition of thionocarbamate compared to other collectors. The flotation recovery is the highest in the presence of thionocarbamate at pH less than 6 and also pH 10, which provides a potential chance to float chalcopyrite at high pH in sea water.

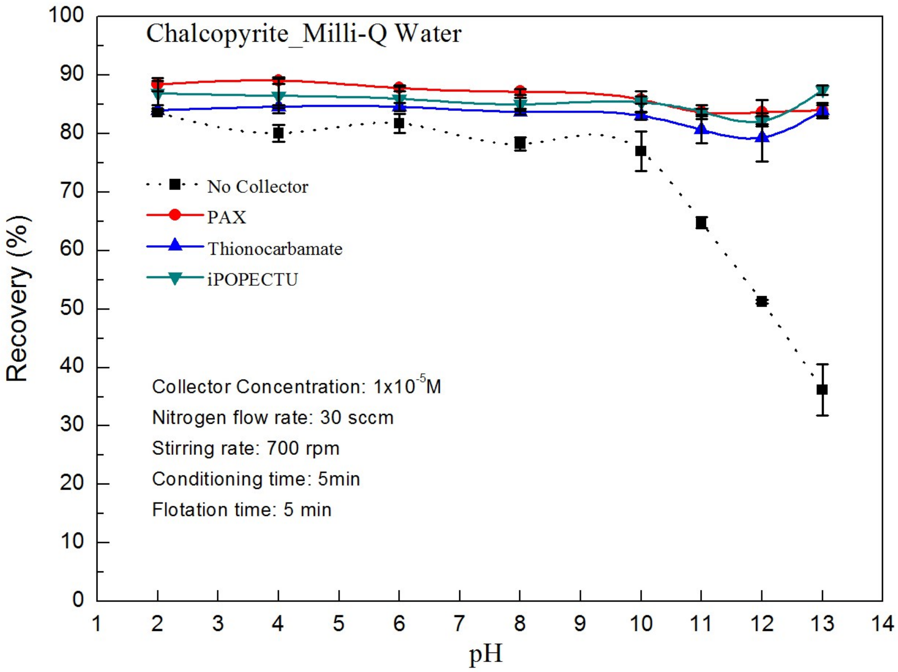

Figure 3.3 Flotation response of chalcopyrite as a function of pH in Milli-Q water with 1×10^{-5} M collector

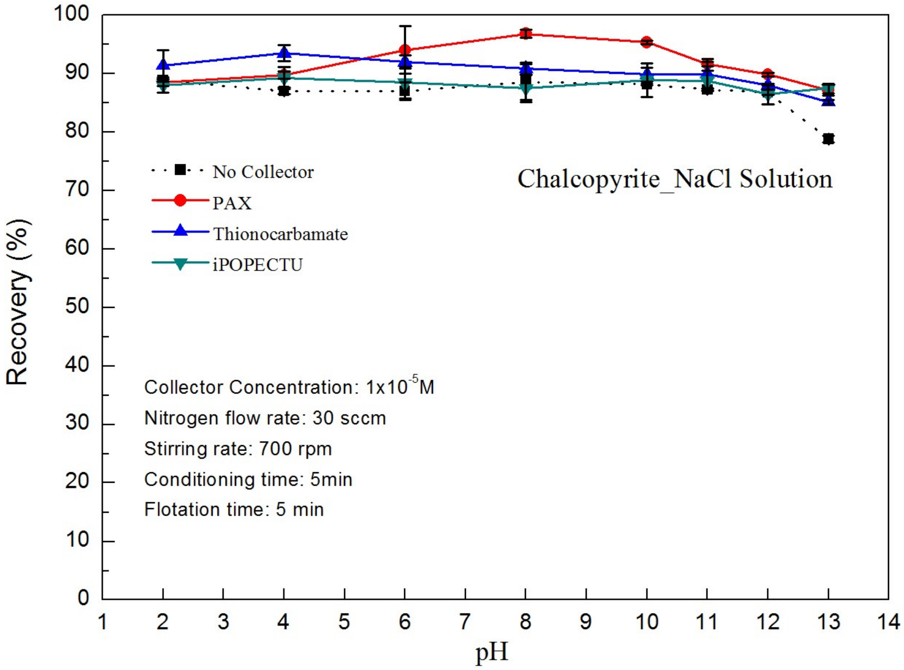

Figure 3.4 Flotation response of chalcopyrite as a function of pH in NaCl solution with 1×10^{-5} M collector

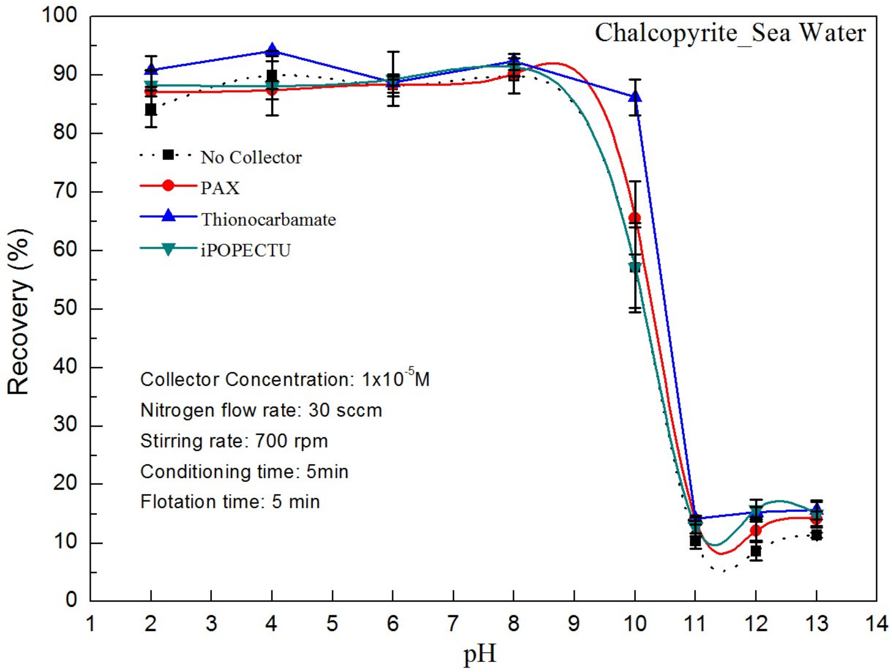

Figure 3.5 Flotation response of chalcopyrite as a function of pH in sea water

with 1×10^{-5} M collector

The flotation recoveries of pyrite in Milli-Q water, NaCl solution and sea water with the addition of collectors at different pHs are shown in Figure 3.6, Figure 3.7 and Figure 3.8, respectively. Figure 3.6 shows that the flotation recovery of pyrite was improved by the addition of collectors. The improvement for pyrite flotation is not very huge with the addition of thioncarbamate and iPOPECTU compared to the collectorless flotation. But the flotation of pyrite was greatly improved by the addition of PAX and even obtained near 100 % flotation at some certain pHs. For the flotation of pyrite using PAX in Milli-Q water, a lower flotation recovery was observed at the pH range of 6-7. Wang and Forssberg (1991) suggested that it is the formation of ferric-hydroxy-xanthate species that caused this low recovery; however, Leppinen, Basilio, and Yoon (1989) and Bulut and Atak (2002) have shown that only dixanthogen is present on the surface of pyrite at that range with FTIR spectroscopy. Lopez-Valdivieso, Sanchez Lopez, and Song (2005) proposed that the low recovery is caused by the high ratio of hydrophilic ferric hydroxide phase to hydrophobic dixanthogen phase caused by an insufficient amount of dixanthogen adsorption. From Figure 3.6, we can get a preliminary conclusion that thionocarbamate and iPOPECTU have less affinity than PAX for the flotation of pyrite in Milli-Q water.

Figure 3.6 and Figure 3.7 show that the flotation of pyrite in these three different collectors was improved in NaCl solution compared to that in Milli-Q water. In Milli-Q water, the flotation recovery of pyrite greatly dropped at near neutral pH. But this low recovery in the near neutral pH range disappeared when the flotation was conducted in NaCl and the flotation recoveries were near 100 % at that pH range, which is a huge improvement. When the pH is less than 6, the flotation response of pyrite is almost the same with the addition of the three different collectors, which has a very high recovery. But when the pH is higher than 6, the flotation recovery of pyrite is the lowest in thionocarbamate and a little bit higher in iPOPECTU but much higher in PAX, which means that the affinity of the three different collectors on the surface of pyrite in NaCl solution is in the ascending order of thionocarbamate, iPOPECTU and PAX.

Figure 3.8 shows that the flotation of pyrite in sea water in these three different collectors was also improved as compared to that in Milli-Q water. And the low recovery of pyrite in PAX in the near neutral pH range disappeared when the flotation was conducted in sea water and reached about 100 % recovery, which is a huge improvement. The flotation recoveries of pyrite in thionocarbamate are the lowest and much higher in iPOPECTU and PAX. The flotation curve of pyrite in thionocarbamate is almost the same with the collectorless flotation in sea water, which means that thionocarbamate has the lowest affinity on the surface of pyrite in sea water.

The flotation of pyrite is greatly dropped at high pH in different process water. The reason is that the formation of hydrophilic ferric hydroxide at high pH might be coated on the surface of pyrite, which depressed the flotation of pyrite. The low recovery in sea water is also probably attributed to the magnesium and calcium hydroxide precipitates at high pH levels. This was confirmed by SEM, EDX, ToF-SIMS and zeta potential measurements. Magnesium hydroxide is believed to be the major cause of the low recovery because its molar concentration in sea water is about five times that of calcium and magnesium hydroxide is less soluble than calcium hydroxide which is indicated by magnesium and calcium speciation diagram (Castro, Rioseco, & Laskowski, 2012; Fuerstenau & Palmer, 1976).

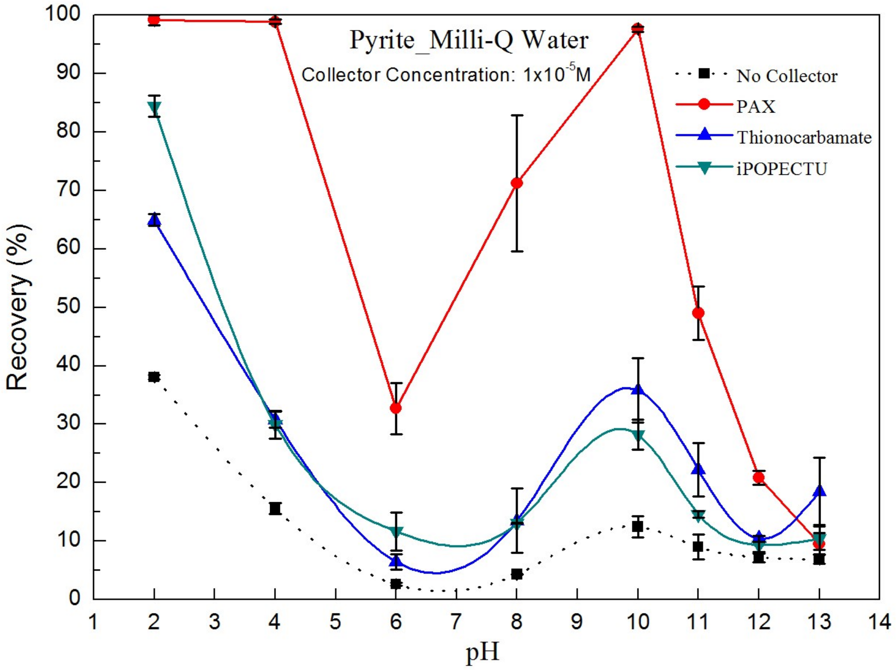

Figure 3.6 Flotation response of pyrite as a function of pH in Milli-Q water with 1×10^{-5} M collector

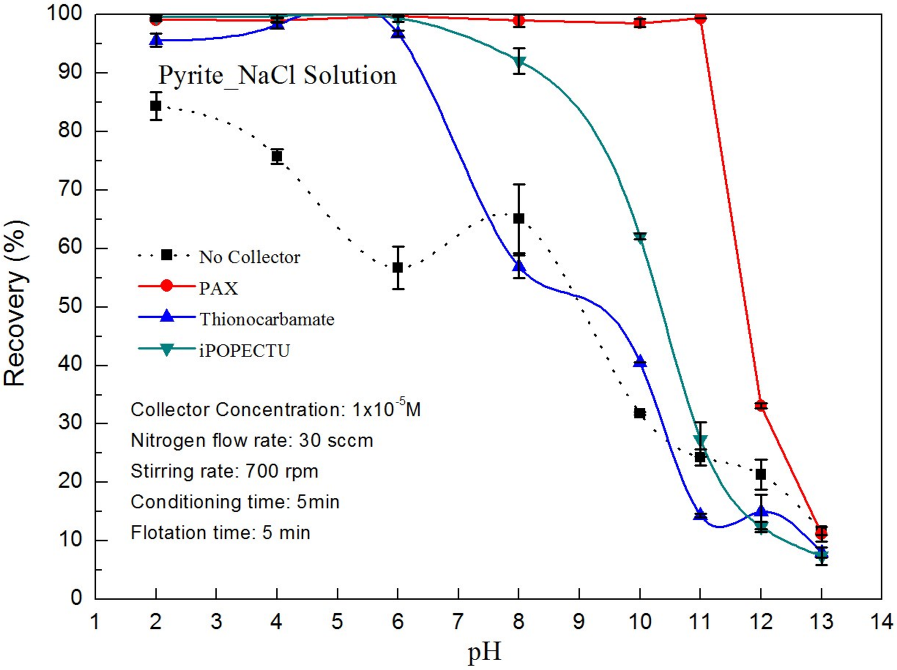

Figure 3.7 Flotation response of pyrite as a function of pH in NaCl solution

with 1×10^{-5} M collector

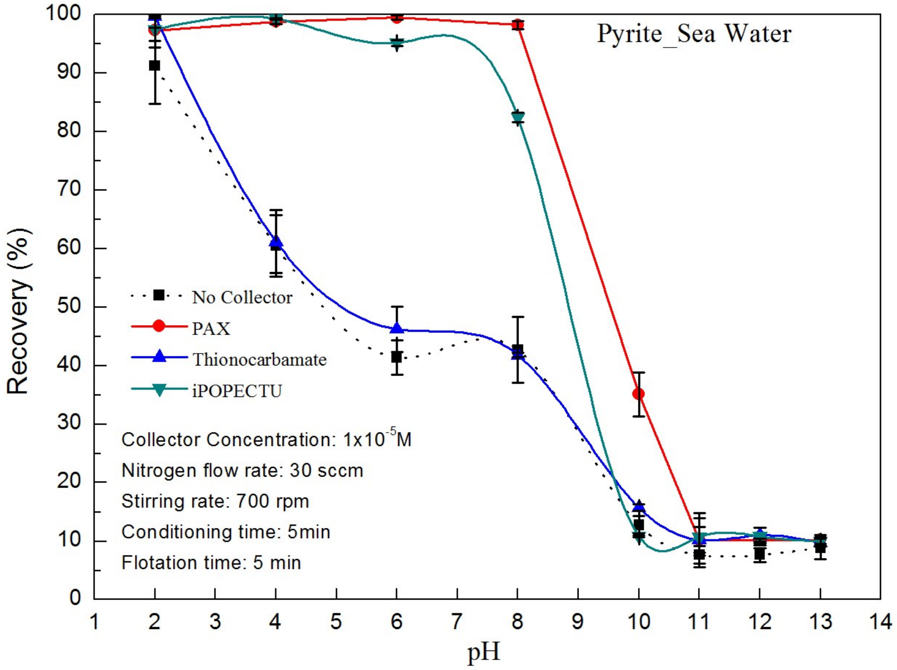

Figure 3.8 Flotation response of pyrite as a function of pH in sea water with 1×10^{-5} M collector

3.3.2 Flotation behavior of chalcopyrite and pyrite mixture

In mineral ores containing more than one sulfide mineral, the interaction between the mineral particles plays an important role in the flotation behavior of each mineral. The effects of mineral-mineral interaction (Nakazawa & Iwasaki, 1985; Rao & Natarajan, 1989a, b) on the flotation have been studied by using different electrochemical techniques and surface characterization methods.

When two sulfide minerals contact with each other in an aqueous solution, electron will transfer from one to another, depending on the conductivity and semiconducting properties of sulfide minerals, which is called galvanic interaction. The origin of galvanic interaction of sulfide minerals is due to their different electrochemical properties, which could be shown by rest potential. Majima (1969) have measured the rest potentials of a number of sulfide minerals in water at pH 4 and 4.6. Pyrite showed the highest rest potential (0.66 V vs the Standard Hydrogen Electrode (S.H.E.) at pH 4) and chalcopyrite (0.56 V) was lower. Rest potential of a sulfide mineral is believed to represent the following redox equilibrium.

$$MS = M^{2+} + S^0 + 2e$$

$$E = E^0 + RT/2F \ln a_{M^{2+}}$$

Since pyrite has the highest rest potential, it is expected to be electrochemically least active thermodynamically. For the interactions of different minerals, a mineral with higher rest potential (noble mineral) acts as a cathode and the mineral with lower rest potential (active mineral) acts as anode electrode. The presence of dissolved oxygen in the solution is of vital importance for galvanic interaction since oxygen acts as an electron acceptor reacting to form OH^- on noble minerals. Different models of galvanic interactions can be established depending on the number of galvanic components in the system (Cheng & Iwasaki, 1992). For a multiple mineral-grinding media and mineral-mineral system, the galvanic interactions become more complex than the two-electrode system.

Since pyrite has the highest rest potential, when pyrite is in contact with other sulfide minerals in aqueous solution, it acts as a cathode absorbing electrons from other sulfide minerals, which give rise to a current called the galvanic current. This process reduces the potential of pyrite, which makes it more reducing. This phenomenon has been discovered by Nakazawa and Iwasaki (1985). The reduction of pyrite was accompanied by simultaneous oxidation of pyrrhotite in their pyrite-pyrrhotite system.

Mehta and Murr (1983) experimentally studied the galvanic interactions between a series of sulfide minerals including the pyrite-chalcopyrite couple. The results showed that the galvanic interactions between pyrite and chalcopyrite significantly affected the leaching and separation of chalcopyrite from pyrite. Pyrite in the slurry led to a 2 - 15 times increase in the rate of dissolution of chalcopyrite. Ekmekci and Demirel (1997) studied the effects of galvanic interactions between pyrite and chalcopyrite during collectorless flotation. They found that galvanic interactions between pyrite and chalcopyrite significantly affected each mineral. The flotation of the pyrite was promoted and chalcopyrite was depressed to some extent.

The flotation test of the mixture of chalcopyrite and pyrite (weight ratio 1:1) are showed in the Figure 3.9 - Figure 3.14. The flotation behaviors of both minerals are quite different with the single mineral flotation. The flotation of chalcopyrite was depressed in Milli-Q water, but the flotation of pyrite is greatly improved. The low flotation recovery of pyrite with the presence of PAX at near neutral pH was disappeared and the flotation recovery is dropped at pH 11. As can be seen from Figure 3.9, chalcopyrite can be separated from pyrite at pH higher than 11 with the presence of 1×10^{-5} M PAX.

It is reported that thionocarbamate and iPOPECTU have very good selectivity for selective separation of chalcopyrite and pyrite minerals by froth flotation (Fairthorne, Fornasiero, & Ralston, 1997; Nagaraj, Basilio, & Yoon, 1989; Mielczarski & Yoon, 1989; Liu et al., 2015; Yuan & Zhong, 2012). The flotation results of single pure mineral in this study also show that thionocarbamate and iPOPECTU have less affinity on pyrite. Figure 3.10 and Figure 3.11 shows the flotation behavior of chalcopyrite and pyrite mixed mineral in Milli-Q water with a 1:1 ratio. The results indicate that the flotation of chalcopyrite is slightly depressed with the addition of pyrite in thionocarbamate and iPOPECTU while the flotation of pyrite is greatly improved. Two different mechanisms for the increased flotation recovery of pyrite after the addition of chalcopyrite have been proposed (Ekmekçi & Demirel, 1997), which is increased proportion of elemental sulfur or metal-deficient sulfur and copper activation on the pyrite surface. In a galvanic cell composed of chalcopyrite and pyrite, pyrite was reduced and the initial oxidation product ferric hydroxide on its surface was reduced to ferrous hydroxide and then to soluble species, which will generate a metal-deficient sulfur-rich hydrophobic surface layer and/or elemental sulfur on pyrite surface resulting in an improved pyrite flotation. For the mechanisms of copper activation, it is generally accepted that the formation of a new copper sulfide phase on the surface of pyrite through the reduction of cupric to cuprous is responsible for the activation of pyrite while sulfide ions are oxidized (Bushell & Krauss, 1962; Weisener & Gerson, 2000). Laajalehto et al. (1999) also found that the copper-activated pyrite exhibited similar S 2p XPS spectrum with copper sulfides (e.g. chalcocite or chalcopyrite) and similar xanthate adsorption behavior as chalcopyrite, which may be due to the formation of a chalcopyrite-like phase ($CuFeS_2$) on the surface during the activation. For binary mineral systems, the heterocoagulation often occurs over the whole range of pH between mineral particles due to the opposite surface charge. Mitchell et al. (2005) found the heterocoagulation phenomenon of chalcopyrite and pyrite. They found that chalcopyrite and pyrite minerals heterocoagulate in the absence and presence of the flotation collectors in acidic medium. Even for thionocarbamate, which is a powerful collector for selective separation of chalcopyrite from pyrite, is impossible to effectively separate chalcopyrite from pyrite at pH 4. However, at pH 10, the two minerals do not heterocoagulate in the presence of the flotation collectors. Therefore, the selective flotation separation of the two minerals is possible at high pH.

As we can see by comparing Figure 3.9, Figure 3.10 and Figure 3.11, the potential separation of chalcopyrite from pyrite by using PAX, thionocarbamate and iPOPECTU is at pHs of 12, 11 and 13 respectively. Even though there are galvanic interaction, pyrite activation and heterocoagulate for the mixed mineral system, the selectivity of thionocarbamate is better than PAX and iPOPECTU for the flotation of chalcopyrite and pyrite mixed mineral.

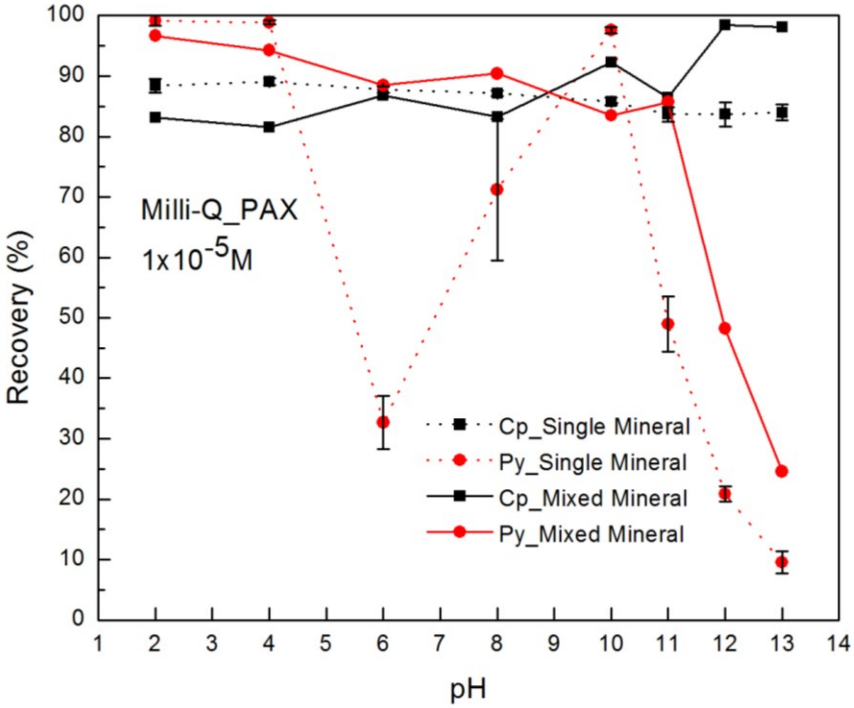

Figure 3.9 Flotation response of chalcopyrite and pyrite mixture (weight ratio 1:1) as a function of pH in Milli-Q water with 1×10^{-5} M PAX (dot curve are the flotation results of single mineral flotation)

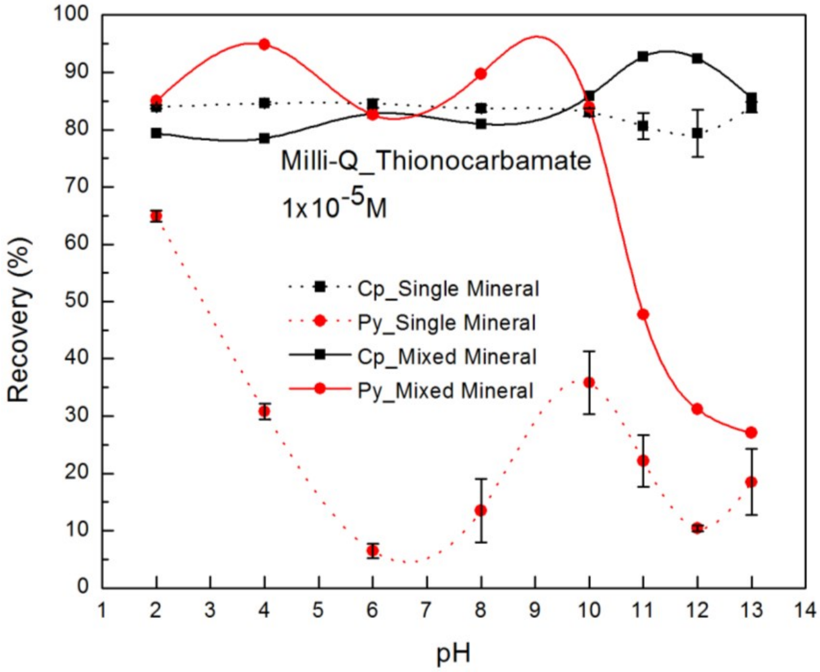

Figure 3.10 Flotation response of chalcopyrite and pyrite mixture (weight

ratio 1:1) as a function of pH in Milli-Q water with 1×10^{-5} M thionocarbamate (dot curve are the flotation results of single mineral flotation)

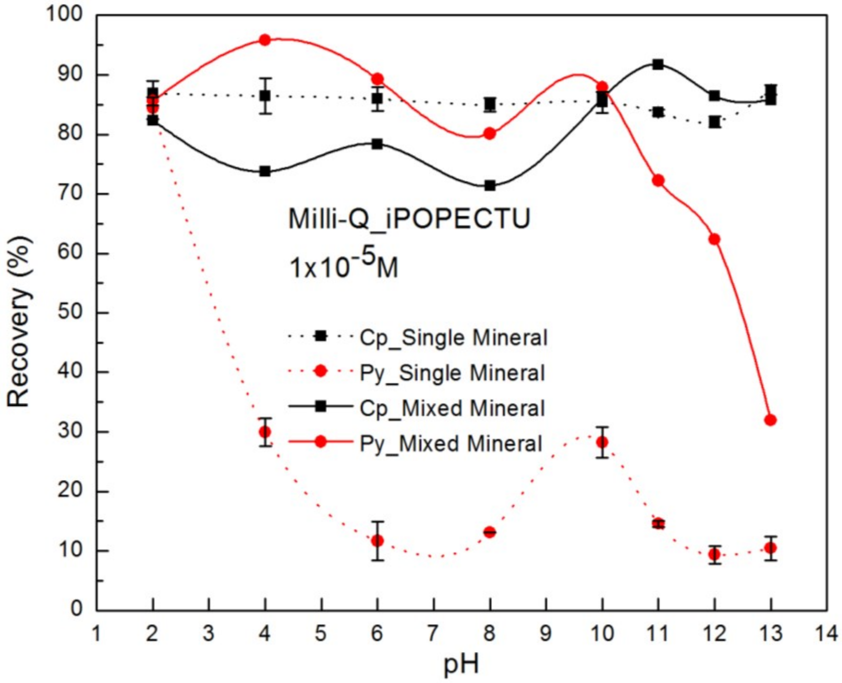

Figure 3.11 Flotation response of chalcopyrite and pyrite mixture (weight ratio 1:1) as a function of pH in Milli-Q water with 1×10^{-5} M iPOPECTU (dot curve are the flotation results of single mineral flotation)

Figure 3.12, Figure 3.13 and Figure 3.14 show the flotation behavior of chalcopyrite and pyrite mixed mineral in NaCl solution with a 1:1 ratio. Figure 3.12 shows that the flotation recovery of chalcopyrite and pyrite are almost the same around 90 % in all the pH range in the presence of PAX, which means poor selectivity. The only possible condition to separate chalcopyrite from pyrite is at pH 13. Figure 3.13 shows that at pH higher than 12, the flotation recovery of chalcopyrite stay very high around 90 %, but the flotation recovery of pyrite is greatly dropped to 20 %, which is very good for the separation of chalcopyrite from pyrite in the presence of thionocarbamate. Figure 3.14 shows that the flotation recovery of chalcopyrite and pyrite is close to each other in the entire pH range even at high alkaline condition, which means poor selectivity in the presence of iPOPECTU in NaCl solution.

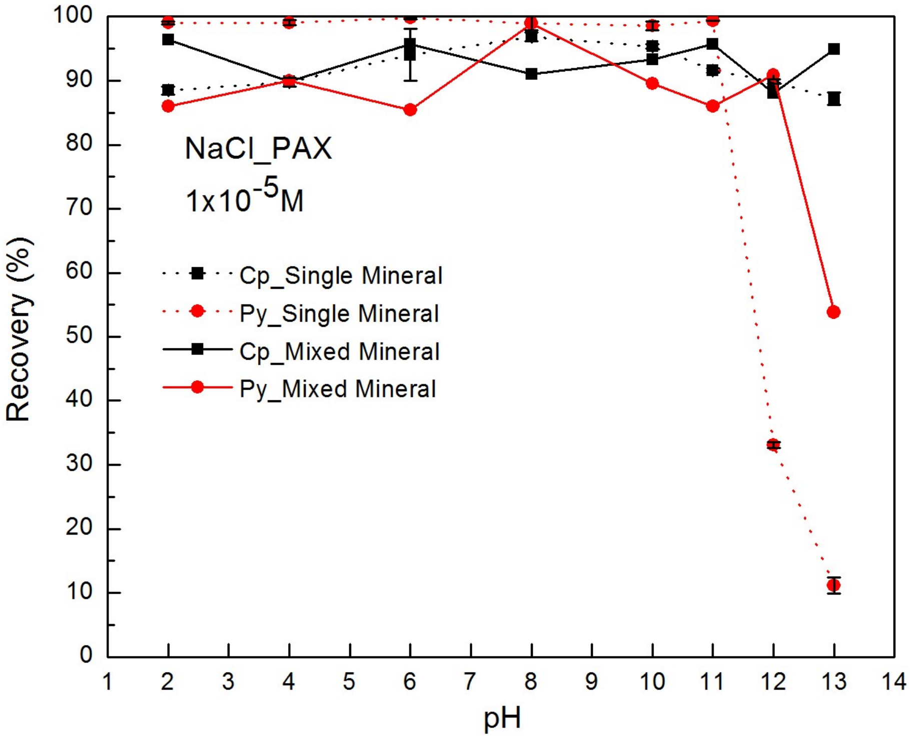

Figure 3.12 Flotation response of chalcopyrite and pyrite mixture (weight ratio 1:1) as a function of pH in NaCl solution with 1×10^{-5} M PAX (dot curve are the flotation results of single mineral flotation)

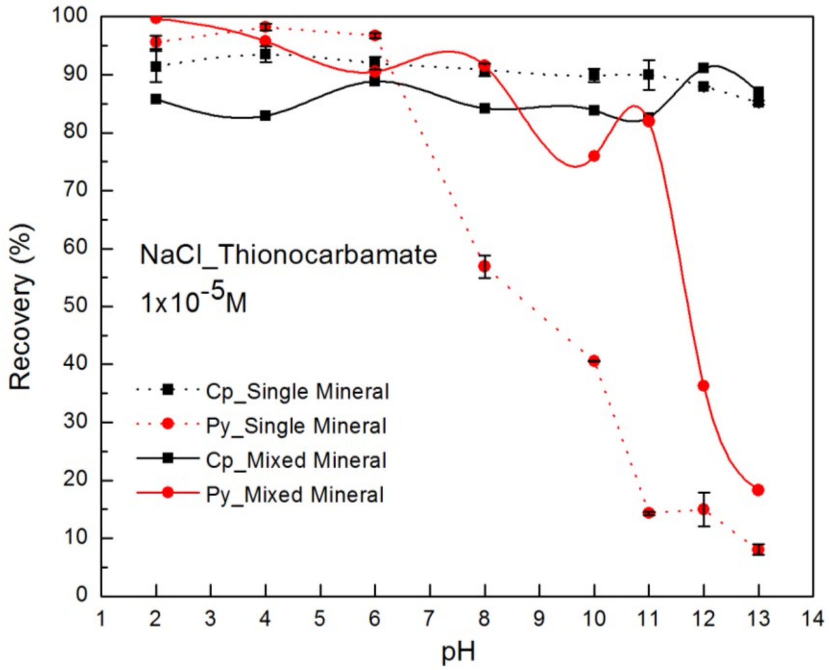

Figure 3.13 Flotation response of chalcopyrite and pyrite mixture (weight ratio 1:1) as a function of pH in NaCl solution with 1×10^{-5} M thionocarbamate (dot curve are the flotation results of single mineral flotation)

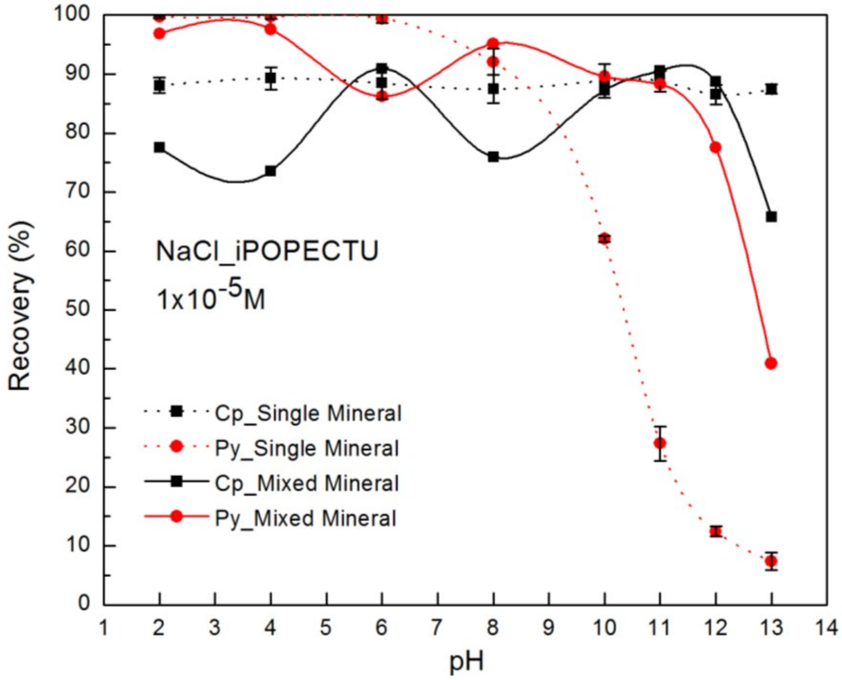

Figure 3.14 Flotation response of chalcopyrite and pyrite mixture (weight

ratio 1:1) as a function of pH in NaCl solution with 1×10^{-5} M iPOPECTU (dot curve are the flotation results of single mineral flotation)

Figure 3.15, Figure 3.16 and Figure 3.17 show the flotation behaviors of chalcopyrite and pyrite mixed mineral in sea water with a 1:1 ratio. It shows that the flotation recovery of chalcopyrite and pyrite are very high in the presence of collector at pH below 8. The only condition which is possible to separate chalcopyrite from pyrite is the small range between pH 9 and pH 11.

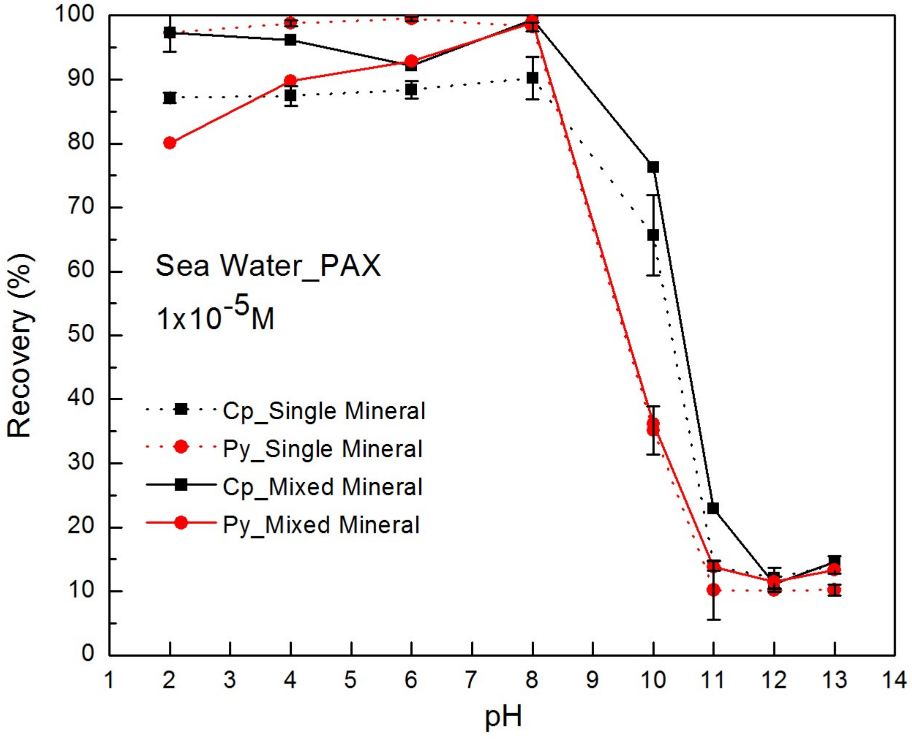

Figure 3.15 Flotation response of chalcopyrite and pyrite mixture (weight ratio 1:1) as a function of pH in sea water with 1×10^{-5} M PAX (dot curve are the flotation results of single mineral flotation)

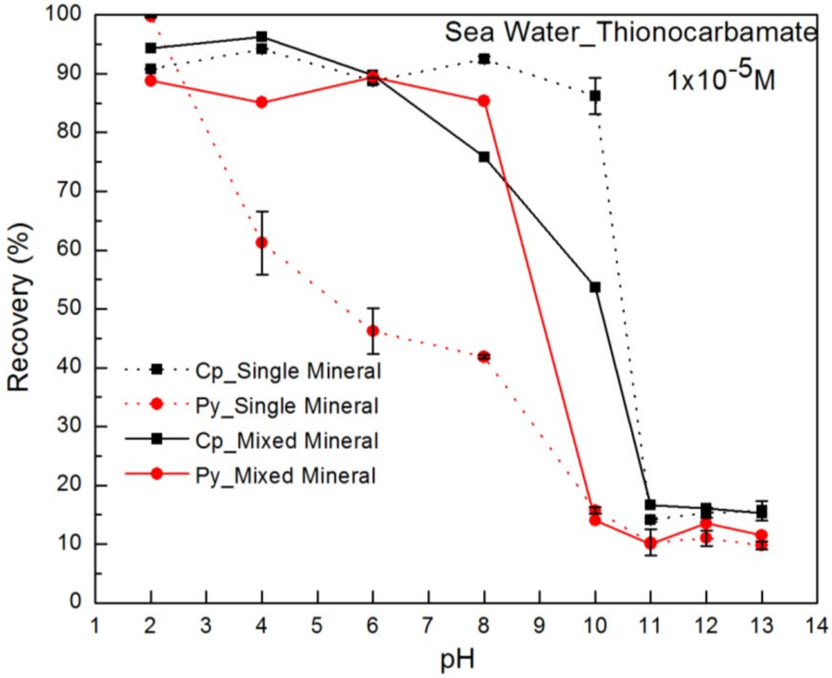

Figure 3.16 Flotation response of chalcopyrite and pyrite mixture (weight ratio 1:1) as a function of pH in sea water with 1×10^{-5} M thionocarbamate (dot curve are the flotation results of single mineral flotation)

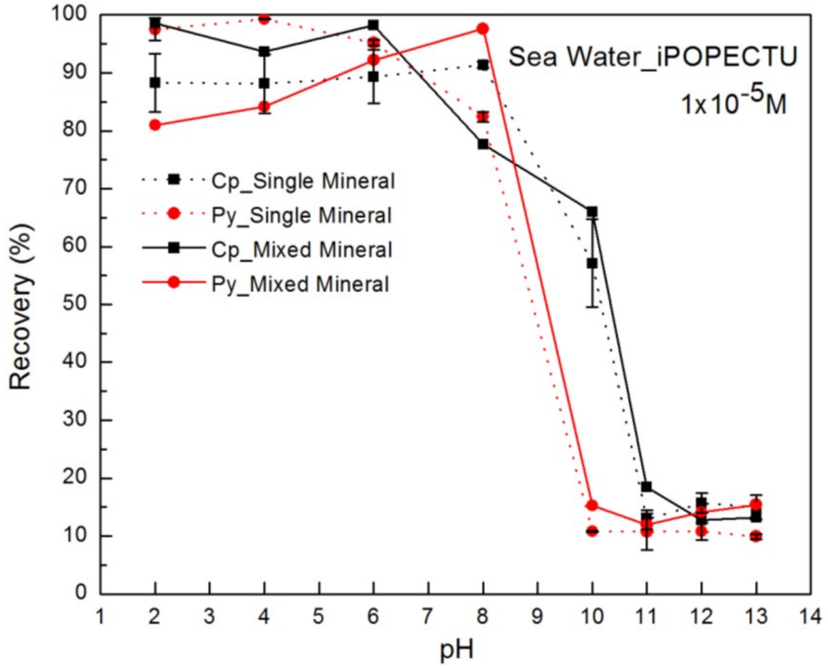

Figure 3.17 Flotation response of chalcopyrite and pyrite mixture (weight

ratio 1:1) as a function of pH in sea water with 1×10^{-5} M iPOPECTU (dot curve are the flotation results of single mineral flotation)

3.3.3 Contact angle measurements

Figure 3.2 shows that the flotation recovery of pyrite in different process water is quite different without the addition of collectors, which is highest in NaCl solution and lowest in Milli-Q water. Contact angle measurements were conducted to explore the surface wettability. Figure 3.18 shows that the contact angle of pyrite is the highest in NaCl solution and is the lowest in Milli-Q water. The contact angle of pyrite in sea water is in between. The contact angle at pH 6 and pH 8 is the lowest in Milli-Q water, which is consistent with the flotation behavior showed in Figure 3.2. By comparing the flotation results shown in Figure 3.2 and surface wettability results shown in Figure 3.18, the surface wettability results are consistent with the flotation results.

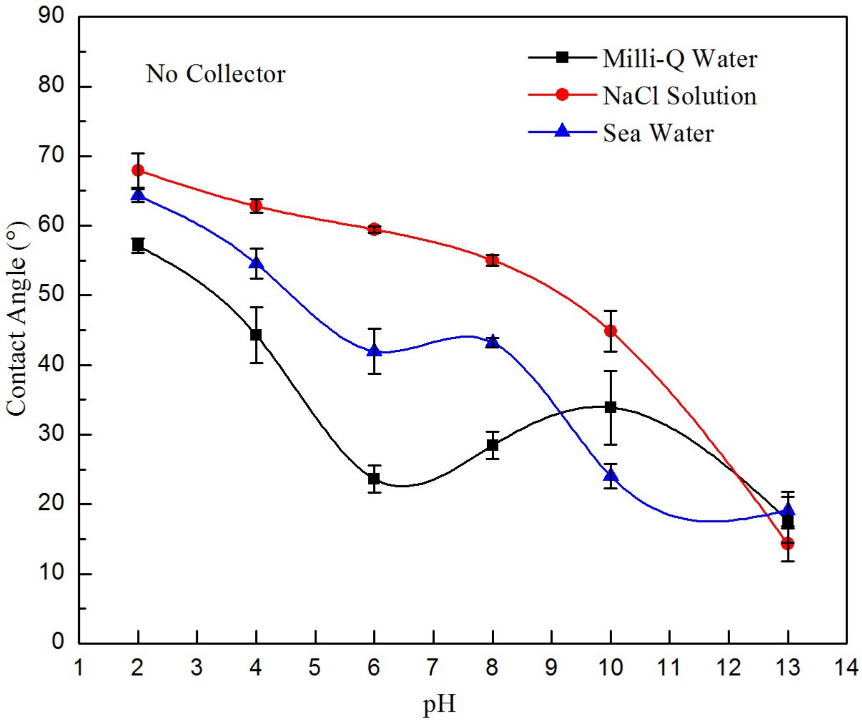

Figure 3.18 Contact angle of pyrite in different solutions at different pHs without the presence of collector

Figure 3.6 shows that the flotation recovery of pyrite in Milli-Q water is quite different with the addition of different collectors, which is highest in PAX and lowest in thionocarbamate and iPOPECTU. Contact angle measurements were conducted to explore the surface hydrophobicity of pyrite in Milli-Q water conditioning with different collectors. Figure 3.19 shows that the contact angle of pyrite is the highest with the addition of PAX and is the lowest with the addition of thionocarbamate, which is slightly higher than the one without the addition of any collectors. The contact angle of pyrite with the addition of iPOPECTU is between that with the addition of PAX and thionocarbamate. The contact angle results show that the affinity of thionocarbamate on the surface of pyrite is the lowest and PAX is the highest among the three collectors in Milli-Q water. The contact angle at pH 6 and pH 8 is the lowest in Milli-Q water, which is consistent with the flotation behavior showed in Figure 3.6. The contact angle results are consistent with the flotation performance of pyrite with the addition of different collectors in Milli-Q water.

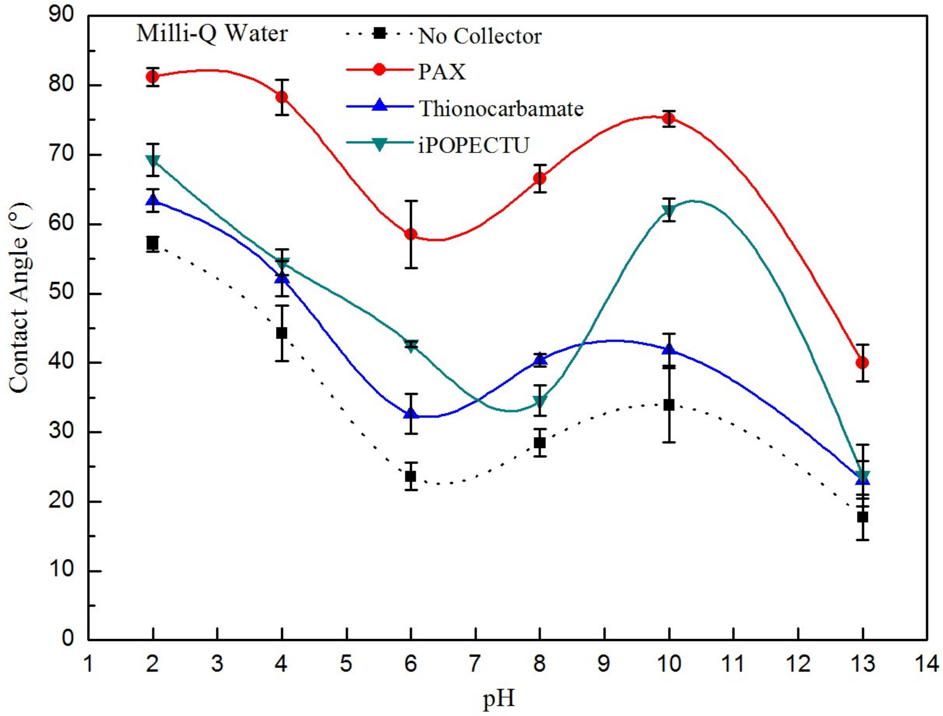

Figure 3.19 Contact angle of pyrite in Milli-Q water at different pHs with the presence of different collector

Figure 3.7 shows that the flotation recovery of pyrite in NaCl solution is greatly improved compared with that in Milli-Q water. The addition of electrolytes makes the surface of pyrite more hydrophobic at near neutral pH. Figure 3.20 also shows that the contact angle of pyrite is the highest with the addition of PAX and is the lowest with the addition of thionocarbamate even though the contact angle is very high. The contact angle of pyrite with the addition of iPOPECTU is between the addition of PAX and thionocarbamate. The contact angle results show that the affinity of thionocarbamate on pyrite surface is the lowest among the three collectors in NaCl solution and PAX is the highest. The contact angle results are consistent with the flotation performance of pyrite with the addition of different collectors in NaCl solution.

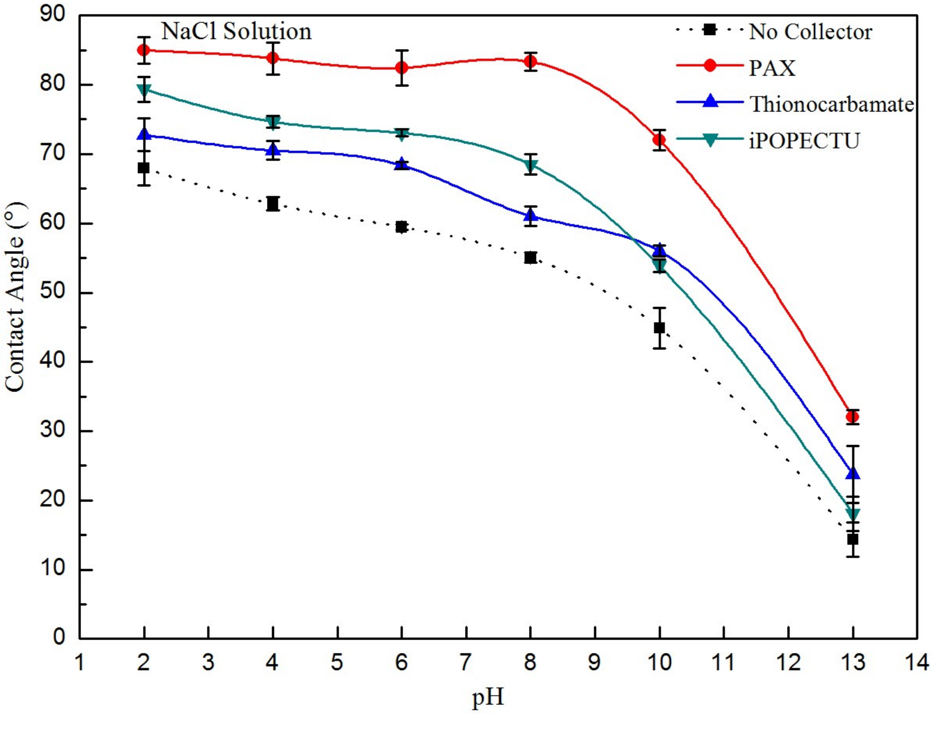

Figure 3.20 Contact angle of pyrite in NaCl solution at different pHs with the presence of different collector

Figure 3.8 shows that the flotation recovery of pyrite in sea water is greatly improved compared with that in Milli-Q water, especially with PAX and iPOPECTU. Figure 3.21 shows that the contact angle of pyrite is the highest with the addition of PAX and the lowest with the addition of thionocarbamate, which are consistent with the flotation results. Besides, the contact angle of pyrite with the addition of thionocarbamate is almost the same with that without any addition of collector in the whole pH range. This means that thionocarbamate almost can't react or adsorb on the surface of pyrite and have the lowest affinity with pyrite in sea water.

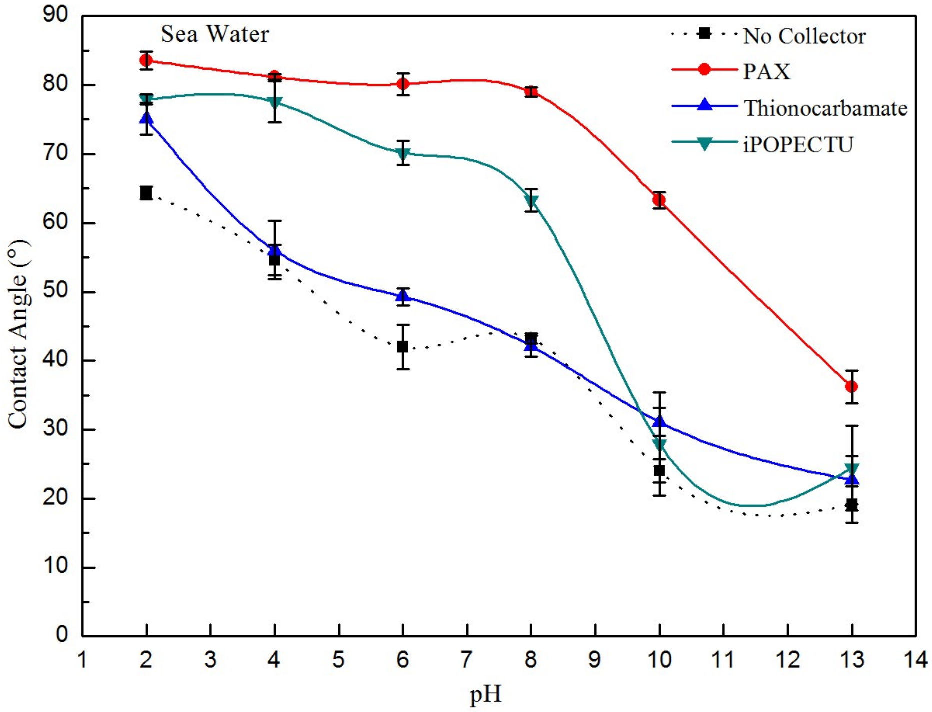

Figure 3.21 Contact angle of pyrite in sea water at different pHs with the presence of different collector

A low floatation recovery is observed in Figure 3.6 at near neutral pH at low xanthate concentration in Milli-Q water. This is consistent with the results reported in literature (Fuerstenau, Kuhn, & Elgillani, 1968). However, as we can see from the comparison of Figure 3.6, Figure 3.7 and Figure 3.8, a higher recovery of pyrite is observed in NaCl solution and sea water over a wide range of pH. Figure 3.19 shows that the contact angle dropped to a minimum at pH 6 and kept dropping from pH 10 to a second minimum at pH 13 in Milli-Q water with the addition of PAX. From Figure 3.20 and Figure 3.21, improved hydrophobicity of pyrite was observed in NaCl solution and sea water at near neutral pH, which corresponds to the flotation results showed in Figure 3.6. The addition of electrolytes makes the surface of pyrite more hydrophobic at near neutral pH. The decreased contact angle at high pH is probably because xanthate oxidation to dixanthogen does not occur on pyrite and the surface of pyrite consists of ferric hydroxide (Fuerstenau, Chander, & Woods, 2007). Barsky relationship also implies competition of collector anions and hydroxyl anions for the mineral surface (Gaudin, 1957; Wark, 1938; Wark & Cox, 1934), which may also cause that the flotation recovery drops at high pH.

3.4 References

Bushell, C. H. G. (1962). Copper activation of pyrite. *Can Min Metall Bull*, *55*(601), 314-318.

Bulut, G., & Atak, S. (2002). Role of dixanthogen on pyrite flotation: solubility, adsorption studies and Eh, FTIR measurements. *Minerals & metallurgical* *processing*, *19*(2), 81-86.

Cheng, X., & IWASAKI, I. (1992). Pulp potential and its implications to sulfide flotation. *Mineral Processing and Extractive Metullargy Review*, *11*(4), 187-210.

Castro, S., & Laskowski, J. S. (2011). Froth flotation in saline water. *Kona, 29*(4), 2011.

Castro, S., Rioseco, P., & Laskowski, J. S. (2012). Depression of molybdenite in seawater. In *Proc. 26th Int. Mineral Processing Congress, New Delhi* (pp. 739-752).

Ekmekçi, Z., & Demirel, H. (1997). Effects of galvanic interaction on collectorless flotation behaviour of chalcopyrite and pyrite. *International journal of mineral processing*, *52*(1), 31-48.

Fairthorne, G., Fornasiero, D., & Ralston, J. (1997). Interaction of thionocarbamate and thiourea collectors with sulphide minerals: a flotation and adsorption study. *International journal of mineral processing*, *50*(4), 227-242.

Fuerstenau, M. C., Chander, S., & Woods, R. (2007). Sulfide mineral flotation. *Froth flotation a century of Innovation. Society for Mining, Metallurgy, and Exploration, Inc. (SME), Littleton, Colorado*, 425-464.

Fuerstenau, M. C., Kuhn, M. C., & Elgillani, D. A. (1968). The role of dixanthogen in xanthate flotation of pyrite. *Trans. AIME*, *241*, 148-156.

Fuerstenau, M. C., & Palmer, B. R. (1976). Anionic flotation of oxides and silicates. *Flotation--A. M. Gaudin Memorial*.

Gaudin, A. M. (1957). Flotation. *McGraw Hill Book Co., Inc, New York (1957).*

Leppinen, J. O., Basilio, C. I., & Yoon, R. H. (1989). In-situ FTIR study of ethyl xanthate adsorption on sulfide minerals under conditions of controlled potential. *International Journal of Mineral Processing*, *26*(3), 259-274.

Laajalehto, K., Leppinen, J., Kartio, I., & Laiho, T. (1999). XPS and FTIR study of the influence of electrode potential on activation of pyrite by copper or lead.*Colloids and Surfaces A: Physicochemical and Engineering Aspects*, *154*(1), 193-199.

Lehmann, M. N., Stichnoth, M., Walton, D., & Bailey, S. I. (2000). The effect of chloride ions on the ambient electrochemistry of pyrite oxidation in acid media. *Journal of the Electrochemical Society*, *147*(9), 3263-3271.

Liu, G., Qiu, Z., Wang, J., Liu, Q., Xiao, J., Zeng, H., Zhong, H., & Xu, Z. (2015). Study of N-isopropoxypropyl-N'-ethoxycarbonyl thiourea adsorption on chalcopyrite using in situ SECM, ToF-SIMS and XPS. *Journal of colloid and interface science*, *437*, 42-49.

Liu, Q., & Zhang, Y. (2000). Effect of calcium ions and citric acid on the flotation separation of chalcopyrite from galena using dextrin. *Minerals*

Engineering, *13*(13), 1405-1416.

Majima, H. (1969). How oxidation affects selective flotation of complex sulphide ores. *Canadian Metallurgical Quarterly*, *8*(3), 269-273.

Mehta, A. P., & Murr, L. E. (1983). Fundamental studies of the contribution of galvanic interaction to acid-bacterial leaching of mixed metal sulfides.*Hydrometallurgy*, *9*(3), 235-256.

Mielczarski, J. A., & Yoon, R. H. (1989). Spectroscopic studies of the structure of the adsorption layer of thionocarbamate: I. On copper and activated zinc sulfide. *Journal of colloid and interface science*, *131*(2), 423-432.

Nagaraj, D. R., Basilio, C., & Yoon, R. H. (1989). The chemistry and structure-activity relationships for new sulphide collectors. In *Processing of Complex Ores: Proceedings of the International Symposium on Processing of Complex Ores, Halifax, August 20-24, 1989* (p. 157). Elsevier.

Nakazawa, H., & Iwasaki, I. (1985). Effect of pyrite-pyrrhotite contact on their floatabilities. *Miner. Metall. Process.*, *2*(4), 206-220.

Rao, M. Y., & Natarajan, K. A. (1989). Effect of electrochemical interactions among sulfide minerals and grinding medium on chalcopyrite flotation. *Minerals and Metallurgical Processing*, *6*(3), 146-151.

Rao, M. Y., & Natarajan, K. A. (1989). Electrochemical effects of mineral-mineral interactions on the flotation of chalcopyrite and sphalerite. *International Journal of Mineral Processing*, *27*(3), 279-293.

Valdivieso, A. L., López, A. S., & Song, S. (2005). On the cathodic reaction coupled with the oxidation of xanthates at the pyrite/aqueous solution interface. *International Journal of Mineral Processing*, *77*(3), 154-164.

Wark, I. W. (1938). Principles of flotation. *Australasian Institute of Mining and Metallurgy*, (a), 187.

Wark, I. W., & Cox, A. B. (1934). Principles of flotation, II—an experimental study of the influence of cyanide, alkalis and copper sulfate on the effect of potassium ethyl xanthate at mineral surfaces. *Transactions AIME*, *112*, 245-266.

Wang, X. H., & Forssberg, K. E. (1991). Mechanisms of pyrite flotation with xanthates. *International journal of mineral processing*, *33*(1), 275-290.

Weisener, C., & Gerson, A. (2000). An investigation of the Cu (II) adsorption mechanism on pyrite by ARXPS and SIMS. *Minerals Engineering*, *13*(13), 1329-1340.

Chapter 4 The Effect of Slime Coating on Surface Properties of Chalcopyrite and Pyrite in Sea Water under Alkaline Conditions

4.1 Introduction

The problem of sea water is its complex chemistry because it contains not only simple electrolytes like NaCl but also some secondary ions like magnesium and calcium with potential depressing effect to minerals, which may interfere with the flotation process. As a result, the flotation behaviour of chalcopyrite and pyrite in sea water is quite different from that in Milli-Q water and NaCl solutions, especially under alkaline conditions. The salinity of sea water is typically between 31 ‰ and 38 ‰, and the concentration of NaCl is about 0.4 – 0.6 M, with important secondary ions such as sulfate ions (0.028 mol/L), magnesium ions (0.053 mol/L), calcium ions (0.010 mol/L), bicarbonate ions (0.002 mol/L), etc, which also have great influence on the flotation process. They may influence the surface chemistry and the floatability of some minerals. Calcium and magnesium ions may form colloidal hydroxides, carbonates and sulfates in alkaline solutions at pH>10 forming a slime coating on the mineral surfaces, which is detrimental to the flotation process. The main precipitation reactions between sea water and lime under flotation conditions are: (Castro, 2012)

$Ca(OH)_2 + Mg^{2+} = Mg(OH)_2 + Ca^{2+}$

$Ca^{2+} + 2OH^- = Ca(OH)_2$

$Ca(OH)_2 + SO_4^{2-} + 2H_20 = CaSO_4 \cdot 2H_20 + 2OH^-$

$Mg(OH)_2 + SO_4^{2-} = MgSO_4 + 2OH^-$

$Ca(OH)_2 + CO_3^{2-} = CaCO_3 + 2OH^-$

$Mg(OH)_2 + CO_3^{2-} = MgCO_3 + 2OH^-$

Previous studies have suggested an electrostatic mechanism for slime-particle interaction (Learmont & Iwasaki, 1984; Gaudin et al., 1960; Fuerstenau et al., 1958; Parsonage, 1985). The slime particles may depress the flotation of sulfide mineral in two ways. First, they can form slime coatings on the surface of sulfide mineral, which reduce the adsorption of collector on mineral surface and reduce the overall wettability of mineral. As a result, both the flotation recovery and flotation rate will be greatly decreased. Secondly, the valuable mineral which is recovered from pulp will have slimes particles on its surface and will greatly dilute the valuable metal concentrates (Pietrobon et al., 1997).

4.2 Experimental methods

4.2.1 Scanning electron microscope measurements

The scanning electron microscopy (SEM) measurement was carried out on a VEGA3 TESCAN scanning electron microscope integrated with an EDX microanalyser. The high vacuum mode (SE) was chosen for the SEM measurements. In EDX measurements, a high energy primary electron beam was utilized to irradiate the sample surface. The test sample was prepared by adding 1.5 g chalcopyrite or pyrite in 150 ml sea water with 1×10^{-5} M PAX at pH 12. The suspension was conditioned in a beaker for five minutes, and the minerals were filtered, washed with sufficient distilled water and dried in a vacuum oven before SEM analysis.

4.2.2 ToF-SIMS measurements

ToF-SIMS images and spectrums were obtained from a ToF-SIMS IV spectrometer (ION-TOF GmbH). For spectra acquisition, a high energy beam of Bi^+ ions (25 kV) was focused on the sample surface. The samples for slime coating study were prepared by collecting the concentrate and tailing of chalcopyrite or pyrite particles after the flotation in sea water at pH 12. The samples were washed by sufficient Milli-Q water and vacuum dried at room temperature.

4.2.3 Zeta potential distribution measurements

The zeta-potential of particles were measured using the Zetasizer (Nano ZS, Malvern Instruments, UK). For the zeta potential distribution measurements of chalcopyrite and pyrite, the mineral particles with the size fraction less than 38 μm were hand ground in an agate mortar. 2 mg mineral particles were dispersed into 400 mL supporting electrolyte solution (1 mM NaCl). The suspensions of precipitates were prepared by adjusting the pH of sea water to 12 and diluting the suspension to 1 mM NaCl solution to obtain the same particle concentration with mineral particles. The pH of each solution was adjusted to 12 and sonicated for 10 min to disperse the particles evenly. The different collectors were added to the suspension with the concentration of 1×10^{-5} M. The mineral particles were conditioned in collector solutions for five minutes before each measurement. The prepared mineral suspensions and precipitates were mixed with a 1:1 mass ratio to make mixture suspensions. The mixture suspensions were then shook for five minutes prior to measurement.

4.3 Results and discussion

4.3.1 SEM measurements

Figure 4.1 shows the SEM images of chalcopyrite conditioned in sea water and Milli-Q water respectively. Figure 4.1 (b) shows that the surface of chalcopyrite conditioned in sea water has a large amount of small particles coated, while Figure 4.1 (a) shows that the surface of chalcopyrite conditioned in Milli-Q water is quite smooth without any particles on it. The

SEM images indicate that precipitates may form on the surface of chalcopyrite when conditioning in sea water, but not in Milli-Q water.

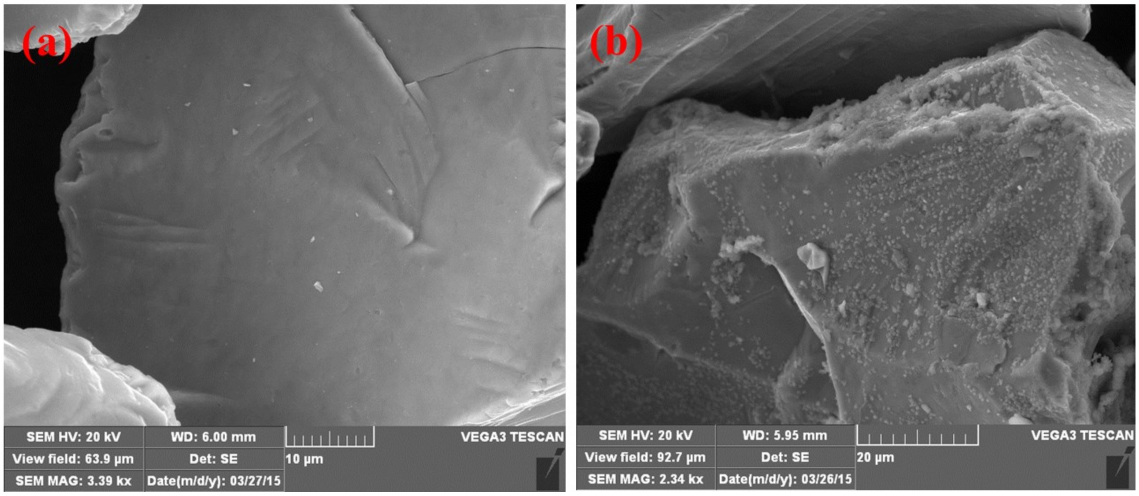

Figure 4.1 SEM images of (a) chalcopyrite conditioning in Milli-Q water, (b) chalcopyrite conditioning in sea water at pH 12 with 1×10^{-5} M PAX

Figure 4.2 shows the SEM images of pyrite conditioning in sea water and Milli-Q water respectively. Figure 4.2 (b) shows that the surface of pyrite have large amount of small particles coated, while Figure 4.2 (a) shows that the surface is quite smooth without any particles on the surface. The SEM images indicate that precipitates may form on the surface of pyrite when the sample was conditioned in sea water, but no precipitate formed when sample was conditioned in Milli-Q water.

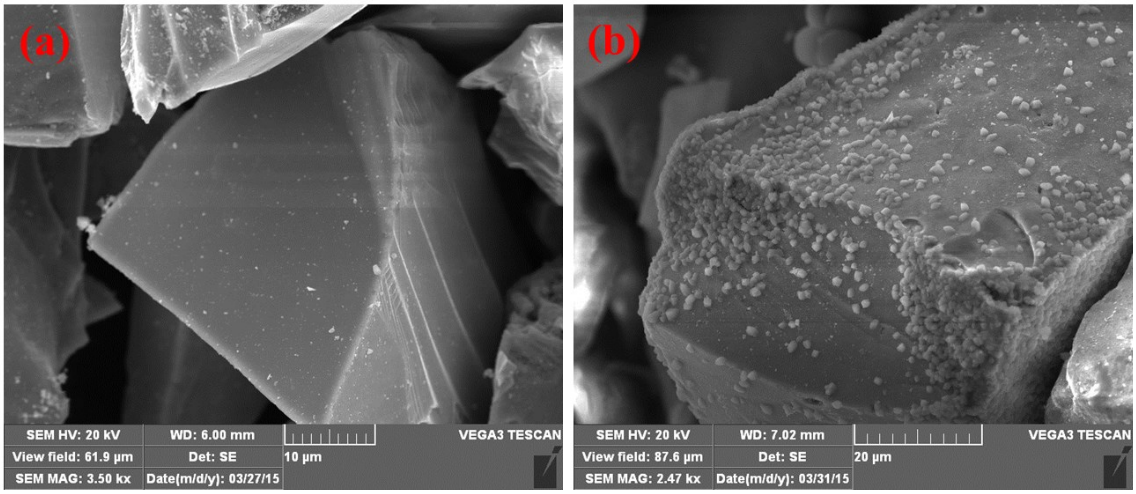

Figure 4.2 SEM images of (a) pyrite conditioning in Milli-Q water, (b) pyrite conditioning in sea water at pH 12 with 1×10^{-5} M PAX

Figure 4.3 shows the distributions of different elements on the surface of chalcopyrite conditioning in sea water at pH 12. The distributions of magnesium and calcium are almost the same as the distributions of copper and sulfur, which indicates that the magnesium and calcium precipitate is homogeneously distributed on the surface of chalcopyrite.

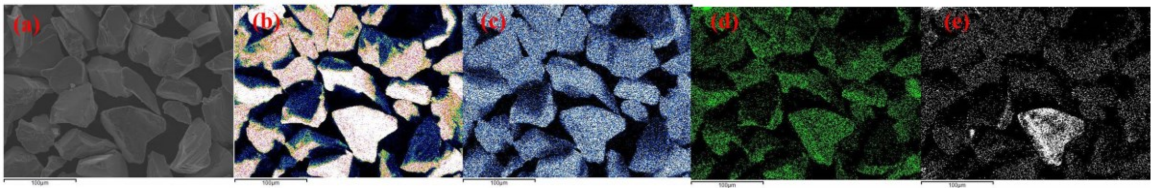

Figure 4.3 EDX mapping images of (a) SEM image, (b) S distribution, (c) Cu element distribution, (d) Mg element distribution, (e) Ca element distribution, of chalcopyrite conditioning in sea water

Figure 4.4 shows the distributions of different elements on the surface of pyrite conditioning in sea water at pH 12. The distributions of magnesium and calcium are almost the same as the distributions of iron and sulfur, which indicates that the magnesium and calcium precipitate is homogeneously distributed on the surface of pyrite.

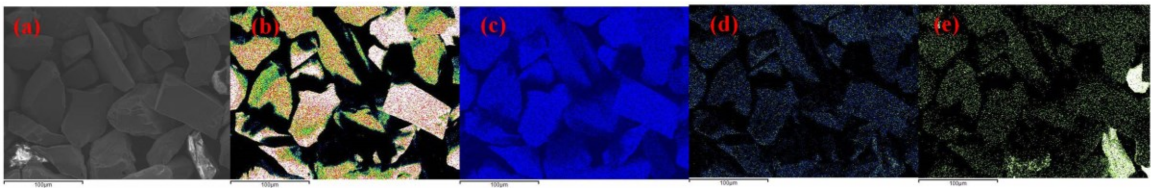

Figure 4.4 EDX mapping images of (a) SEM image, (b) S distribution, (c) Fe element distribution, (d) Mg element distribution, (e) Ca element distribution of pyrite conditioning in sea water

4.3.2 ToF-SIMS measurements

Prior to the ToF-SIMS analysis, the SIMS data were normalized by dividing the intensity of specific ion by the intensity of the total ions. Figure 4.5 shows that the concentration of Mg^+ and $MgOH^+$ is much higher in chalcopyrite tail than that in chalcopyrite concentrate, but Ca^+ and $CaOH^+$ is a little bit lower in tail than that in concentrate. Magnesium hydroxide species is believed to be the major cause of the low recovery because its molar concentration in sea water is about five times that of calcium, and magnesium hydroxide is less soluble than calcium hydroxide which is indicated by magnesium and calcium speciation diagram (Castro, Rioseco, & Laskowski, 2012; Fuerstenau & Palmer, 1976). Mg^+ intensity is the direct indication of magnesium hydroxide species. The results shown in Figure 4.5 indicate that the slime coating have detrimental effect on the flotation of chalcopyrite by comparing the concentration of magnesium hydroxide species in concentrate and tail.

Figure 4.6 shows that the concentration of Mg^+, $CaOH^+$ and $MgOH^+$ is much higher in pyrite tail than that in pyrite concentrate. This also implies that the slime coating have depressing effect on the flotation of pyrite at high pH in sea water.

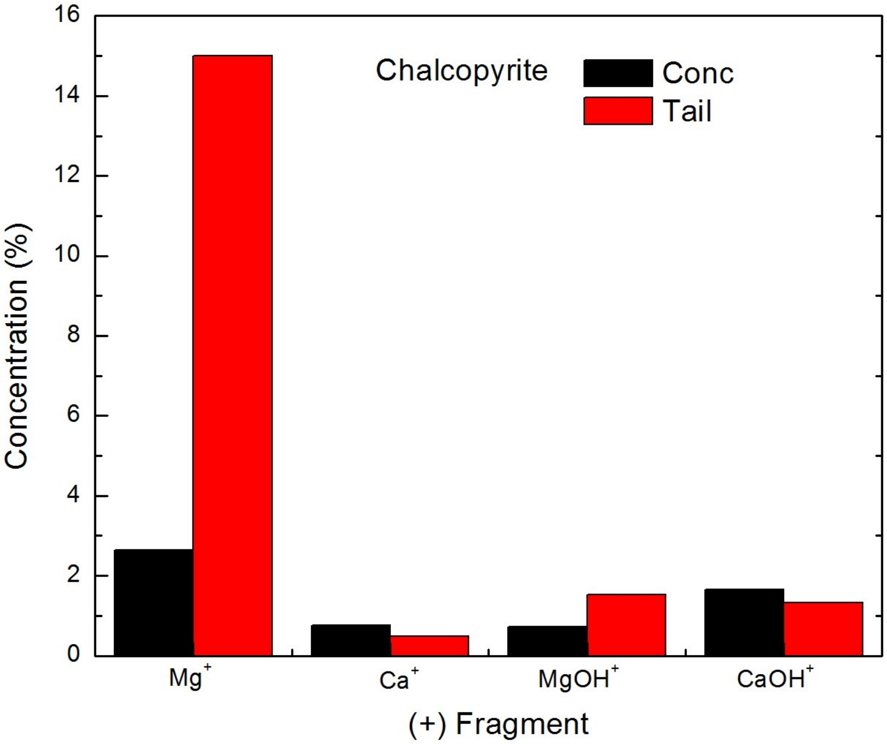

Figure 4.5 Positive ions concentration of chalcopyrite concentrate and tail samples at pH 12

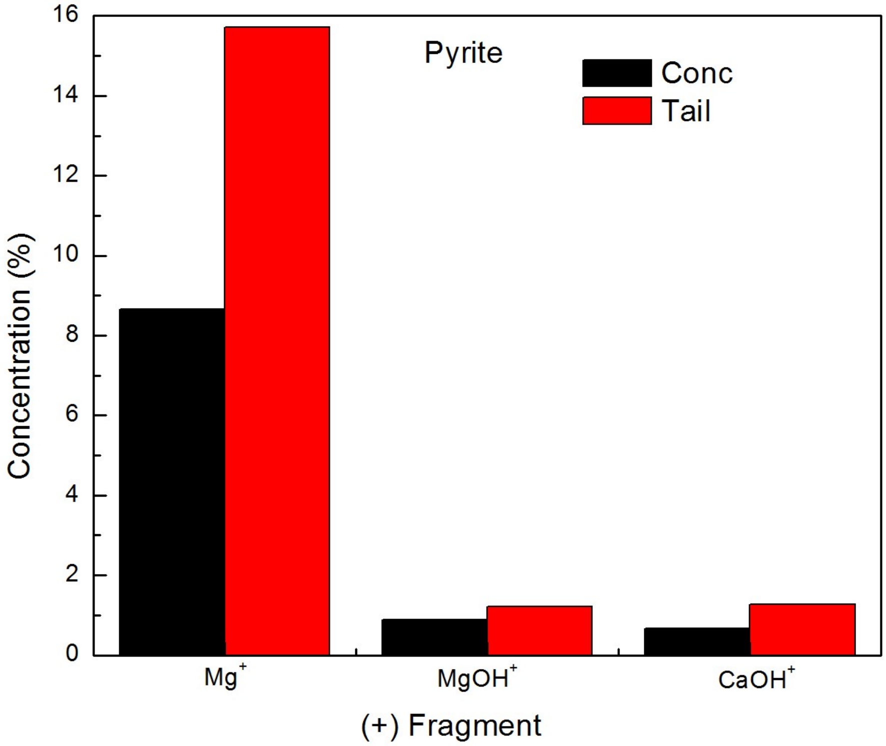

Figure 4.6 Positive ions concentration of pyrite concentrate and tail samples at pH 12

Figure 4.7 and Figure 4.8 show the ToF-SIMS images from chalcopyrite and pyrite conditioning in sea water at pH 12. As chalcopyrite and pyrite were the only sources of iron, the distribution of chalcopyrite could be visualized by iron distribution. The distribution and concentration of precipitates could be visualized by the distribution and intensity of magnesium and calcium. By comparing the images (a) and (b) in Figure 4.7 and Figure 4.8 respectively, it was obviously showing that the distributions of magnesium and calcium have the similar patterns with Fe. Besides, the intensity of magnesium and calcium species is much higher in tail than that in concentrate and magnesium has much stronger intensity than calcium, which confirmed that magnesium hydroxide is the major cause responsible for the depression of chalcopyrite and pyrite flotation in sea water at high pH.

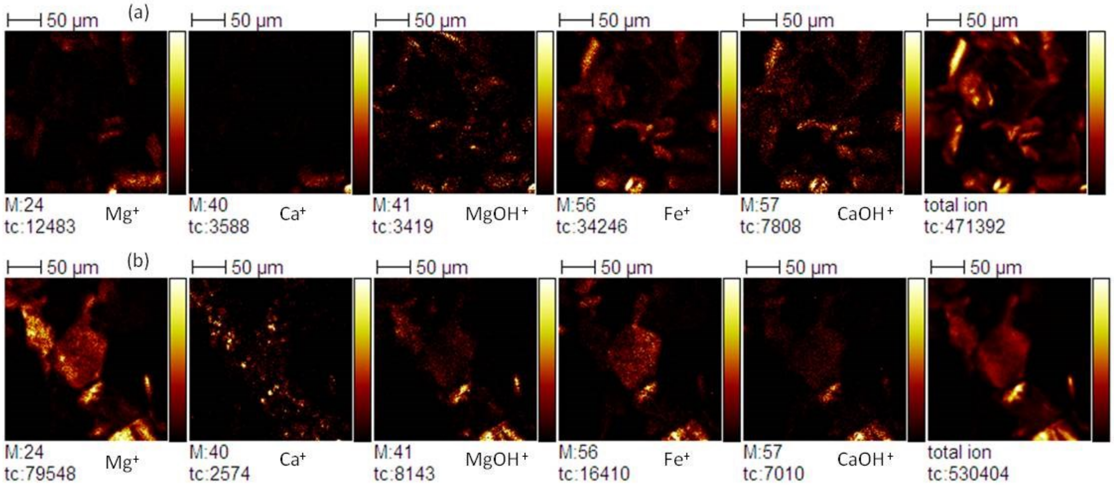

Figure 4.7 ToF-SIMS positive ions mapping of chalcopyrite (a) concentrate and (b) tail samples at pH 12

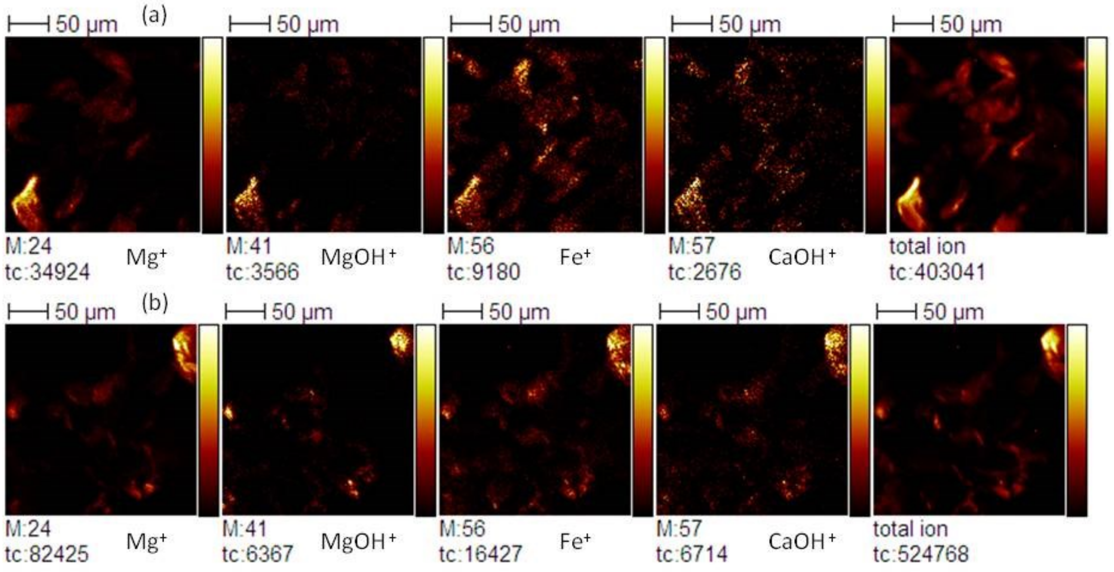

Figure 4.8 ToF-SIMS positive ions mapping of pyrite (a) concentrate and (b) tail samples at pH 12

4.3.3 Zeta potential distribution measurements

Zeta potential distribution measurements have been used to study the interaction of two different particles by comparing the zeta potential distributions of single particles and mixed particles (Liu et al., 2002; Liu et al., 2004a; 2004b; 2005; Xu et al., 2003). Figure 4.9 shows the principles by using zeta potential distribution measurements to analyze the interaction between valuable mineral and gangue mineral. ζ_V and ζ_G are the zeta potential distributions of valuable mineral and gangue mineral in suspension with the similar condition. When the valuable mineral and gangue mineral are mixed together under the same conditions, the interaction between the two mineral particles greatly affects the distribution of the mixture's zeta potential. If the valuable mineral and the gangue mineral don't interact with each other, a bimodal zeta potential distribution with two peaks centered at almost the same peak at ζ_V and ζ_G will be observed in Figure 4.9 (b). If the valuable mineral and the gangue mineral strongly interact with each other, only one distribution peak will be observed in Figure 4.9 (c) or Figure 4.9 (d). The position of the single peak will be depended by the ratio of the gangue mineral covered on the surface of valuable mineral. If there is weak attraction, a bimodal zeta potential distribution will be observed in Figure 4.9 (e).

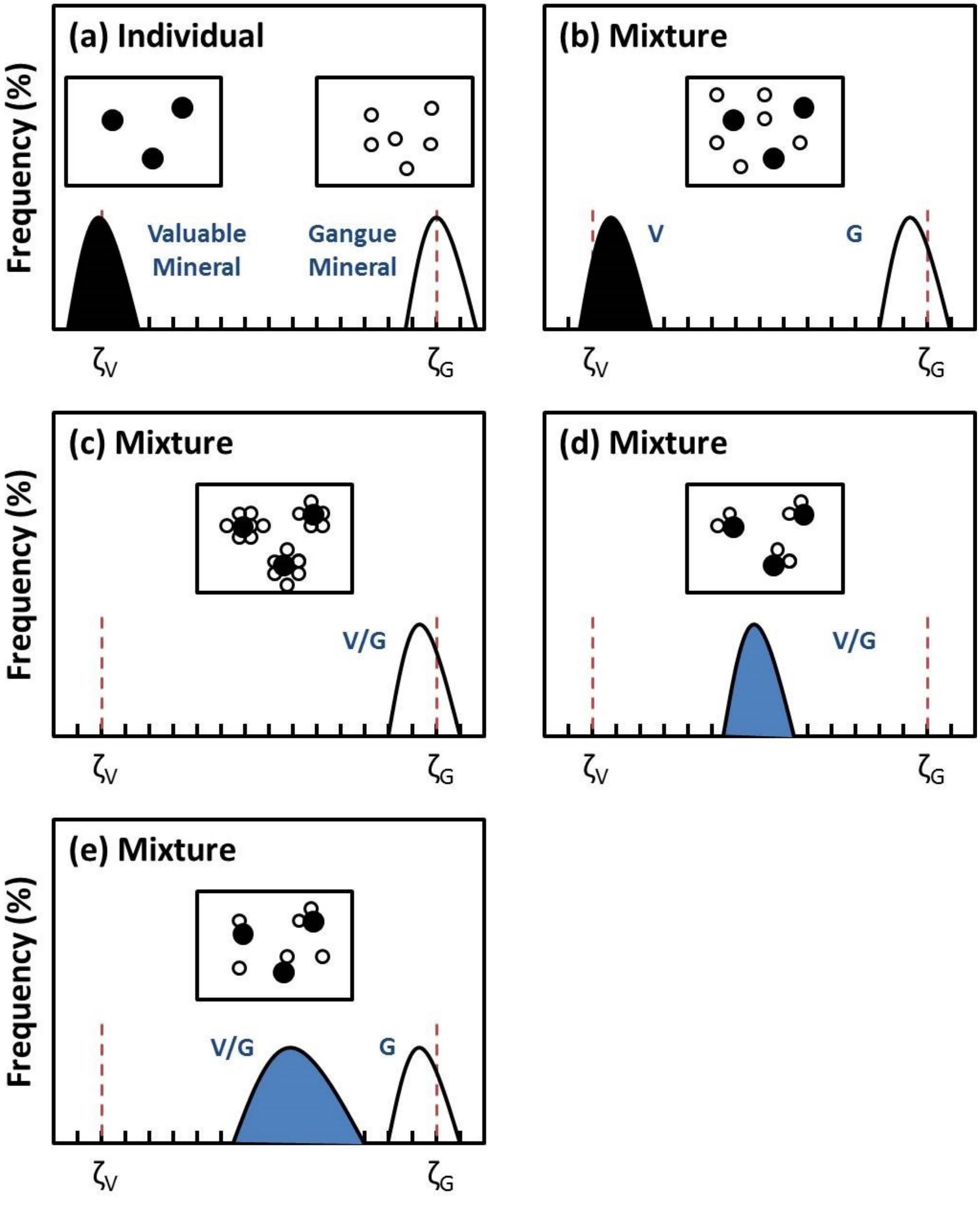

Figure 4.9 Schematics of zeta potential distributions, illustrating: (a) the individual zeta potential distributions of valuable and gangue minerals, (b) the binary mixture with no attraction, (c) strong attraction in the binary mixture (valuable mineral is fully coated with gangue mineral), (d) strong attraction in the binary mixture (valuable mineral is partially coated with

insufficient amount of gangue mineral), and (e) weak attraction in the binary mixture (valuable mineral is partially coated with some amount of gangue mineral unattached). The figures are adapted from Liu et al. (2002).

As shown from the SEM, EDX and ToF-SIMS analysis, the surface of chalcopyrite uniformly formed magnesium and calcium precipitates when the mineral was conditioned in sea water at pH 12. To determine whether slime coating really occurs between mineral particles and precipitates in water, zeta potential distribution measurements were conducted at pH 12. As shown in Figure 4.10, 4.11 and 4.12, each suspension of chalcopyrite and precipitates gives a zeta potential distribution of their own when measured individually. When mixing the two particles together under the same condition with a weight ratio of 1:1, a single zeta potential distribution peak with almost the same position with precipitates was observed in Figure 4.9 (c). The result suggests that a strong slime coating of magnesium and calcium precipitates on chalcopyrite occurred. When hydrophilic precipitates are coated on the mineral surface, it greatly decreased the probability of collector adsorption on the chalcopyrite surface and the bubble-mineral attachment.

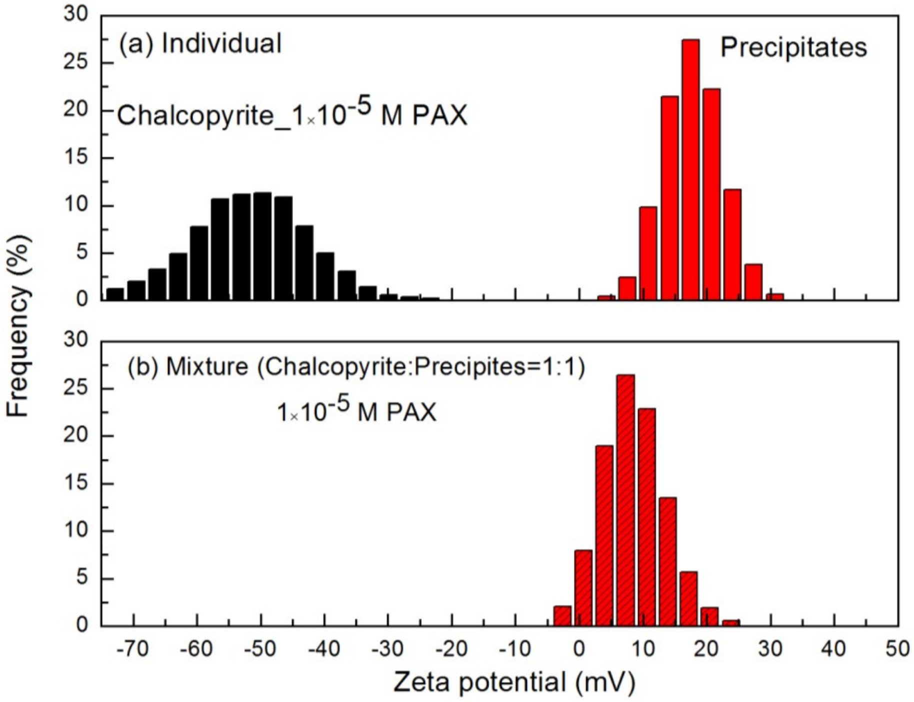

Figure 4.10 Zeta potential distributions for (a) individual chalcopyrite in PAX and precipitate suspensions, (b) chalcopyrite and precipitate 1:1 mixture in PAX at pH 12 in 1 mM NaCl solution

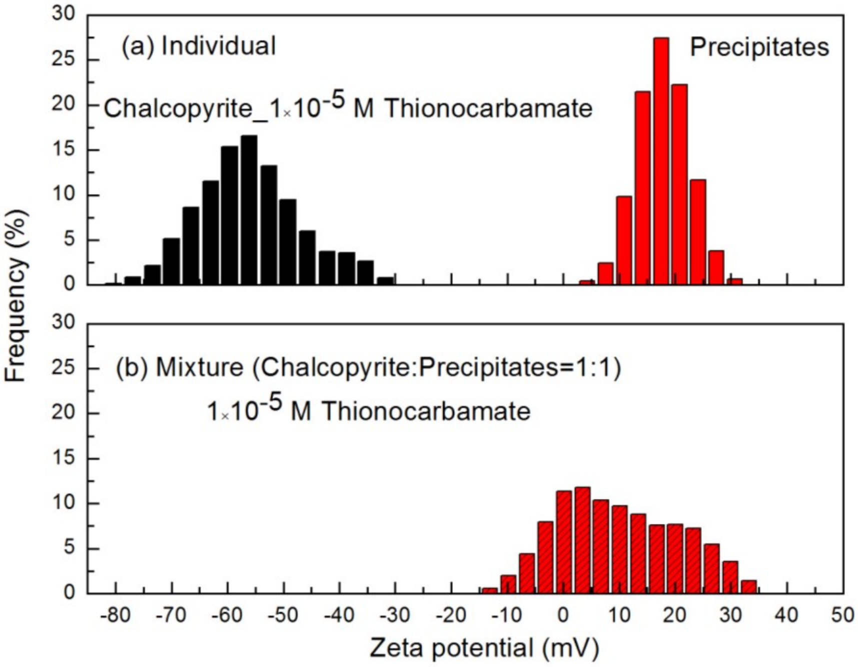

Figure 4.11 Zeta potential distributions for (a) individual chalcopyrite in

thionocarbamate and precipitate suspensions, (b) chalcopyrite and precipitate 1:1 mixture in thionocarbamate at pH 12 in 1 mM NaCl solution

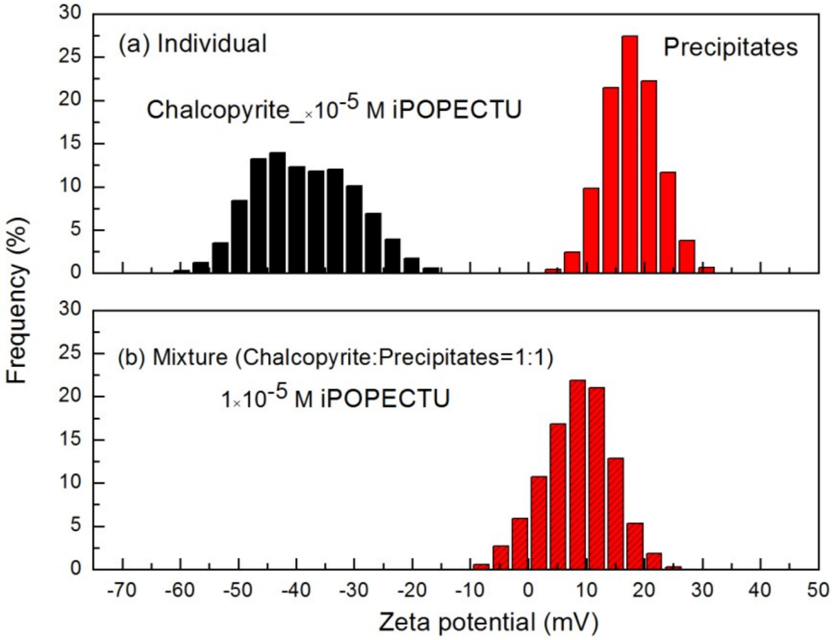

Figure 4.12 Zeta potential distributions for (a) individual chalcopyrite in iPOPECTU and precipitate suspensions, (b) chalcopyrite and precipitate 1:1 mixture in iPOPECTU at pH 12 in 1 mM NaCl solution

As shown in Figure 4.13, 4.14 and 4.15, each suspension of pyrite and precipitate gives a zeta potential distribution of their own when measured individually. When mixing the two suspensions together under the same conditions with a weight ratio of 1:1, a single zeta potential distribution peak with almost the same position with precipitate was observed in Figure 4.9 (c). The result suggests that a strong slime coating of magnesium and calcium precipitates on pyrite surface occurred. When hydrophilic precipitates coated on the mineral surface, it greatly decreased the probability of collector adsorption on the pyrite surface and the following bubble-mineral attachment. The advantage of using the zeta potential distribution measurements to confirm the slime coating is that all the tests are conducted in-situ, which avoids the complex changes of some ex-situ characterizations that occurs when minerals are dried.

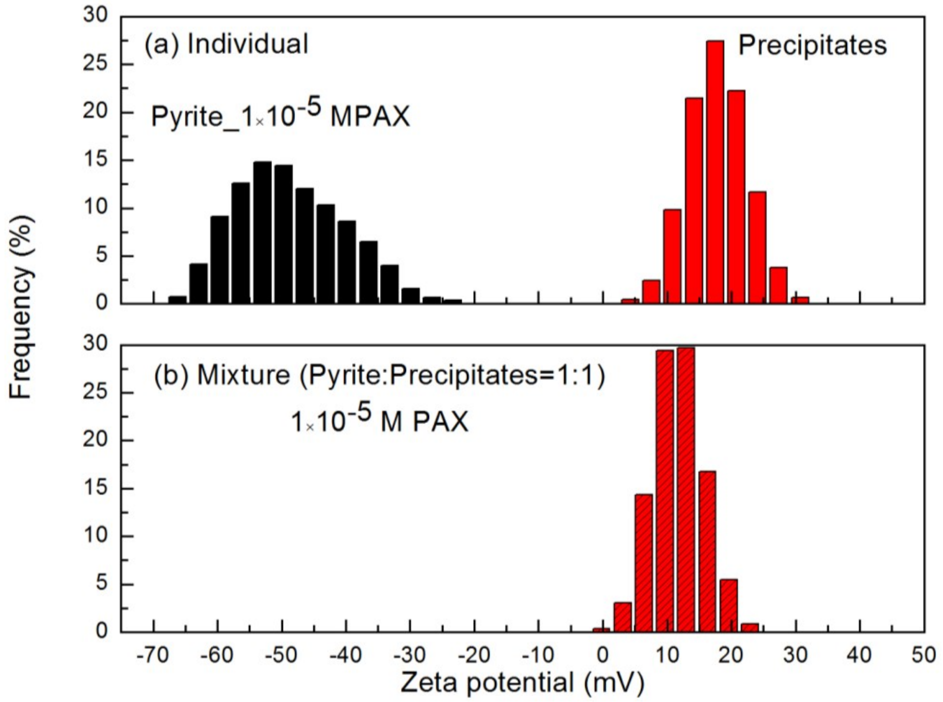

Figure 4.13 Zeta potential distributions for (a) individual pyrite in PAX and precipitate suspensions, (b) pyrite and precipitate 1:1 mixture in PAX at pH 12 in 1 mM NaCl solution

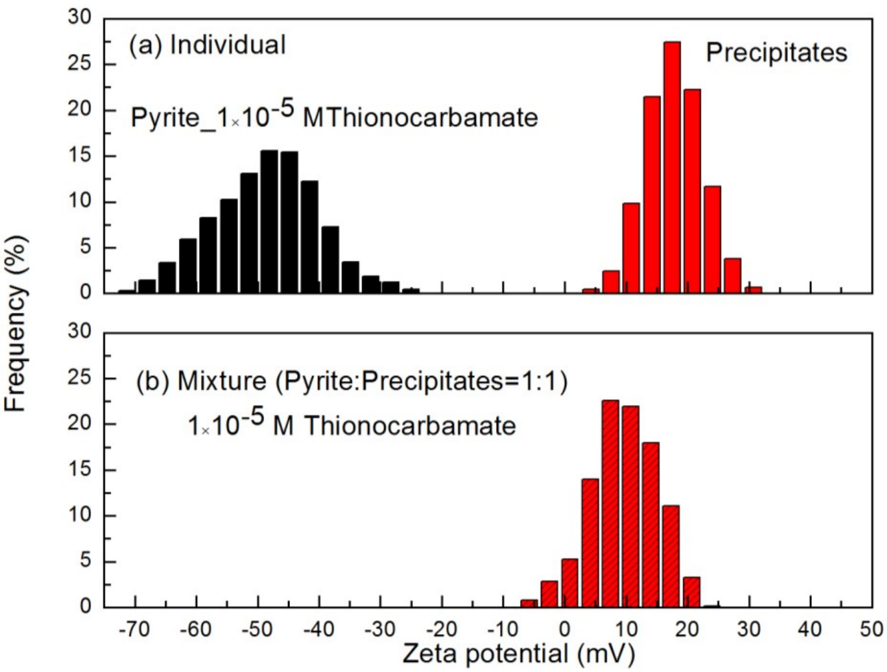

Figure 4.14 Zeta potential distributions for (a) individual pyrite in thionocarbamate and precipitate suspensions, (b) pyrite and precipitate 1:1 mixture in thionocarbamate at pH 12 in 1 mM NaCl solution

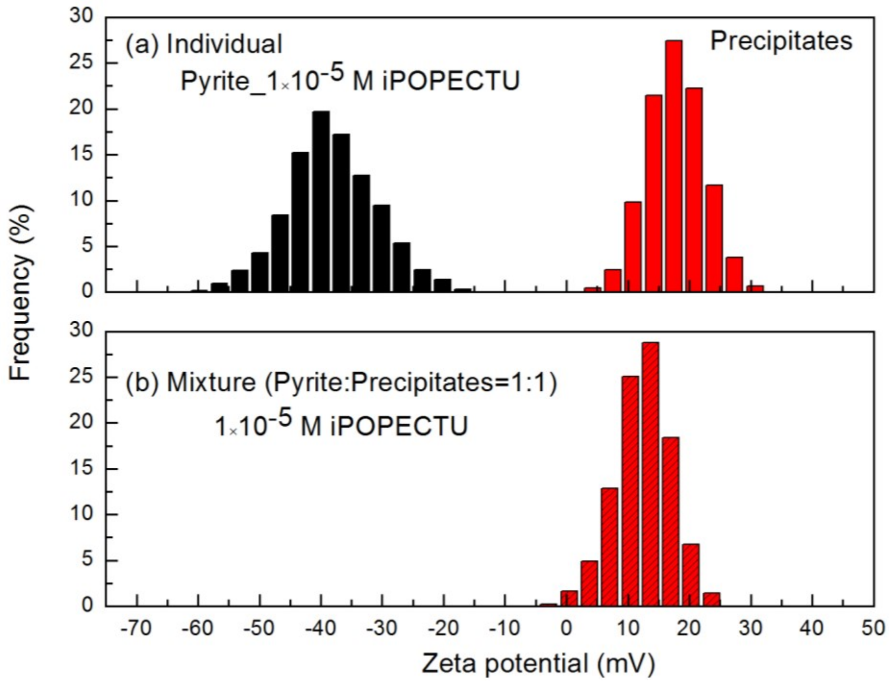

Figure 4.15 Zeta potential distributions for (a) individual pyrite in iPOPECTU

and precipitate suspensions, (b) pyrite and precipitate 1:1 mixture in iPOPECTU at pH 12 in 1 mM NaCl solution

4.4 References

Castro, S. (2012). Challenges in flotation of Cu-Mo sulfide ores in sea water. In*Water in Mineral Processing–Proc. of the First International Symposium (J. Drelich, Ed.), SME* (pp. 29-40).

Castro, S., Rioseco, P., & Laskowski, J. S. (2012). Depression of molybdenite in seawater. In *Proc. 26th Int. Mineral Processing Congress, New Delhi* (pp. 739-752).

Fuerstenau, M. C., & Palmer, B. R. (1976). Anionic flotation of oxides and silicates. *Flotation--A. M. Gaudin Memorial*.

Fuerstenau, D. W., Gaudin, A. M., & Miaw, H. L. (1958). The influence of alumina slimes on galena flotation. *Amer. Inst. Min. Eng. Trans*, *211*, 792-795.

Gaudin, A. M., Fuerstenau, D. W., & Miaw, H. L. (1960). Slime coatings in galena flotation. *CIM Bulletin*, *53*, 960-963.

Learmont, M. E., & Iwasaki, I. (1984). Effect of grinding media on galena flotation. *Minerals and Metallurgical Processing*, *1*(2), 136.

Liu, J., Xu, Z., & Masliyah, J. (2004). Interaction between bitumen and fines in oil sands extraction system: Implication to bitumen recovery. *The*

Canadian Journal of Chemical Engineering, *82*(4), 655-666.

Liu, J., Xu, Z., & Masliyah, J. (2004). Role of fine clays in bitumen extraction from oil sands. *AIChE journal*, *50*(8), 1917-1927.

Liu, J., Xu, Z., & Masliyah, J. (2005). Interaction forces in bitumen extraction from oil sands. *Journal of colloid and interface science*, *287*(2), 507-520.

Liu, J., Zhou, Z., Xu, Z., & Masliyah, J. (2002). Bitumen–clay interactions in aqueous media studied by zeta potential distribution measurement. *Journal of colloid and interface science*, *252*(2), 409-418.

Parsonage, P. G. (1984). Effects of slime and colloidal particles on the flotation of galena. *Flotation of sulphide minerals*, 111-139.

Pietrobon, M. C., Grano, S. R., Sobieraj, S., & Ralston, J. (1997). Recovery mechanisms for pentlandite and MgO-bearing gangue minerals in nickel ores from Western Australia. *Minerals Engineering*, *10*(8), 775-786.

Xu, Z., Liu, J., Choung, J. W., & Zhou, Z. (2003). Electrokinetic study of clay interactions with coal in flotation. *International Journal of Mineral Processing*,*68*(1), 183-196.

Chapter 5 The Mechanisms of Different Flotation Behavior of Pyrite in Different Process Water

5.1 Introduction

Water represents 80 - 85 % of the total volume of mineral pulp processed in flotation circuits (Levay, Smart, & Skinner, 2001). The quality of the process water in flotation plays an important role in mineral flotation and the shortage of freshwater resource is a major challenge for the mineral processing industry. In order to minimize the competition for freshwater resources with others, the mining industry began to use alternative water resource like sea water, groundwater and sewage water (Dunne, 2012). Since only 0.8 % of the earth's total water is considered to be fresh water (Greenlee, et al., 2009), the use of sea water for flotation has gained more and more attention.

It has been reported that the floatability of natural hydrophobic mineral is significantly improved in concentrated electrolyte solutions (Klassen & Mokrousov, 1963). Therefore, the salinity itself is not detrimental to flotation but can enhance the efficiency of flotation (Castro & Laskowski, 2011). Ionic strength can directly improve particle-particle (coagulation/flocculation) and particle-bubble (flotation) interactions.

Paulson and Pugh (1996) proposed that reduced bubble sizes and increased population in electrolyte solutions can increase the encounter efficiency of bubble-particle attachment. Fuerstenau, Rosenbaum and Laskowski (1983) attributed the increased bubble-particle attachment to the reduction of zeta potential of both bubbles and particles resulting from the compression of electrical double-layer in the presence of electrolytes. Another possible mechanism proposed is that the inorganic electrolytes destabilize the hydrated layers surrounding mineral particles and reduce their surface hydration thereby enhancing the bubble-particle attachment (Klassen & Mokrousov, 1963). Depending on the effect of ions on the water structure, soluble salts can be classified either as a structure maker, in which intermolecular hydrogen bonding between water molecules is stabilized, or as a structure breaker, in which intermolecular hydrogen bonding between water molecules is disrupted (Du & Miller, 2007, 2008; Hancer, Celik, & Miller, 2001). Castro (2011) proposed that because hydrophobic surfaces usually carry electrical charges, the attachment of the hydrophobic particles to bubbles is opposed by an electrical double layer repulsive force. When ionic strength increases, such a repulsive force is reduced and flotation of hydrophobic solids is improved. Bubble coalescence is prevented at such salt concentrations, reducing the bubble size. Extensive researches have been conducted to understand the effects of electrolytes on bubble coalescence (Craig, 2004; Horn, Del Castillo, & Ohnishi, 2011; Craig, Ninham, & Pashley, 1993a). It was found that some electrolytes reduce bubble coalescence whereas others have no effect using combining rules base on assigned properties of the ions for a range of common cations and anions (Craig, Ninham, & Pashley, 1993b; Boström, Williams, & Ninham, 2001).

Pyrite (FeS_2) is the most abundant sulfide associated with the Earth's surface region, which is commonly referred to as “Fool’s gold”. Pyrite itself usually has little economic value but it’s often associated with other valuable sulfide minerals like chalcopyrite, galena and sphalerite. In most cases, pyrite is a gangue mineral and should be removed from the associated sulfides. Accordingly, a comprehensive knowledge of the surface properties of pyrite, in addition to those valuable metal sulfides, is very important for the deep understanding of flotation process to separate pyrite from other sulfide minerals.

For the flotation behavior of pyrite using PAX solution, a lower flotation recovery was observed at the pH range of 6-7 (Fuerstenau, Kuhn & Elgillani, 1968; Fornasiero & Ralston, 1992). Wang and Forssberg (1991) suggested that it is the formation of ferric-hydroxy-xanthate species that caused this low recovery; however, Leppinen, Basilio, and Yoon (1989) and

Bulut and Atak (2002) had shown that only dixanthogen is present on the surface of pyrite at that range with FTIR spectroscopy. Lopez-Valdivieso, Sanchez Lopez, and Song (2005) proposed that the low recovery is caused by the high ratio of hydrophilic ferric hydroxide phase to hydrophobic dixanthogen phase caused by an insufficient amount of dixanthogen adsorption.

The surface oxidation of sulfide minerals can not only influence the interactions with flotation collectors but also impart hydrophobicity or hydrophilicity to the mineral surface. For example, the presence of elemental sulfur or metal-deficient sulfide species on the mineral surfaces can render a strong surface hydrophobicity (Finkelstein et al., 1975; Buckley & Woods, 1987). On the contrary, metal hydroxides and metal oxides formed on the surface can render strong surface hydrophilicity of mineral and greatly depress the flotation (Sutherland & Wark, 1955).

Iron hydroxides and oxides have previously been found not only on pyrite surfaces from aqueous oxidation (Buckley & Woods, 1987; Demoisson, Mullet, & Humbert, 2007; Giannetti et al., 2001; Nesbitt, 1998; Goldhaber, 1983) but also on surfaces exposed to atmospheric gases (Todd, Sherman, & Purton, 2003; Donato et al., 1993; Eggleston, Ehrhardt, & Stumm, 1996; Knipe et al., 1995), which are suggested to form as an accumulation of oxidation products. Moreover, the iron hydroxides and iron oxides found on pyrite surface are the result of the oxidation processes and not from precipitates of dissolved iron from solution (Chandra & Gerson, 2010). Precipitates of dissolved iron on pyrite surfaces will occur only under neutral to alkaline conditions, where a thick coating of goethite retards oxidation by blocking oxidant diffusion (Lowson, 1982; Todd, Sherman, & Purton, 2003; Huminicki & Rimstidt, 2009).

The acidic anions in solutions have an influence on the leaching and oxidation rate of pyrite. Previous studies of aqueous oxidation of pyrite by hydrogen peroxide with different leaching media found oxidation rates are different according to $HClO_4 < HCl < H_2SO_4$ (Antonijevic, Dimitrijevic, & Jankovic, 1997; Antonijevic, 2005; Dimitrijevic, 1996; Dimitrijevic, 1990). Increasing the concentrations of HCl or H_2SO_4 had a negative effect on oxidation rates of pyrite (Antonijevic, Dimitrijevic, & Jankovic, 1997; Dimitrijevic, 1990). Additions of Cl^- or SO_4^{2-} had a similar effect. Chloride ions have been shown to behave as aggressive anions, able to destroy passive films on iron by initially adsorbing and then absorbing into the hydrated hydroxide/oxide coatings (Pou et al., 1984; Jovancicevic et al., 1986). It was suggested that Cl^- and SO_4^{2-} adsorb onto the pyrite surface and inhibit the access of oxidants. Studies by Lehmann et al. (2000) showed the role of Cl^-

ions in preventing the deposition of S^0 and S_n^{2-} on reacting pyrite surfaces and also inhibiting the buildup of passive iron hydroxides and oxides coatings. Being a strong Lewis base, Cl^- is able to replace hydroxyl ions or water molecules in the hydrated iron hydroxide/oxide surface layers, which results in the formation of iron-chloride complexes and dissolution in solution. The exact effect of acidic anions on the aqueous oxidation rate of pyrite remains poorly understood, which is due to the effect caused by other more predominant factors such as solution Eh. There are also contrasting views on the effect of Cl^-, whether it has a positive or negative effect on rates and the actual mechanism involved is unknown (Chandra & Gerson, 2010). This study provides a basic understand of the surface properties and flotation behaviours of pyrite in different process water.

5.2 Experimental methods

5.2.1 Atomic absorption spectroscopy

Atomic absorption spectroscopy (AAS) is an analytical procedure to quantitatively determine the chemical elements using the absorption of optical radiation (light) by free atoms in the gaseous state. A Varian SpectrAA-220FS (Varian, USA) atomic absorption spectrometer (AAS) was used to do this analysis. The atomic absorption spectroscopy was used to determine the leaching speed of pyrite in different process water. 1 g mineral particles with the size fractions between 38 μm and 75 μm were mixed with 150 ml process water (Milli-Q water, NaCl solution and sea water). The pH of all the solution was adjusted to 6 to make comparable results. PAX was added to the solution with a concentration of 1×10^{-5} M. The samples were conditioned in a beaker with a stir bar at 700 rpm for 5 min. After the conditioning, the suspension was filtrated by a filter with 0.22 μm hole. The supernatant was used to doing the AAS analysis to characterize the concentration of iron leaching in the solution. Each sample was analyzed for three times to get repeatable results.

5.2.2 UV-Vis spectroscopy

UV-Vis-NIR (Shimadzu UV-3600) spectrophotometer determines absorption of ultraviolet, visible and near infrared radiation by samples. The concentration of an organic compound in solution can be determined by measuring the absorbance at some wavelength. The amount of collector adsorption on the surface of mineral was determined indirectly by measuring the collector stay in the solution which isn't adsorbed by mineral. The sample preparation procedure is the same with the AAS. The supernatant was used to doing the UV-Vis analysis to characterize the concentration of collector remaining in the solution.

5.2.3 Electrochemical impedance spectroscopy

Electrochemical impedance is the response of an electrochemical system to an applied potential. It is usually measured by applying an AC potential to an electrochemical cell and then measuring the current through the cell, which makes it also called AC impedance. These measurements are carried out at different ac frequencies and the frequency dependence of this impedance can reveal underlying chemical processes. Electrochemical impedance spectroscopy (EIS) is widely used as a standard characterization technique for many material systems and applications (corrosion, plating, batteries, fuel cells, etc.). The EIS measurements were conducted by using a 1255B Frequency Response Analyzer from Solartron Analytical. The pH of solution (with or without collector) was adjusted to 6. A three electrode system was applied to this measurement. A 1×1 cm^2 platinum foil was used as counter electrode and a calomel electrode was used as a reference electrode. A high purity pyrite chunk was used to make the working electrode. A rectangular pyrite chunk was connected with a copper wire by means of soldering and then set in mounting epoxy. The electrode was ground on successive grades of silicon carbide paper down to 1000 grade to minimize the surface contact resistance. The surface area of the pyrite electrode was measured by optical microscope, which is 0.65 cm^2. The working electrode was conditioned for 10 min before impedance measurements to reach the steady-state. An AC signal of 10 mV amplitude with frequencies ranging from 0.01 to 5×10^4 Hz was then applied to the electrode. The measured impedance spectra were fitted to equivalent circuit models using ZSimpWin software to obtain the resistance values.

5.2.4 Bubble size distribution measurements

Flotation recovery of mineral is greatly determined by the bubble–particle interaction, in which bubble acts as a carrier for the mineral particle. It is essential to accurately measure the bubble size to understand the bubble-particle interaction in flotation systems. However, only a small number of techniques are available which can operate at any scale from laboratory to plant and most of the approaches are collecting bubble samples and analyzing them off-line. The devices developed by the University of Cape Town and McGill University (capillary and imaging, respectively) are two that have been tested both under plant and laboratory conditions (Hernandez-Aguilar et al., 2004). The working principle of the McGill University technique is directly sampling bubbles into a viewing chamber where they are exposed and photographed with a digital camera. In this study, the McGill University technique was used to measure the size of bubble in Milli-Q water and NaCl solution. The viewing chamber is made of glass with a ruler scale on it. In order to improve the image contrast, a strong lamp is put at the back of the viewing chamber. The chamber is sloped at a 15° angle to spread the bubbles into a single layer to limit overlap and provide an unambiguous plane of focus. The flow rate of the nitrogen used is 30 sccm.

5.2.5 ToF-SIMS measurements

ToF-SIMS images and spectrums were obtained from a ToF-SIMS IV spectrometer (ION-TOF GmbH). For spectra acquisition, a high energy beam of Bi^+ ions (25 kV) was focused on the sample surface. The samples were prepared by conditioning 1.5 g pyrite particles in desired solution with 1×10^{-5} M collector for five minutes. The samples were washed three times by Milli-Q water and vacuum dried at room temperature.

5.2.6 XPS measurements

The adsorption products of PAX on pyrite in different solutions were characterized by using XPS at room temperature and 130 K (Cryo-XPS). The mineral particle samples were conditioning in desired solutions at pH of interest for 5 min. The particles were then filtrated and rinsed with sufficient Milli-Q water to remove the surface residual. The samples were vacuum dried at room temperature in a vacuum oven. The samples were loaded for the XPS analysis. The XPS measurements were performed on a Kratos AXIS-165 instrument at the Alberta Centre for Surface Engineering and Science, University of Alberta. The base pressure in the analytical chamber (SAC) was better than 1 ×10^{-9} torr. A monochromatic 210-W Al Kα X-ray (hν=1486.6 ev) was used as the incident beam. The charge neutralization was applied to stabilize the spectra during the measurements. Casa XPS software was used to analyze the XPS spectrum. The spectrums were calibrated by using the C 1s BE of 284.6 eV.

5.3 Results and discussion

5.3.1 Iron leaching measurements

The concentration of chloride ions in Milli-Q water, NaCl solution and sea water used in the research is listed in Table 5.1. The concentration of chloride ion is the highest in sea water, which is 0.546 M. Figure 5.1 shows the concentration of solubilized iron in different process water after the 5 min conditioning. The concentration of solubilized iron in Milli-Q water is about 0.037 ppm, but is much higher in NaCl solution and sea water, which is 0.153 and 0.233 ppm respectively. The order of the solubilized iron concentration in different process water after conditioning is consistent with the order of chloride concentration in the process water. This phenomenon results in the replacement of chloride ions with hydroxyl ions or water molecules in the hydrated iron hydroxides/oxides surface layers and the formation of iron-chloride complexes which readily dissolve in solution. The removal of iron hydroxides/oxides from the surface by chloride ions prevents the oxidation process and inhibits the buildup of hydrophilic passive iron hydroxides/oxides coatings, forming a clean reacting surface. As chloride ions displace hydroxyl ions or water molecules, the breakdown rate of the passive iron hydroxides/oxides coatings would be proportional to the chloride ion concentration, which corresponds to the results shown in Figure 5.1.

Table 5.1 Chloride ion concentration of different process water

Milli-Q Water	NaCl Solution	Sea Water
0	0.4 M	0.546 M

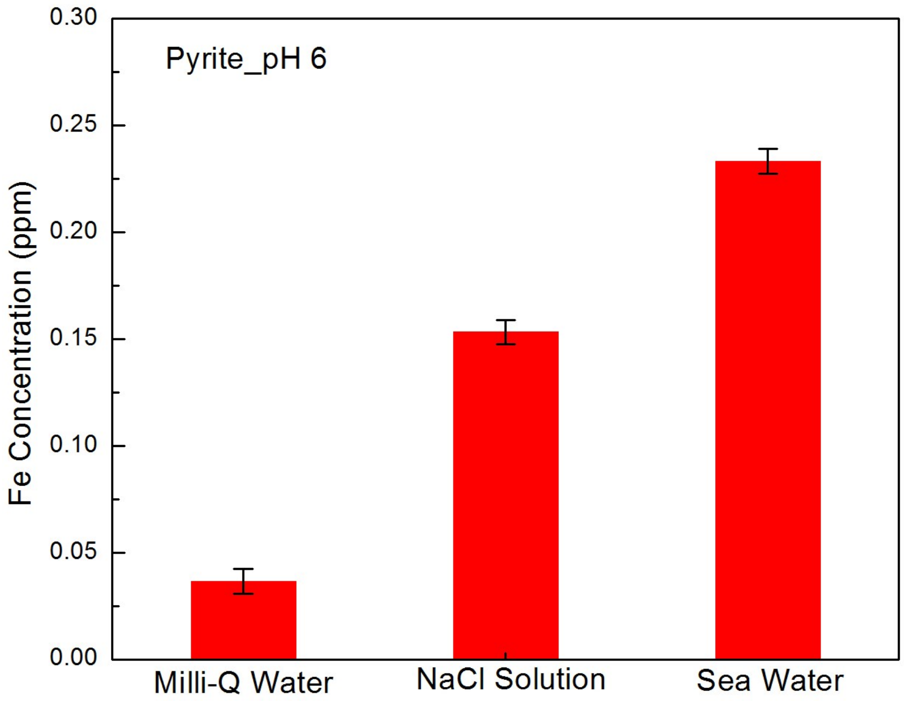

Figure 5.1 Solubilized iron concentration of pyrite in different process water

at pH 6 after 5 min conditioning

5.3.2 PAX adsorption measurements

UV-vis spectroscopy was used to study the xanthate-mineral interaction to monitor the collectors remaining in solution after adsorption. UV-vis absorption spectra of PAX were recorded in Milli-Q water, NaCl solution and sea water after 5 min conditioning. The peak at 300 nm is the absorption peak of xanthate. The peak is the highest for PAX remaining in Milli-Q water and is the lowest in NaCl solution. The peak in sea water is slightly higher than that in NaCl solution, indicating the absorption of xanthate on the surface of pyrite is slightly lower in sea water. A series of standard solutions of PAX with different concentration were measured and the standard line of concentration versus absorbance peak intensity was calculated. The consumption percentage of PAX was calculated by dividing the concentration change by the initial concentration. The results of consumption percentage of PAX in different process water at pH 6 were plotted in Figure 5.2. The schematic of xanthate adsorption on pyrite surface was shown in Figure 5.3. The extent of iron hydroxide/oxide formation is expected to determine the xanthate/dixanthogen coverage required to render the pyrite surface hydrophobic (Gardner & Woods, 1977). The results show that the consumption of PAX is lowest in Milli-Q water and much higher in NaCl solution and sea water. The lowest consumption percentage for PAX in Milli-Q water is consistent with the contact angle results shown in Figure 3.19 and flotation results shown in Figure 3.6, where a small contact angle and low flotation recovery is observed. The much higher consumption percentage for PAX in NaCl solution is also consistent with the contact angle results shown in Figure 3.20 and Figure 3.21 and flotation results shown in Figure 3.7 and Figure 3.8, in which contact angle is larger than 80 ° and near 100 % flotation recovery is observed. The reason why the consumption percentage is slightly higher in NaCl solution compared to that in sea water might be that calcium and magnesium ions forming hydroxyl species coating on the surface of pyrite and inhibit the absorption of PAX.

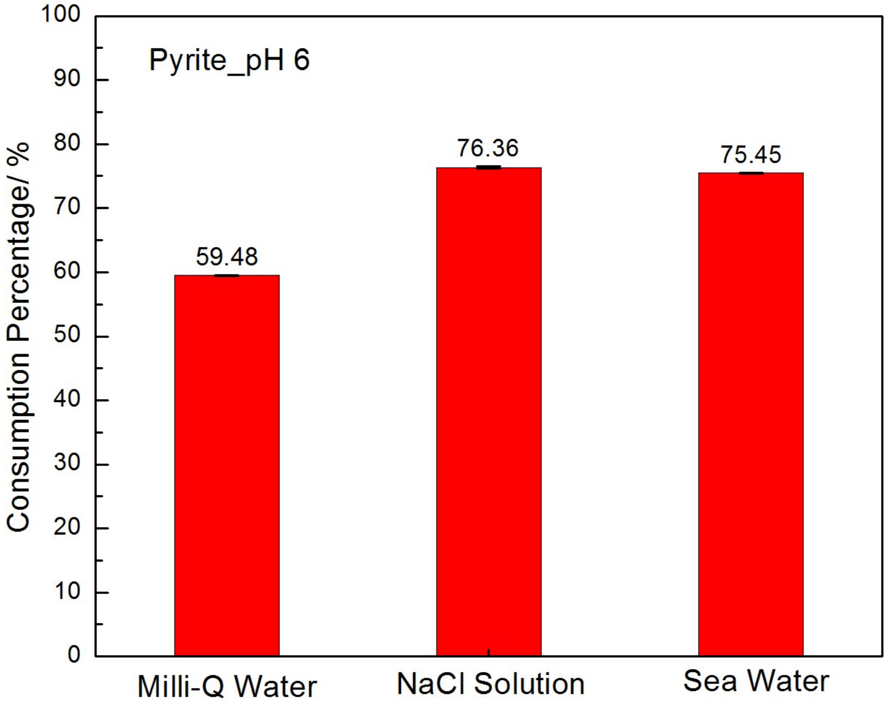

Figure 5.2 Consumption percentage of PAX in different process water at pH 6

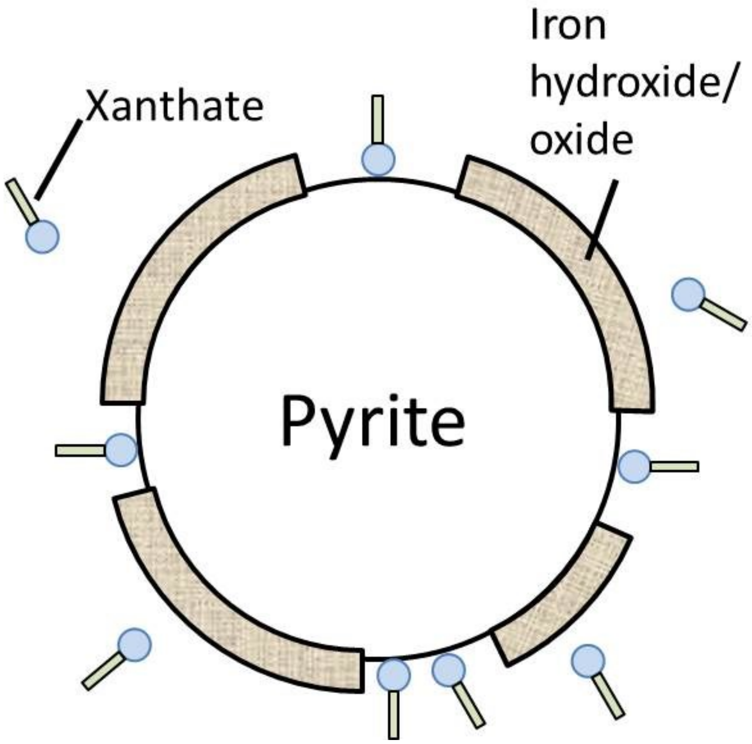

Figure 5.3 Schematic of xanthate adsorption on pyrite surface

5.3.3 Electrochemical impedance spectroscopy

There are several different electrochemical processes on the surface of sulfide mineral in the flotation system, which involving surface oxidation, dissolution, adsorption, surface reaction and precipitation. The related literature is huge and sometimes controversial, and a detailed discussion of all the aspects is beyond the range of this research. In this section, the discussion is focused on the growth and properties of the surface coating on pyrite surface. In fact, coatings can be hydrophilic which form by oxidation of the mineral and hydrophobic which form after treatment with collectors, after mild oxidation of the mineral or after mild oxidation of the mineral treated with solution containing sulfide ions (Chander, 1991). There was evidence repeated in literature with the conclusion that there was an iron hydroxide/oxide layer on pyrite surface even when the surface was freshly ground (Janetski, Woodburn & Woods, 1977). The presence of the hydrophilic iron hydroxide/oxide layer can also counteract the hydrophobic effect of organic collector, which is proved by Gardner and Woods (1977) that a large quantity of dixanthogen can be present on the mineral surface while the contact angle remains zero. The amount of hydrophilic iron hydroxide/oxide is expected to change the coverage of dixanthogen that render the pyrite surface hydrophobic.

Electrochemical impedance spectroscopy (EIS) is one of the techniques for the in-situ characterization of the solid/liquid interfaces. This technique has been used to study the properties of surface films (Chander, 1991; Pang & Chander, 1990; Chander & Briceno, 1987). In the cited examples, the impedance spectra was fitted by the most suitable model in which two layers were considered to be on the mineral surface. The first inner layer is near the unreacted mineral and is considered to be an iron-deficient sulfide. The second layer is near the liquid phase to be metal hydroxides or sulfates (Chander, 1991). Tolley et al. (1996) measured the impedance for different freshly crushed sulfide minerals in borate solution and found that the resistance to electrical current flow through the surface increases as the amount of iron in the mineral increases, which is attributed to the increasing amounts of iron hydroxides on the mineral surface. In general, oxidation will adversely affect the flotation process. It can reduce both the selectivity and the recovery in flotation by forming adherent surface layers of hydroxides (Rogers, 1962; Palagi & Stillar, 1976). As a result, the mineral surface appears as a hydroxide/oxide.

The results of the electrochemical impedance spectra and the equivalent circuit models of pyrite in Milli-Q water and saline water are shown in Figure 5.5 and Figure 5.6. The equivalent circuit models are adopted from several literatures (Pang, Briceno & Chander, 1990; Chander, 1991; Velásquez et al., 2001; Hung et al., 2008). The circuit models are the basis of the double-layers models which could be used to describe the contribution of a porous layer at the solid/solution interface (Chander, 1991). The elements shown in the circuits are: R_e - the resistance of the electrolyte, R_p - the resistance of the pore, R_t - the resistance of the charge transfer, C_c - the capacitance of the coating layer, C_d - the capacitance of the double-layer and L - the inductance of adsorption-layer. The schematic of pyrite surface with porous non-conductive coating layer in electrolyte with the resulting equivalent circuit was shown in Figure 5.4.

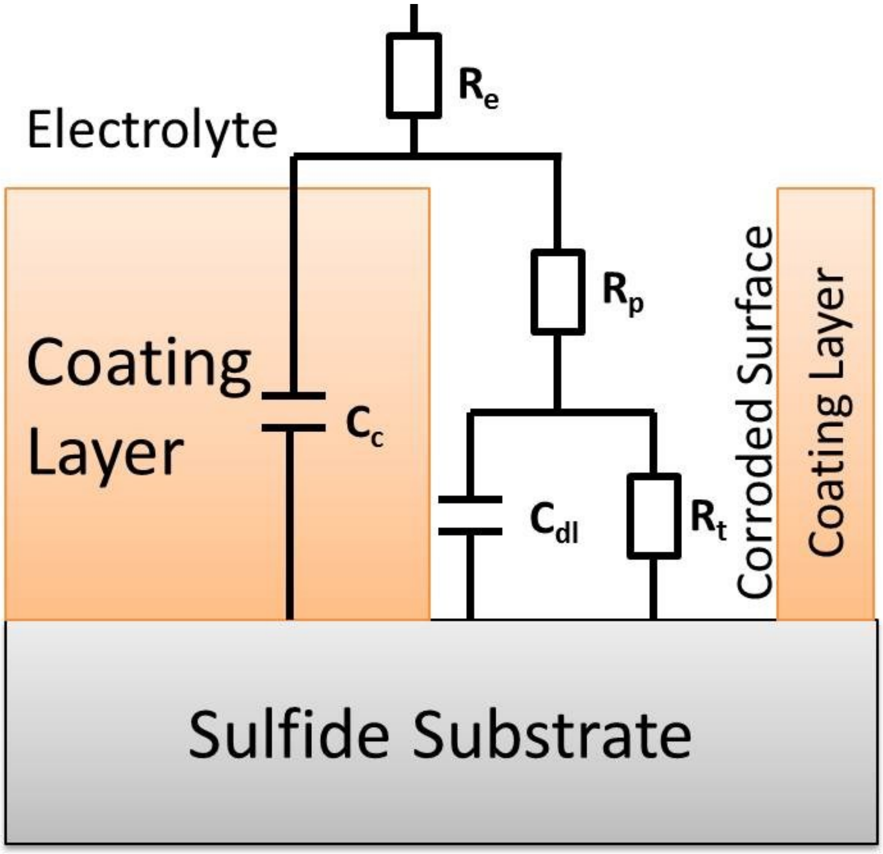

Figure 5.4 Schematic of pyrite surface with porous non-conductive coating layer in electrolyte with the resulting equivalent circuit

Table 5.2 summarizes the calculated R_p and R_t of pyrite with and without the addition of PAX in different process water. By comparing the value of R_p and R_t when no collector is added into the solution, it could be found that both the value of R_p and R_t are much larger in Milli-Q water than in NaCl solution and sea water. The smaller charge transfer resistance (R_t) of pyrite in NaCl solution and sea water indicates less formation of non-conductive layer of iron hydroxides/oxides on the surface. The much smaller pore resistance (R_p) indicates that the porosity of the iron hydroxides/oxides layer of pyrite is much higher in NaCl solution and sea water than that in Milli-Q water and the pore resistance is slightly smaller in sea water than that in NaCl solution. This indicates the pore resistance inversely proportional to the concentration of chloride containing in different solutions. The chloride ions are very aggressive ions and can adsorb on the surface of pyrite to replace hydroxyl ions or water molecules in the hydrated iron hydroxides/oxides layer and form the iron-chloride complexes and dissolve in solution (Lehmann et al., 2000), which leading to less pore resistance and higher porosity. The effect of chloride can also explain the less formation of non-conductive iron hydroxides/oxides layer on the surface of pyrite in salt water and the more solubilized iron in salt water than that in Milli-Q water.

By comparing the value of R_p and R_t of pyrite before and after the addition of PAX, it was found that the charge transfer resistance (R_t) of pyrite in all the three solutions increase, which indicates the adsorption of xanthate on the surface forming a passivation layer. However, the pore resistance of pyrite in Milli-Q water increases after the addition of PAX, but the pore resistance decreases in NaCl solution and sea water after the addition of PAX. This indicates that the adsorption of xanthate creates porosity in the surface of pyrite in salt water but not in Milli-Q water (Tolley et al., 1996).

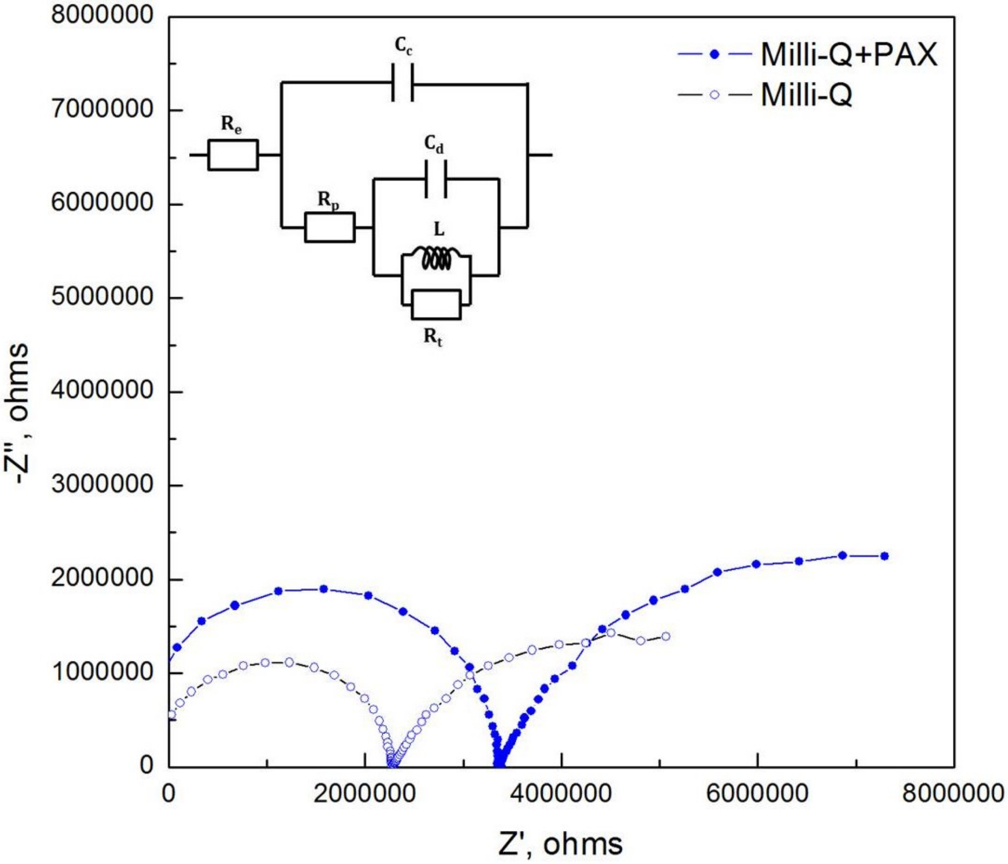

Figure 5.5 Nyquist plots of AC impedance data and equivalent circuit model for pyrite in Milli-Q water with and without the addition of PAX at pH 6

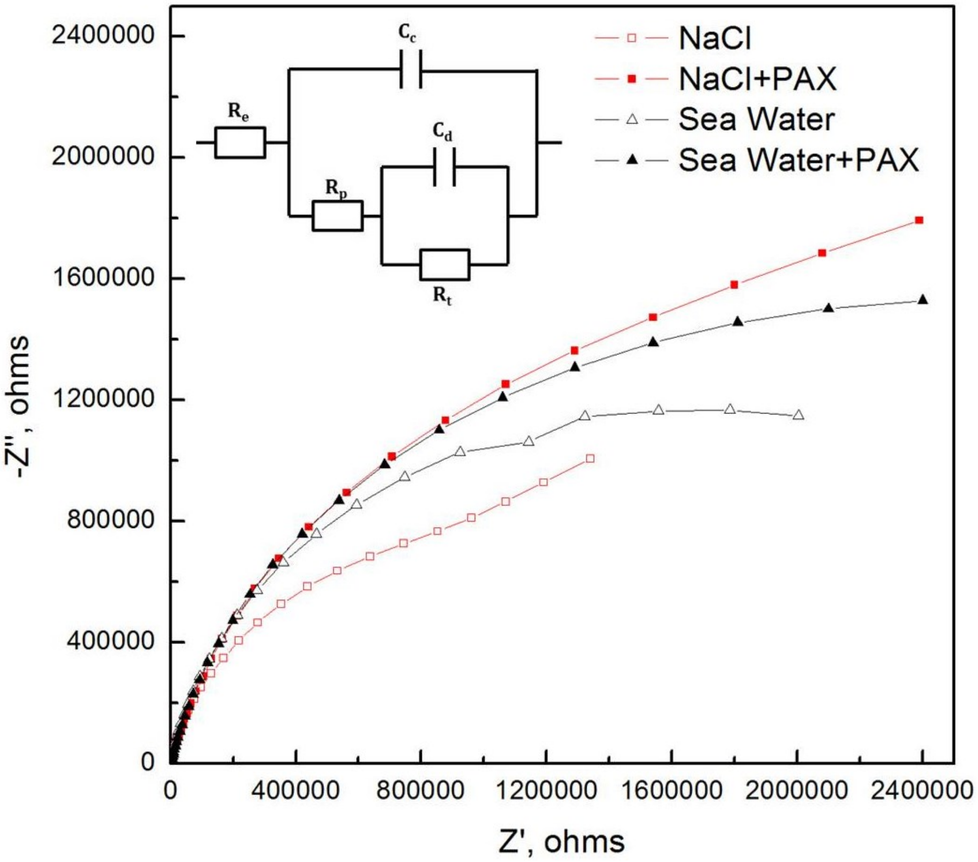

Figure 5.6 Nyquist plots of AC impedance data and equivalent circuit model for pyrite in NaCl solution and sea water with and without the addition of PAX

Table 5.2 Calculated R_p and R_t with and without the addition of PAX in different process water at pH 6

Process Water	R_p/kΩ		R_t/kΩ	
	No PAX	With PAX	No PAX	With PAX
Milli-Q Water	1514	2261	1807	2827
NaCl Solution	232	137	932	1823
Sea Water	145	81	1360	1717

5.3.4 Bubble size distributions

Figure 5.7 shows the size distribution and picture in the viewing chamber of bubble in Milli-Q water (right) and NaCl solution (left). The bubble size distribution in sea water is almost the same with that in NaCl solution, which was not plotted out. The mean value of the bubble size distribution is about 1.4 mm in Milli-Q water and about 0.4 mm in NaCl solution. The bubble size is more than three times larger in Milli-Q water than that in NaCl solution. Sutherland (1948) assumed that the probability of a bubble to collect particle (P) can be represented by,

$$P = P_c P_a (1-P_d)$$

where P_c is the collision probability between bubble and particle, P_a is the adhesion/attachment probability of particle after collision, and P_d is the probability that subsequent detachment would occur. Using numerical solution techniques, people showed that the collision probability (P_c) between bubbles and particles could be given by,

$$Pc \propto (\frac{Dp}{Db})^2$$

where D_p and D_b, are the diameters of particles and bubbles, respectively (Flint & Howarth, 1971; Weber, 1981; Weber, 1983; Yoon & Luttrell, 1989). This relationship indicates that the collision probability (P_c) could be improved by decreasing the bubble size. In that case, the collision probability between bubbles and particles are about nine times in NaCl solution compared to that in Milli-Q water. The difference of bubble size in Milli-Q water and salt water is one of the reasons that caused the different flotation response in different process water.

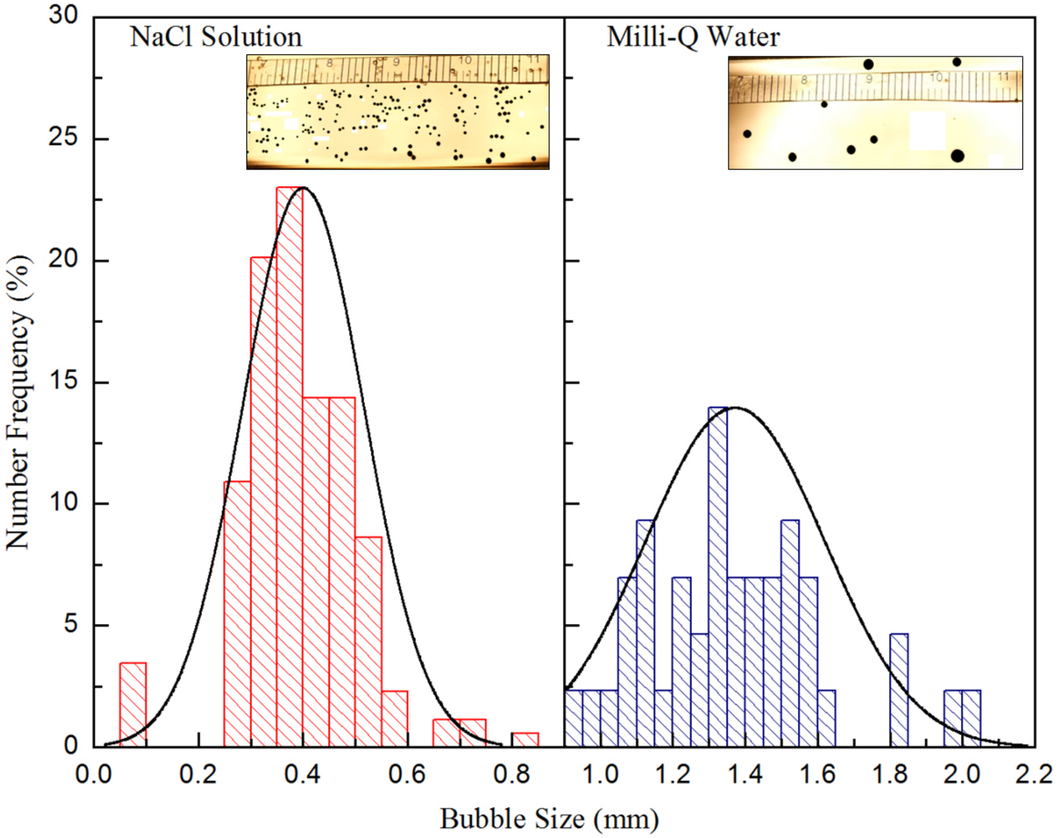

Figure 5.7 Distribution of bubble size in Milli-Q water and NaCl solution at pH 6

5.3.5 ToF-SIMS analysis

Figure 5.8 shows the ToF-SIMS spectra of Fe^+ and $FeOH^+$ fragment of pyrite in different process water with and without the addition of PAX. Table 5.3 shows the $FeOH^+/Fe^+$ ratio. By comparing the data in Table 5.3 vertically, it shows that the presence of chloride can greatly depress the formation of iron-hydroxides species on the surface of pyrite with and without the presence of xanthate (Lehmann et al., 2000). By comparing the data in Table 5.3 horizontally, it shows that the presence of xanthate can also decrease the formation of iron-hydroxides species on the surface of pyrite (Tolley et al., 1996). The results of the $FeOH^+/Fe^+$ ratio in Table 5.3 are almost corresponding to the contact angle and flotation recovery results, which indicate that the iron-hydroxides species have great influence on the surface hydrophobicity and flotation response of pyrite. The decrease content of iron-hydroxides species will greatly increase the surface hydrophobicity and the flotation performance of pyrite.

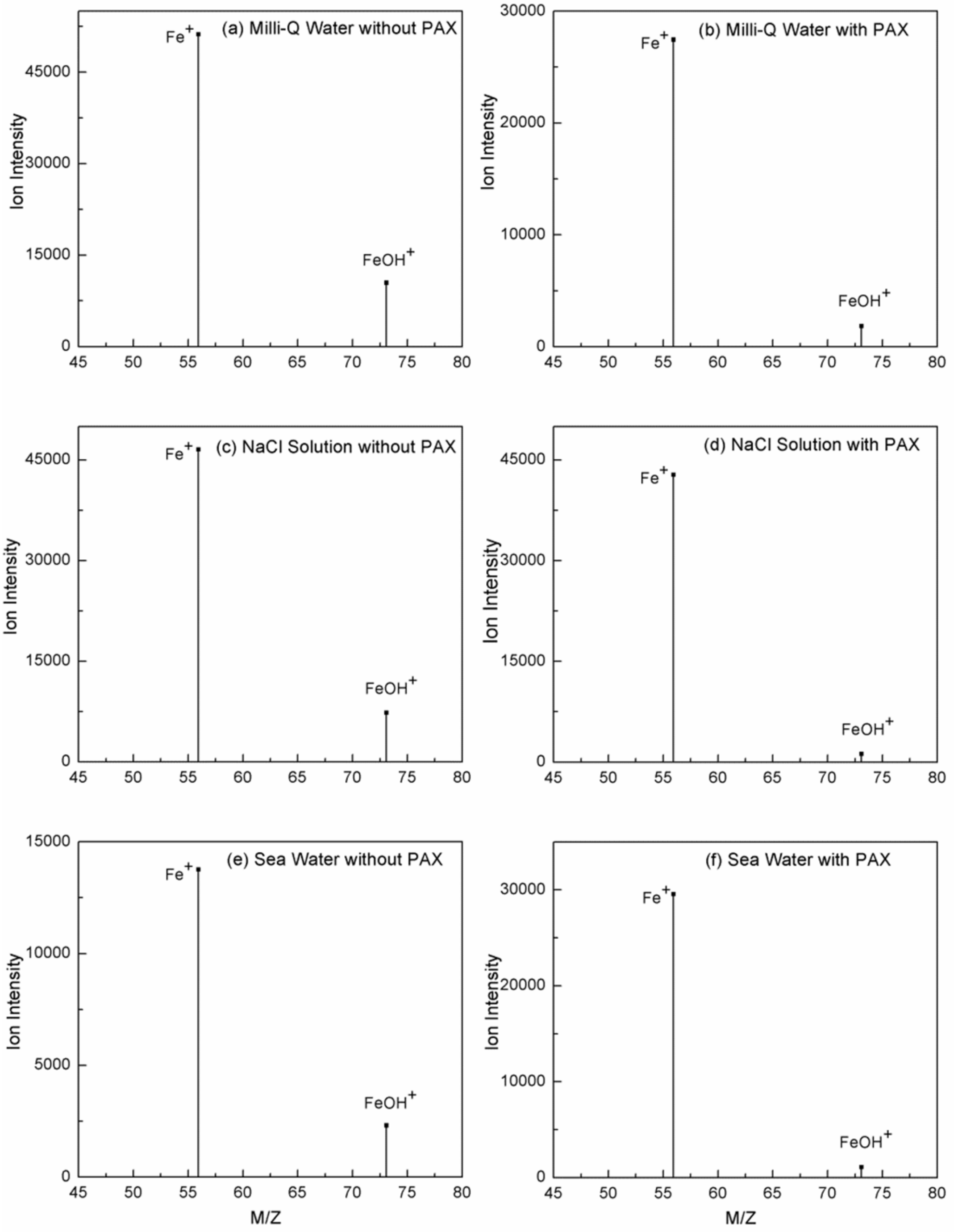

Figure 5.8 Part of positive ions ToF-SIMS spectra from the surface of pyrite in (a) Milli-Q water (b) NaCl solution (c) sea water at pH 6

Table 5.3 $FeOH^+/Fe^+$ ratio with and without the addition of PAX in different process water at pH 6

Process Water	$FeOH^+/Fe^+$ Ratio	
	No PAX	With PAX
Milli-Q Water	0.204	0.068
NaCl Solution	0.157	0.028
Sea Water	0.168	0.037

Figure 5.9 shows the ToF-SIMS spectra of negative ions from the surface of pyrite with the addition of PAX in different process water. The three spectrums are almost the same as most peaks. However, the peaks at m/z 148 and 223 are very weak for pyrite conditioned in Milli-Q water, but very strong in NaCl solution and sea water. The structure of the two fragments are assigned to amyl monothiocarbonate (m/z 148) and fragment of amyl carbonate disulphide (m/z 223), which is shown in Figure 5.10. Evidence has suggested that derivatives other than metal xanthates and dixanthogens may be a product when xanthate solutions react in the presence of oxygen (Granville et al., 1972). Spectrophotometric studies have shown that a species was formed during the decomposition of xanthate solutions (Finkelstein, 1967) and during the reaction between unoxidized galena surfaces and oxygen-containing solutions of xanthate (Finkelstein, 1970). These findings are consistent with the earlier studies that monothiocarbonates are formed as

intermediates in the decomposition of xanthate (Phillip & Fichte, 1960; Fleming, 1952).

Dixanthogen have been identified as the only xanthate derivative as a product of reaction at pyrite surfaces (Fuerstenau, Kuhn & Elgillani, 1968; Allison et al., 1972). However, the available evidences can't exclude the possibility that iron xanthate and iron hydroxide xanthate complexes and other derivatives could be present at the pyrite surface (Wang, Forssberg & Bolin, 1989; Critchley & Hunter, 1986; Sheikh & Leja, 1977). The formation of monothiocarbonate (MTC) on pyrite surfaces is proposed by Harris and Finkelstein (1975) that it is formed from a minor adsorbed species of the compound $FeOHX_2$ (Sheikh & Leja, 1973; Fornasiero & Ralston, 1992). The reactions are as followed (X^- stands for the xanthate ion):

$$FeS_2 \xrightarrow{O_2, X^-} FeOHX_2 + S^0 \text{ (or sulphoxides)}$$

$$FeOHX_2 + OH^- \rightarrow FeSX + MTC + H_2O$$

Finkelstein (1970) also proposed another substitution reaction of xanthate accounted for the formation of monothiocarbonate as followed (R stands for hydrocarbon):

$$ROCS_2^- + \frac{1}{2} O_2 \rightarrow RO_2CS^- + S^0$$

Therefore, monothiocarbonate is formed by a parallel reaction, either between $FeOHX_2$ and oxygen or direct from pyrite, oxygen and xanthate

(Harris & Finkelstein, 1975). For carbonate disulphide, it is formed by the reaction analogous to the oxidation of xanthates to dixanthogens as the following reaction (Reid, 1958; Murphy & Winter, 1973).

$$RO_2CS^- \xrightarrow{oxidation} RO_2CSSCO_2R$$

The potential value for monothiocarbonate and carbonate disulphide in sulfide mineral flotation has been mentioned (Wark & Wark, 1933; Winter & Woods, 1973). The contact angle of pyrite surface in the presence of butyl monothiocarbonate can reach 72 ° (Wark & Wark, 1933). The flotation performance of ethyl carbonate disulphide is even higher than ethyl dixanthogen in galena flotation (Winter & Woods, 1973). Those studies confirmed the potential collecting capacity of the monothiocarbonate and its corresponding carbonate disulphide.

The peaks at m/z 148 and 223 on the surface of pyrite in NaCl solution and sea water as shown in Figure 5.9 indicate the formation of amyl monothiocarbonate and amyl carbonate disulphide. The presence of these two xanthate derivatives may indicate the formation of iron hydroxide xanthate complexes other than dixanthogen in NaCl solution and sea water which contribute addition collecting power for pyrite flotation at pH 6. Besides, the presence of amyl monothiocarbonate and amyl carbonate disulphide themselves can also act as a “collector” to improve the flotation of pyrite at pH 6. This may be another reason for the high flotation recovery of pyrite in NaCl solution and sea water at pH 6.

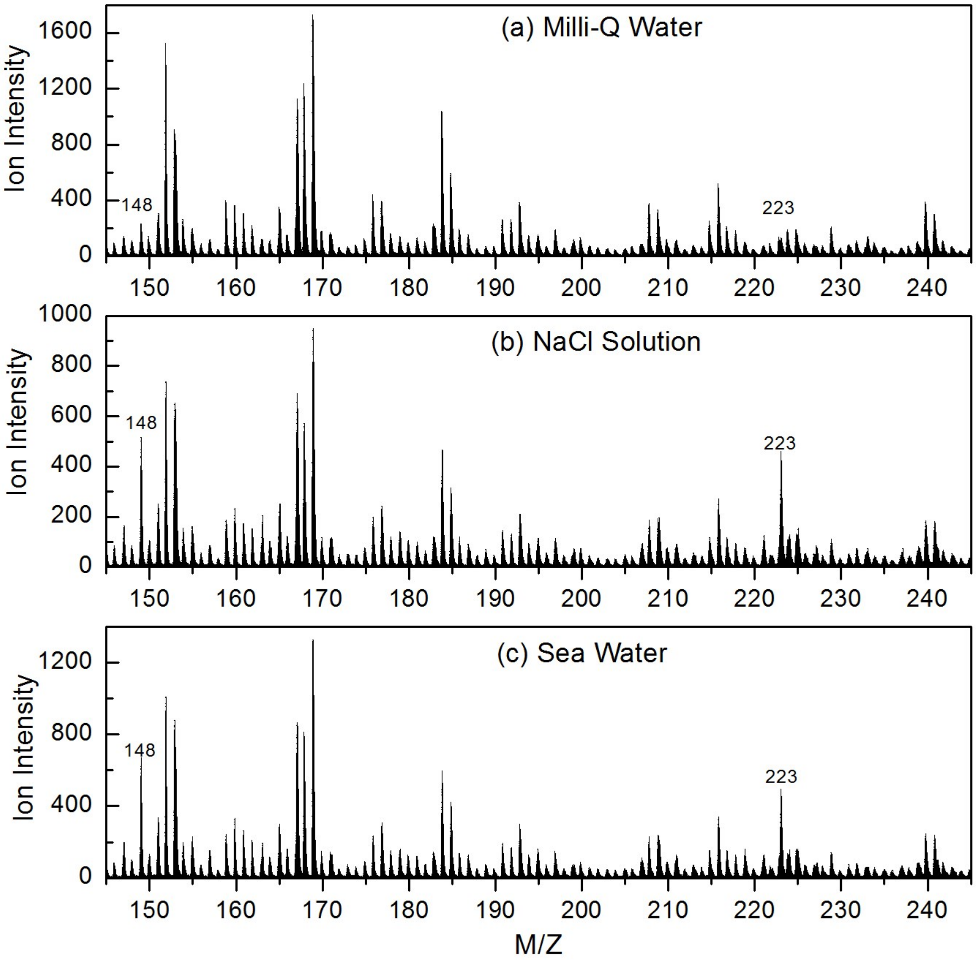

Figure 5.9 Negative ions ToF-SIMS spectra from the surface of pyrite in (a) Milli-Q water (b) NaCl solution (c) sea water with the addition of PAX at pH 6

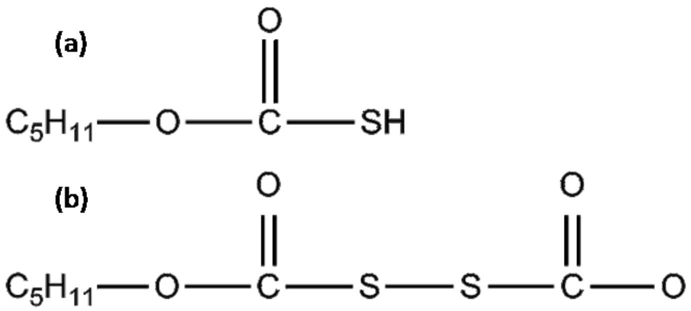

Figure 5.10 Molecular structure of (a) amyl monothiocarbonate (b) fragment of amyl carbonate disulphide

5.3.6 XPS analysis

Figure 5.11 shows the C 1s and S 2p spectra of pyrite conditioned in pH 6 Milli-Q water with 1×10^{-5} M PAX by both room temperature and Cryo-XPS. From Figure 5.11 (a), it could be found that the room temperature XPS C 1s spectrum of pyrite has only one peak at 284.6 eV. However, when the sample was analyzed at 130 K, two more peaks appear at 286.5 eV and 288.7 eV which indicates the existence of dixanthogen (Szargan, Karthe & Suoninen, 1992). For the two S 2p spectrums, the doublet at 162.5 eV is consistent with the peak of bulk pyrite (Khan et al., 1991; Pillai, Young & Bockris, 1985; Laajalehto et al., 1999). For the Cryo-XPS spectra, an extra peak was found at 164.5 eV. The spectrum can be well fitted by three doublets, with 162.5 eV (high intensity), 162.5 eV (low intensity), and 164.5 eV (Cases et al., 1993; Kartio et al., 1992; Szargan, Karthe & Suoninen, 1992; Khan et al., 1991; Pillai, Young & Bockris, 1985; Smart et al., 2003; Wang & Forssberg, 1991). The low intensity doublet at 162.5 and the doublet at 164.5 are indications of the existence of the adsorbed dixanthogen (Deng et al., 2013). The difference of spectra between room temperature XPS and Cryo-XPS indicates the successful detection of dixanthogen on pyrite surface by Cryo-XPS but not room temperature XPS, which is because that dixanthogen are not stable compounds at room temperature and will be pumped away under ultrahigh vacuum (Fielding, Porter & Winter, 1980). In order to figure out the difference of the interaction between pyrite and xanthate in different solutions at pH 6, all the following results shown are acquired by Cyro-XPS analysis.

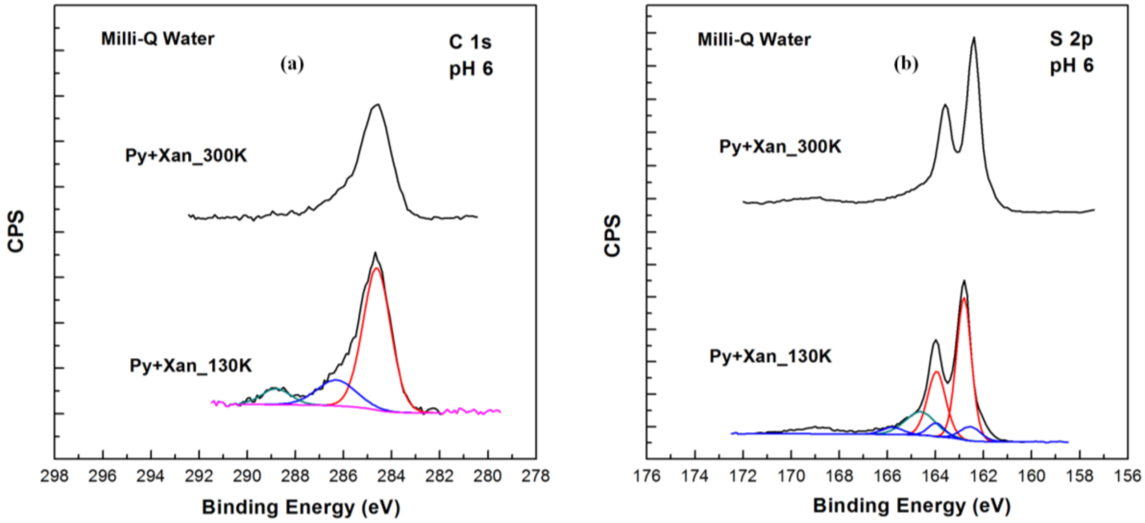

Figure 5.11 Cryo-XPS and room temperature XPS spectra from pyrite conditioned in pH 6 Milli-Q water with 1×10^{-5} M PAX (a) C 1s spectra, (b) S 2p spectra

Figure 5.12 shows the C 1s spectra of pyrite conditioned at pH 6 with 1×10^{-5} M PAX in different solutions. All of the spectrums can be well fitted by the three peaks at 284.6 eV, 286.5 eV and 288.1 eV. The three peaks can be attributed to hydrocarbon contaminants (Deng et al., 2013; Ikumapayi, Johansson & Rao, 2012; Miller, Biesinger & McIntyre, 2002). The C 1s peak at 286.3 eV can also be attributed to the C-O in adsorbed xanthate (Deng et al., 2013; Ikumapayi, Johansson & Rao, 2012; Wang et al., 2015). The C 1s peak at 288.1 eV is close to the CS_2 (Ranta et al., 1981) and dixanthogen (Szargan, Karthe & Suoninen, 1992). By comparing the C 1s spectra of pyrite treated in different solutions, the C 1s spectra of pyrite treated in NaCl solution and sea water show a relative high intensity at 286.5 eV, which potentially indicate the increase adsorption of xanthate on pyrite conditioned in NaCl solution and sea water compared to pyrite in conditioned Milli-Q water (Deng et al., 2013; Ikumapayi, Johansson & Rao, 2012). This result is also consistent with the xanthate adsorption results shown in this study.

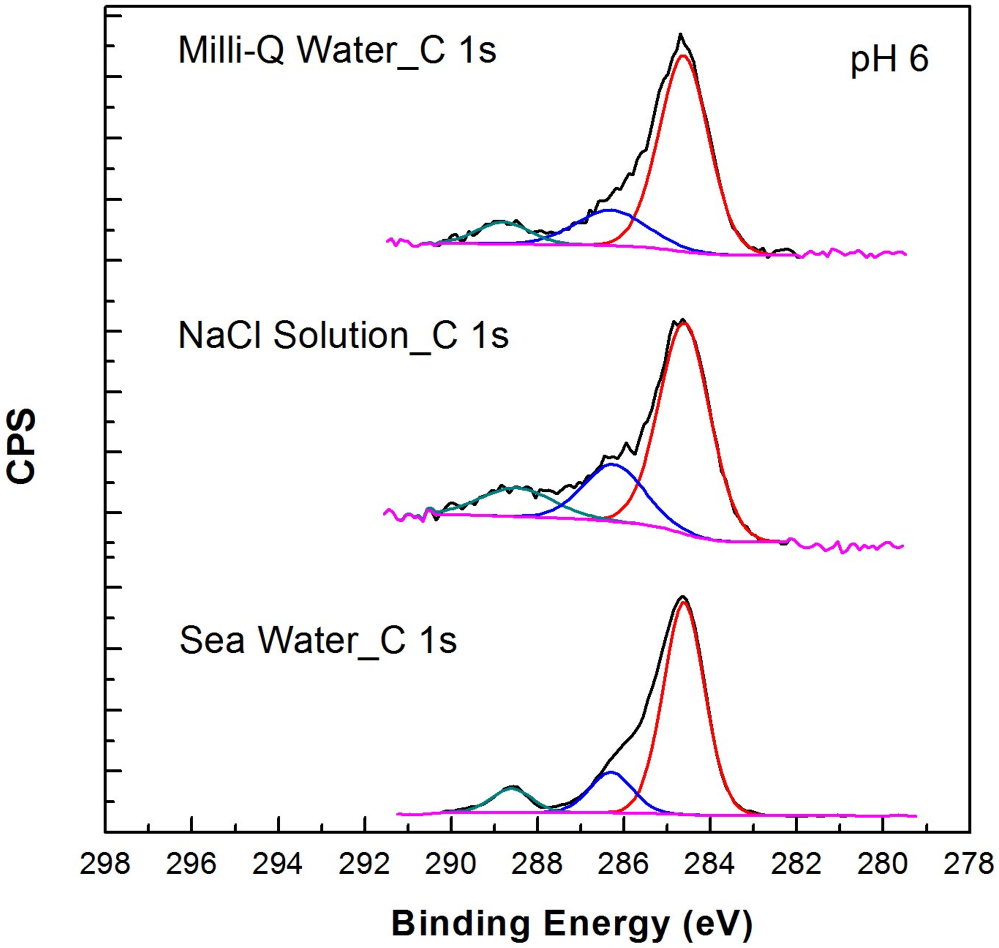

Figure 5.12 C 1s spectra of pyrite conditioned at pH 6 with 1×10^{-5} M PAX in different solutions

The S 2p spectra of pyrite treated in different solutions can be well fitted by three doublets mentioned in previous section, except for the pyrite treated in sea water, which have an extra peak near 169 eV. This peak is attribute to sulfate (Descostes et al., 2000), which is caused by the sulfate ion in sea water adsorbed onto the surface of pyrite. The peak at 164.5 eV can be attributed to dixanthogen, which indicates the formation of dixanthogen on pyrite surface in all three solutions with NaCl solution having the highest adsorption of xanthate.

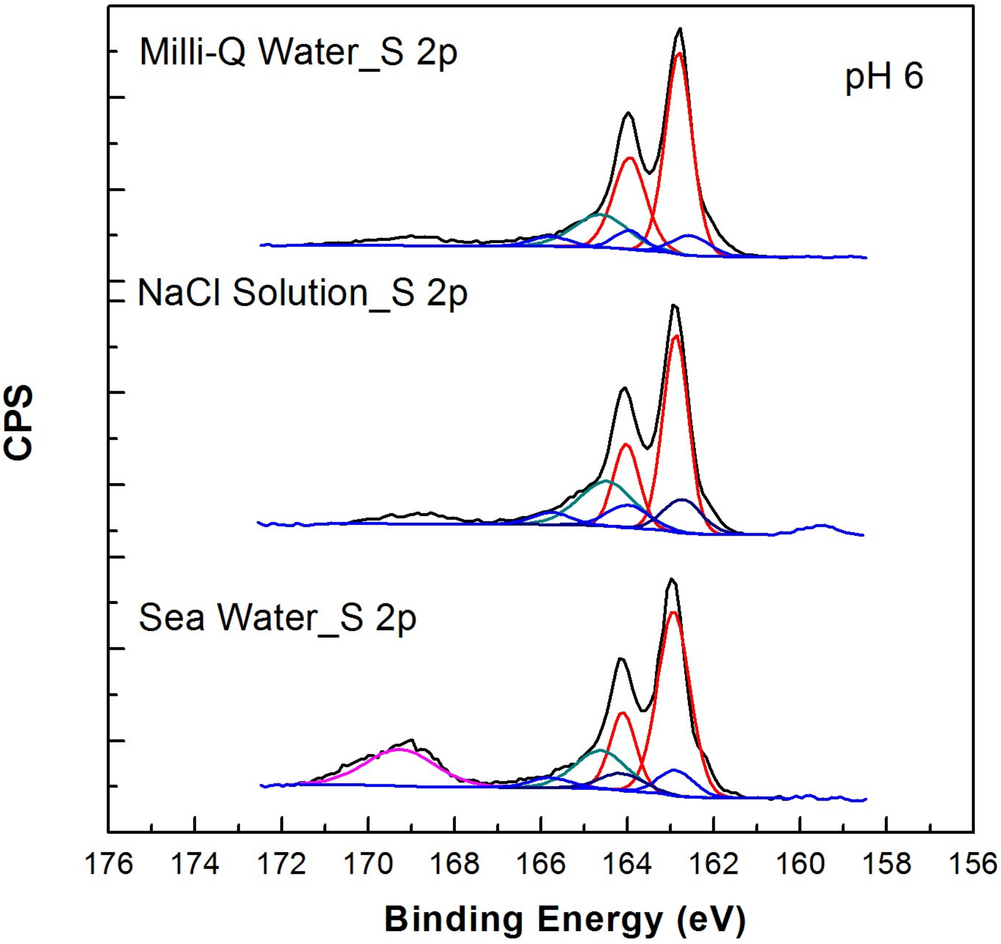

Figure 5.13 S 2p spectra of pyrite conditioned at pH 6 with 1×10^{-5} M PAX in different solutions

Figure 5.14 shows the Fe 2p spectra of pyrite conditioned in different solutions, which could be well fitted by three peaks. The high intensity of the peak at 711.5 eV for pyrite conditioned in Milli-Q water, which is attributed to iron-oxides/hydroxides (Deng et al., 2013), indicates the oxidation of pyrite in Milli-Q water. The intensity of this peak is much smaller in NaCl solution and sea water, which indicates that the oxidation of pyrite to form iron hydroxides/oxides is inhabited in NaCl solution and sea water.

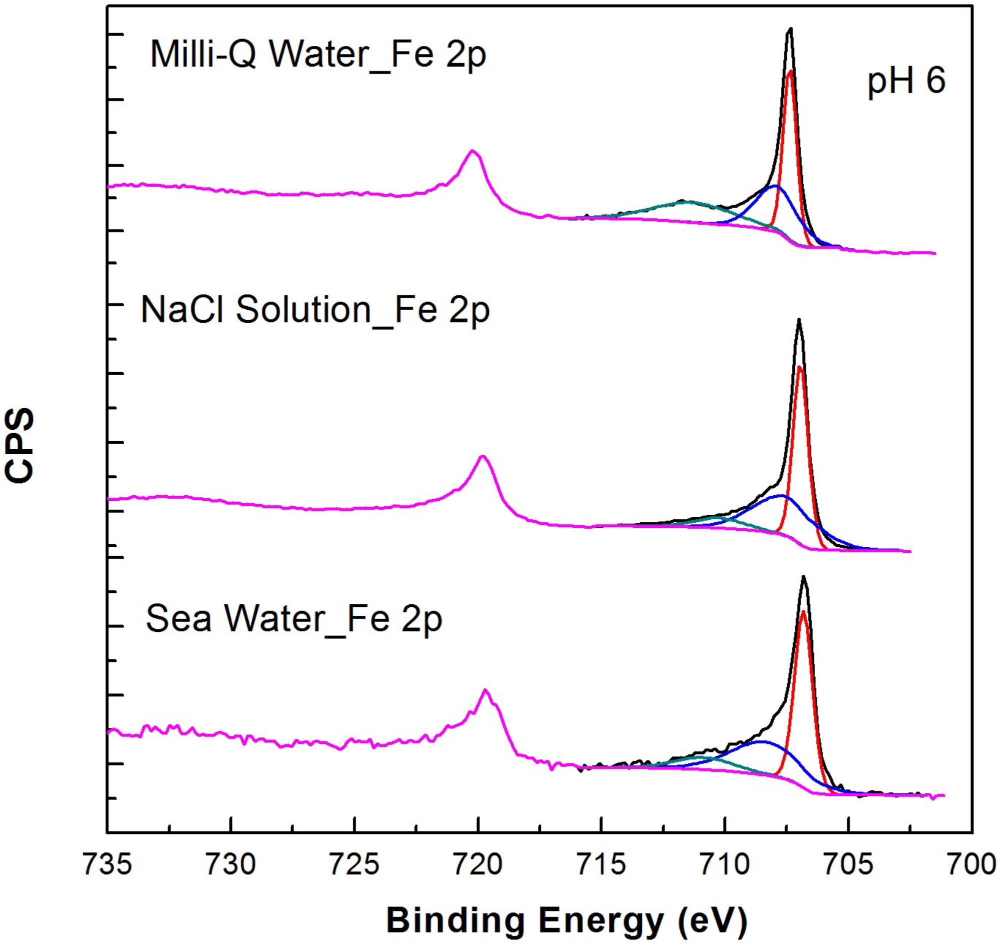

Figure 5.14 Fe 2p spectra of pyrite conditioned at pH 6 with 1×10^{-5} M PAX in different solutions

Figure 5.15 shows the O 1s spectra of pyrite conditioned in different solutions, which could be well fitted by three peaks. The peak at 533 eV can be attributed to the adsorption of xanthate (Ihs et al., 1993; Mielczarski et al., 1983) or dixanthogen (Deng et al., 2013). The dominant peak at 531.5 eV for pyrite conditioned in Milli-Q water is attributed to surface oxidation

(Gonzalez-Elipe et al., 1990; Khmeleva et al., 2005; Ikumapayi et al., 2012; Deng et al., 2013). By comparing the relative intensity of the three peaks in the O 1s spectrums, it could be found that there are less surface oxidation and more xanthate adsorption on the surface of pyrite conditioned in NaCl solution and sea water compared to that in Milli-Q water.

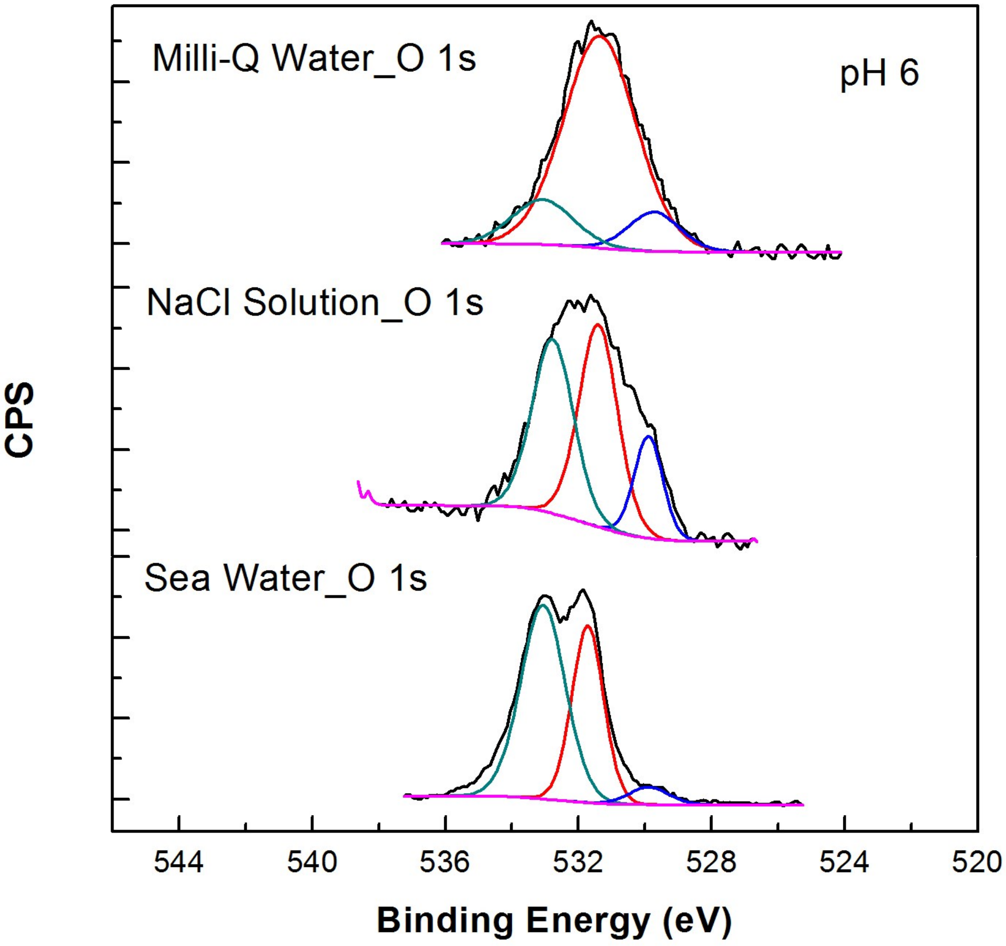

Figure 5.15 O 1s spectra of pyrite conditioned at pH 6 with 1×10^{-5} M PAX in different solutions

From the XPS analysis mentioned above, it's quite easy to confirm the formation of dixanthogen on the surface of pyrite in the three different solutions. However, the iron xanthate compounds was not identified since the peak of iron xanthate compounds at 162.6 eV (Buckley & Woods, 1990; Szargan, Karthe & Suoninen, 1992; Deng et al., 2013) will overlap with that of dixanthogen. The XPS analysis shows that dixanthogen and xanthate are adsorbed on the surface of pyrite conditioned in Milli-Q water, NaCl solution and sea water, with the pyrite conditioned in NaCl solution adsorbing the largest amount, which is consistent with the xanthate adsorption result. The larger amount of iron hydroxides/oxides on the surface of pyrite conditioned in Milli-Q water indicates more surface oxidation of pyrite conditioned in Milli-Q water as compared to that conditioned in NaCl solution and sea water, which is consistent with the ToF-SIMS results and electrochemical impedance spectroscopy results.

5.4 References

Antonijević, M. M., Dimitrijević, M., & Janković, Z. (1997). Leaching of pyrite with hydrogen peroxide in sulphuric acid. *Hydrometallurgy*, *46*(1), 71-83.

Antonijević, M. M., Dimitrijević, M. D., Šerbula, S. M., Dimitrijević, V. L. J., Bogdanović, G. D., & Milić, S. M. (2005). Influence of inorganic anions on electrochemical behaviour of pyrite. *Electrochimica acta*, *50*(20), 4160-4167.

Allison, S. A., Goold, L. A., Nicol, M. J., & Granville, A. (1972). A determination of the products of reaction between various sulfide minerals and aqueous xanthate solution, and a correlation of the products with electrode rest potentials. *Metallurgical Transactions*, *3*(10), 2613-2618.

Bulut, G., & Atak, S. (2002). Role of dixanthogen on pyrite flotation: solubility, adsorption studies and Eh, FTIR measurements. *Minerals & metallurgical processing*, *19*(2), 81-86.

Buckley, A. N., & Woods, R. (1987). The surface oxidation of pyrite. *Applied Surface Science*, *27*(4), 437-452.

Buckley, A. N., & Woods, R. (1990). X-ray photoelectron spectroscopic and electrochemical studies of the interaction of xanthate with galena in relation to the mechanism proposed by Page and Hazell. *International Journal of Mineral Processing*, *28*(3), 301-311.

Boström, M., Williams, D. R., & Ninham, B. W. (2001). Surface tension of electrolytes: specific ion effects explained by dispersion forces. *Langmuir*, *17*(15), 4475-4478.

Craig, V. S. (2004). Bubble coalescence and specific-ion effects. *Current opinion in colloid & interface science*, *9*(1), 178-184.

Chander, S. (1991). Electrochemistry of sulfide flotation: growth characteristics of surface coatings and their properties, with special reference to chalcopyrite and pyrite. *International journal of mineral processing*, *33*(1), 121-134.

Chander, S., & Briceno, A. (1987). Kinetics of pyrite oxidation. *Minerals and Metallurgical Processing*, *4*(3), 170-176.

Chandra, A. P., & Gerson, A. R. (2010). The mechanisms of pyrite oxidation and leaching: a fundamental perspective. *Surface Science Reports*, *65*(9), 293-315.

Critchley, J. K., & Hunter, C. J. (1986). Solubility products of ferric xanthates. *TRANSACTIONS OF THE INSTITUTION OF MINING AND METALLURGY SECTION C-MINERAL PROCESSING AND EXTRACTIVE METALLURGY*, *95*, C173-C175.

Cases, J. M., Kongolo, M., De Donato, P., Michot, L. J., & Erre, R. (1993). Interaction between finely ground pyrite and potassium amylxanthate in flotation: 1. Influence of alkaline grinding. *International journal of mineral processing*, *38*(3), 267-299.

Castro, S., & Laskowski, J. S. (2011). Froth flotation in saline water. *KONA Powder and Particle Journal*, *29*(4).

Craig, V. S. J., Ninham, B. W., & Pashley, R. M. (1993a). Effect of electrolytes on bubble coalescence. *Nature*, *364*(6435), 317-319.

Craig, V. S. J., Ninham, B. W., & Pashley, R. M. (1993b). The effect of electrolytes on bubble coalescence in water. *The Journal of Physical Chemistry*, *97*(39), 10192-10197.

Dunne, R. (2012). Water Water Everywhere and not a Drop to Drink, Nor do I Know its Whereabouts. *SME Annual Meeting*, 1.

Dimitrijevic, M., Antonijevic, M. M., & Jankovic, Z. (1996). Kinetics of pyrite dissolution by hydrogen peroxide in perchloric acid. *Hydrometallurgy*, *42*(3), 377-386.

Dimitrijević, M., Antonijević, M. M., & Dimitrijević, V. (1999). Investigation of the kinetics of pyrite oxidation by hydrogen peroxide in hydrochloric acid solutions. *Minerals Engineering*, *12*(2), 165-174.

Deng, M., Karpuzov, D., Liu, Q., & Xu, Z. (2013). Cryo‐XPS study of xanthate adsorption on pyrite. *Surface and Interface Analysis*, *45*(4), 805-810.

Du, H., & Miller, J. D. (2007). Interfacial water structure and surface charge of selected alkali chloride salt crystals in saturated solutions: A molecular dynamics modeling study. *The Journal of Physical Chemistry C*, *111*(27), 10013-10022.

Demoisson, F., Mullet, M., & Humbert, B. (2007). Investigation of pyrite oxidation by hexavalent chromium: Solution species and surface chemistry. *Journal of colloid and interface science*, *316*(2), 531-540.

De Donato, P., Mustin, C., Benoit, R., & Erre, R. (1993). Spatial distribution of iron and sulphur species on the surface of pyrite. *Applied Surface Science*, *68*(1), 81-93.

Descostes, M., Mercier, F., Thromat, N., Beaucaire, C., & Gautier-Soyer, M. (2000). Use of XPS in the determination of chemical environment and oxidation state of iron and sulfur samples: constitution of a data basis in binding energies for Fe and S reference compounds and applications to the evidence of surface species of an oxidized pyrite in a carbonate medium. *Applied Surface Science*, *165*(4), 288-302.

Eggleston, C. M., Ehrhardt, J. J., & Stumm, W. (1996). Surface structural controls on pyrite oxidation kinetics: An XPS-UPS, STM, and modeling study. *American Mineralogist*, *81*(9), 1036-1056.

Finkelstein, N. P. (1967). Kinetic and thermodynamic aspects of the interaction between potassium ethyl xanthate and oxygen in aqueous solution. *Trans. Inst. Min. Metall.*, *76*, C51-C59.

Finkelstein, N. P. (1970). Quantitative aspects of the role of oxygen in the interaction between xanthate and galena. *Separation Science*, *5*(3), 227-256.

Fleming, M. G. (1952). Effects of alkalinity on the flotation of lead minerals. *Min. Eng*, *4*(12), 1231-1236.

Finkelstein, N. P., Allison, S. A., Lovell, V. M., & Stewart, B. V. (1975). Natural and induced hydrophobicity in sulfide mineral systems. In *Advances in*

Interfacial Phenomena of Particulate/Solution/Gas Systems (Vol. 71, pp. 165-175). Am Inst Chem Eng, Symp Ser New York.

Flint, L. R., & Howarth, W. J. (1971). The collision efficiency of small particles with spherical air bubbles. *Chemical Engineering Science*, *26*(8), 1155-1168.

Fuerstenau, M. C., Kuhn, M. C., & Elgillani, D. A. (1968). The role of dixanthogen in xanthate flotation of pyrite. *Trans. AIME*, *241*, 148-156.

Fielding, L. J., Porter, Q. N., & Winter, G. (1980). Sigmatropic rearrangements of unsaturated dixanthogens. *Australian Journal of Chemistry*, *33*(12), 2615-2619.

Fornasiero, D., & Ralston, J. (1992). Iron hydroxide complexes and their influence on the interaction between ethyl xanthate and pyrite. *Journal of colloid and interface science*, *151*(1), 225-235.

Fuerstenau, D. W., Rosenbaum, J. M., & Laskowski, J. (1983). Effect of surface functional groups on the flotation of coal. *Colloids and Surfaces*, *8*(2), 153-173.

Goldhaber, M. B. (1983). Experimental study of metastable sulfur oxyanion formation during pyrite oxidation at pH 6-9 and 30oC. *American Journal of Science*, *283*(3), 193-217.

Giannetti, B. F., Bonilla, S. H., Zinola, C. F., & Rabóczkay, T. (2001). A study of the main oxidation products of natural pyrite by voltammetric and photoelectrochemical responses. *Hydrometallurgy*, *60*(1), 41-53.

Gonzalez-Elipe, A. R., Espinos, J. P., Fernandez, A., & Munuera, G. (1990). XPS study of the surface carbonation/hydroxylation state of metal oxides.*Applied Surface Science*, *45*(2), 103-108.

Granville, A., Finkelstein, N. P., & Allison, S. A. (1972). Review of reactions in the flotation system galena-xanthate-oxygen. *Trans. IMM*, *81*, C1-C30.

Greenlee, L. F., Lawler, D. F., Freeman, B. D., Marrot, B., & Moulin, P. (2009). Reverse osmosis desalination: water sources, technology, and today's challenges. *Water research*, *43*(9), 2317-2348.

Gardner, J. R., & Woods, R. (1977). Electrochemical investigation of contact angle and of flotation in the presence of alkylxanthates. II. Galena and pyrite surfaces. *Australian Journal of Chemistry*, *30*(5), 981-991.

Hernandez-Aguilar, J. R., Coleman, R. G., Gomez, C. O., & Finch, J. A. (2004). A comparison between capillary and imaging techniques for sizing bubbles in flotation systems. *Minerals Engineering*, *17*(1), 53-61.

Horn, R. G., Del Castillo, L. A., & Ohnishi, S. (2011). Coalescence map for bubbles in surfactant-free aqueous electrolyte solutions. *Advances in colloid and interface science*, *168*(1), 85-92.

Hancer, M., Celik, M. S., & Miller, J. D. (2001). The significance of interfacial water structure in soluble salt flotation systems. *Journal of Colloid and Interface Science*, *235*(1), 150-161.

Harris, P. J., & Finkelstein, N. P. (1975). Interactions between sulphide minerals and xanthates, I. The formation of monothiocarbonate at galena and pyrite surfaces. *International Journal of Mineral Processing*, *2*(1), 77-100.

Hung, C. C., Lee, W. H., Hu, S. Y., Chang, S. C., Chen, K. W., & Wang, Y. L. (2008). Investigation of Bis-(3-sodiumsulfopropyl disulfide) (SPS) decomposition in a copper-electroplating bath using mass spectroscopy. *Journal of The Electrochemical Society*, *155*(5), H329-H333.

Huminicki, D. M., & Rimstidt, J. D. (2009). Iron oxyhydroxide coating of pyrite for acid mine drainage control. *Applied Geochemistry*, *24*(9), 1626-1634.

Ikumapayi, F., Sis, H., Johansson, B., & Rao, K. H. (2012). Recycling process water in sulfide flotation, Part B: Effect of H. *Minerals & Metallurgical Processing*, *29*(4), 192-198.

Ihs, A., Uvdal, K., & Liedberg, B. (1993). Infrared and photoelectron spectroscopic studies of ethyl and octyl xanthate ions adsorbed on metallic and sulfidized gold surfaces. *Langmuir*, *9*(3), 733-739.

Jovancicevic, V., Bockris, J. M., Carbajal, J. L., Zelenay, P., & Mizuno, T. (1986). Adsorption and absorption of chloride ions on passive iron systems.

Journal of The Electrochemical Society, *133*(11), 2219-2226.

Janetski, N. D., Woodburn, S. I., & Woods, R. (1977). An electrochemical investigation of pyrite flotation and depression. *International Journal of Mineral Processing*, *4*(3), 227-239.

Khan, S. U. M., Baltrus, J. P., Lai, R. W., & Richardson, A. G. (1991). X-ray photoelectron spectroscopic study of the interaction of xanthate with coal pyrite and mineral pyrite surfaces. *Applied surface science*, *47*(4), 355-363.

Khmeleva, T. N., Georgiev, T. V., Jasieniak, M., Skinner, W. M., & Beattie, D. A. (2005). XPS and ToF-SIMS study of a chalcopyrite–pyrite–sphalerite mixture treated with xanthate and sodium bisulphite. *Surface and interface analysis*, *37*(8), 699-709.

Kartio, I., Laajalehto, K., Suoninen, E., Karthe, S., & Szargan, R. (1992). Technique for XPS measurements of volatile adsorbed layers: application to studies of sulphide flotation. *Surface and interface analysis*, *18*(12), 807-810.

Klassen, V. I., & Mokrousov, V. A. (1963). *An introduction to the theory of flotation*. Butterworths.

Knipe, S. W., Mycroft, J. R., Pratt, A. R., Nesbitt, H. W., & Bancroff, G. M. (1995). X-ray photoelectron spectroscopic study of water adsorption on iron sulphide minerals. *Geochimica et Cosmochimica Acta*, *59*(6), 1079-1090.

Lowson, R. T. (1982). Aqueous oxidation of pyrite by molecular oxygen.*Chemical Reviews*, *82*(5), 461-497.

Laajalehto, K., Leppinen, J., Kartio, I., & Laiho, T. (1999). XPS and FTIR study of the influence of electrode potential on activation of pyrite by copper or lead. *Colloids and Surfaces A: Physicochemical and Engineering Aspects*, *154*(1), 193-199.

Lehmann, M. N., Stichnoth, M., Walton, D., & Bailey, S. I. (2000). The effect of chloride ions on the ambient electrochemistry of pyrite oxidation in acid media.*Journal of the Electrochemical Society*, *147*(9), 3263-3271.

Levay, G., Smart, R. S. C., & Skinner, W. M. (2001). The impact of water quality on flotation performance. *Journal of the South African Institute of Mining and Metallurgy (South Africa)*, *101*(2), 69-75.

Miller, D. J., Biesinger, M. C., & McIntyre, N. S. (2002). Interactions of CO_2 and CO at fractional atmosphere pressures with iron and iron oxide surfaces: one possible mechanism for surface contamination?. *Surface and interface analysis*, *33*(4), 299-305.

Murphy, C. N., & Winter, G. (1973). Monothiocarbonates and their oxidation to disulphides. *Australian Journal of Chemistry*, *26*(4), 755-760.

Mielczarski, J., Werfel, F., & Suoninen, E. (1983). XPS studies of interaction of xanthate with copper surfaces. *Applications of surface science*, *17*(2), 160-174.

Nesbitt, H. W., & Muir, I. J. (1998). Oxidation states and speciation of secondary products on pyrite and arsenopyrite reacted with mine waste waters and air. *Mineralogy and Petrology*, *62*(1-2), 123-144.

Pang, J., Briceno, A., & Chander, S. (1990). A study of pyrite/solution interface by impedance spectroscopy. *Journal of The Electrochemical Society*, *137*(11), 3447-3455.

Pang, J., & Chander, S. (1990). Oxidation and wetting behavior of chalcopyrite in the absence and presence of xanthates. *Minerals and Metallurgical Processing*, *7*, 149-155.

Phillip, B., & Fichte, C. (1960). Kinetische Untersuchungen zur Zersetzung von Xanthogenaten. *Faserforsch. Tex. Tech.*, *11*, 118-124.

Pou, T. E., Murphy, O. J., Young, V., Bockris, J. O. M., & Tongson, L. L. (1984). Passive films on iron: the mechanism of breakdown in chloride containing solutions. *Journal of the Electrochemical Society*, *131*(6), 1243-1251.

Palagi, C. G., & Stillar, S. S. (1976). Anaconda C. E. Weed Concentrator. *Flotation--A. M. Gaudin Memorial* (pp. 1029-1042). AIME New York, NY.

Pillai, K. C., Young, V. Y., & Bockris, J. M. (1985). X-ray photoelectron spectroscopy studies of xanthate adsorption on pyrite mineral surfaces.*Journal of colloid and interface science*, *103*(1), 145-153.

Reid, E. E. (1958). *Organic chemistry of bivalent sulfur* (Vol. 1). Chemical Publishing Company.

Rogers, J. (1962). Principles of sulfide mineral flotation. In *Froth Flotation* (pp. 139-169). AIME New York, NY.

Ranta, L., Minni, E., Suoninen, E., Heimala, S., Hintikka, V., Saari, M., & Rastas, J. (1981). XPS studies of adsorption of xanthate on sulfide surfaces. *Applications of surface science*, *7*(4), 393-401.

Sutherland, K. L. (1948). Physical chemistry of flotation. XI. Kinetics of the flotation process. *The Journal of Physical Chemistry*, *52*(2), 394-425.

Smart, R. S., Amarantidis, J., Skinner, W. M., Prestidge, C. A., La Vanier, L., & Grano, S. R. (2003). *Surface analytical studies of oxidation and collector adsorption in sulfide mineral flotation* (pp. 3-62). Springer Berlin Heidelberg.

Szargan, R., Karthe, S., & Suoninen, E. (1992). XPS studies of xanthate adsorption on pyrite. *Applied surface science*, *55*(4), 227-232.

Sheikh, N., & Leja, J. (1977). Mössbauer spectroscopy of Fe xanthates. *Separation Science*, *12*(5), 529-540.

Sheikh, N., & Leja, J. (1973). Evaluation of iron xanthates by mossbauer spectroscopy. *Can. Min. Metall. Bull.*, *66*(8), 31.

Sutherland, K. L., & Wark, I. W. (1955). Principles of Flotation, Australasian Institute of Mining and Metallurgy. *Inc., Melbourne*, *164*.

Tolley, W., Kotlyar, D., & Van Wagoner, R. (1996). Fundamental electrochemical studies of sulfide mineral flotation. *Minerals Engineering*,*9*(6), 603-637.

Todd, E. C., Sherman, D. M., & Purton, J. A. (2003). Surface oxidation of pyrite under ambient atmospheric and aqueous (pH= 2 to 10) conditions: electronic structure and mineralogy from X-ray absorption spectroscopy. *Geochimica et Cosmochimica Acta*, *67*(5), 881-893.

Valdivieso, A. L., López, A. S., & Song, S. (2005). On the cathodic reaction coupled with the oxidation of xanthates at the pyrite/aqueous solution interface. *International Journal of Mineral Processing*, *77*(3), 154-164.

Velásquez, P., Leinen, D., Pascual, J., Ramos-Barrado, J. R., Cordova, R., Gómez, H., & Schrebler, R. (2001). XPS, SEM, EDX and EIS study of an electrochemically modified electrode surface of natural chalcocite (Cu 2 S).*Journal of Electroanalytical Chemistry*, *510*(1), 20-28.

Weber, M. E. (1981). Collision efficiencies for small particles with a spherical collector at intermediate Reynolds numbers. *J. Separation Process Tcchnol*, *2*, 29-33.

Wang, X. H., & Forssberg, K. E. (1991). Mechanisms of pyrite flotation with xanthates. *International journal of mineral processing*, *33*(1), 275-290.

Wang, X., Forssberg, K. E., & Bolin, N. J. (1989). Thermodynamic calculations on iron-containing sulphide mineral flotation systems, I. The stability of iron-xanthates. *International Journal of Mineral Processing*, *27*(1), 1-19.

Weber, M. E., & Paddock, D. (1983). Interceptional and gravitational collision efficiencies for single collectors at intermediate Reynolds numbers. *Journal of Colloid and Interface Science*, *94*(2), 328-335.

Wark, E. E., & Wark, I. W. (1933). The Physical Chemistry of Flotation. III. The Relationship between Contact Angle and the Constitution of the Collector. *The Journal of Physical Chemistry*, *37*(6), 805-814.

Winter, G., & Woods, R. (1973). The relation of collector redox potential to flotation efficiency: monothiocarbonates. *Separation Science*, *8*(2), 261-267.

Wang, J., Xie, L., Liu, Q., & Zeng, H. (2015). Effects of salinity on xanthate adsorption on sphalerite and bubble–sphalerite interactions. *Minerals Engineering*, *77*, 34-41.

Yoon, R. H., & Luttrell, G. H. (1989). The effect of bubble size on fine particle flotation. *Mineral Processing and Extractive Metallurgy Review*, *5*(1-4), 101-122.

Chapter 6 The Effect of High Saline Water on the Electrochemical Flotation Performance of Chalcopyrite and Pyrite

6.1 Introduction

The floatabilities of sulfide mineral are controlled by the surface hydrophobicity. Conventional models for the flotation of sulfide mineral are by the addition of collectors. Some sulfide minerals also demonstrate good floatabilities in the absence of the collectors at suitable electrochemical conditions, which are called collectorless flotation. Collectorless flotation of sulfide minerals is neither a new nor an unimportant concept. It has been commercially practiced since nearly the start of last century. A lot of studies have been conducted on floatability of sulfide minerals without collector since it was first recognized by Ravitz and Porter in 1933. Similar results of collectorless flotation have also been found for chalcopyrite, pyrite and arsenopyrite (Finkelstein et al., 1975; Lepetic, 1974; Plaksin, 1959). Fuerstenau and Sabacky (1981) reported that galena, chalcopyrite, chalcocite, pyrite and copper-activated sphalerite were almost completely floatable without collector in water containing less than 5 ppb of oxygen with single mineral and in anaerobic laboratory conditions.

It is very important to distinguish the term "natural floatability" and "collectorless flotation". The differences between those two concepts are quite subtle. Minerals such as orpiment, realgar, and stibnite are very easy to float without the addition of collectors and no specific Eh is required for flotation, which are natural floatability. They also don’t display any differences in the floatability at different Eh. This behavior is linked to the chemical bonding and the crystal structure of each single mineral. A relatively nonpolar surface will be exposed after fracture (Arbiter et al., 1964). Other sulfide minerals like chalcopyrite don’t display the natural floatability. The collectorless flotation is only possible under certain Eh conditions for these minerals. From the literature, it is possible to rank sulfide minerals in the approximate order of relative ease of collectorless flotation (Hayes, 1987). Table 6.1 lists the relative order of the sulfide minerals in collectorless flotation, even though the exact ranking of some of the minerals are questionable. Heyes and Trahar (1979) and Guy and Trahar (1985) have also ranked the descending order of collectorless floatability as: chalcopyrite, galena, pyrrhotite, pentlandite, covellite, bornite, chalcocite, sphalerite, pyrite and arsenopyrite. The collectorless flotation of first four minerals is quite high over a wide range of particles size and the last four minerals display little collectorless floatability. We could see that the order of collectorless floatability as shown in Table 6.1 is the same order with the rest potential even though chalcopyrite has an anomalous position, which indicates that the collectorless floatability have a good correspondence with the rest potential of mineral. It seems like that the more cathodic or reducing the rest potential, the more readily it floats without a collector (Hayes, 1987).

Table 6.1 Approximate order of collectorless flotation of sulfide minerals (descending order of floatability)

Rest potentials for sulfide minerals in water at pH 4 are also give (Majima, 1969)

Mineral		Rest potential (V vs. SHE)	
Molybdenite	MoS_2	0.11	
Stibnite	Sb_2S_3	0.12	
Argentite	AgS	0.28	
Galena	PbS	0.40	
Bornite	Cu_5FeS_4	0.42	
Covellite	CuS	0.45	
Sphalerite	ZnS	0.46	
(Chalcopyrite	$CuFeS_2$	0.56)*	
Marcasite	(Zn, Fe)S	0.63	
Pyrite	FeS	0.66	most readily oxidized

* (anomalous)

The hydrophobic species responsible for the collectorless flotation for each single sulfide mineral are still debatable. Sulphur-based compounds, i.e. elemental sulfur, sulfur-enriched metal-deficient sulfide or a metal polysulfide are commonly expected as the source of collectorless flotation and the surface species may be quite different in different circumstances for different sulfide minerals (Smart, 1991). All of the studies about collectorless flotation imply that an oxidizing potential is required for the collectorless flotation. As mentioned by Gaudin (1974), only extremely low levels of oxygen are required to establish an oxidizing Eh in water at near neutral pH.

There are two methods to control the Eh, which are potentiostatic control method and chemical control method. The potentiostatic control is achieved with a platinum mesh working electrode contacting with mineral particles. It is much cleaner than chemical control since it doesn't need to add any redox agents into the flotation pulp which may induce some certain interactions with mineral. Besides, potentiostatic control can also be directly controlled to any desired value, whereas chemical control is less flexible and the addition of redox agents can't be quantified to obtain a certain Eh.

Most of the studies on the collectorless flotation have been undertaken on isolated minerals. For mixed minerals or real minerals, there are more than one sulfide minerals contacting with aqueous electrolyte, which make the galvanic interaction play an important role in the flotation of these minerals. The effect of mineral-mineral interaction on flotation has been studied by using electrochemical methods and surface characterization methods (Nakazawa, 1985; Rao & Natarajan, 1989a, b). The formation of galvanic interaction between mineral is because the difference in the rest potentials. The mineral with higher rest potential (noble mineral) acts as a cathode and the one with lower rest potential (active mineral) acts as an anode electrode. A galvanic current flow between the minerals will alter the mineral surfaces. The presence of dissolved oxygen in the pulp is very significant for the galvanic interaction since oxygen acts as an electron acceptor reacting to form hydroxide on noble minerals.

In this study, the collectorless flotation of chalcopyrite and pyrite and the minerals in different process water were explored and cyclic voltammetry was used to explore the difference on the flotation behaviors.

6.2 Experimental methods

6.2.1 Collectorless flotation by potentiostatic control

For the collectorless flotation by potentiostatic control, a modified Hallimond flotation tube with a three electrodes system was used (Figure 2.3). The reference electrode was calomel electrode. The counter electrode was platinum foil. The working electrode was a cylinder without bottom made by platinum mesh. The three electrodes system was controlled by CHI600E series electrochemical analyzer/workstation (CH Instruments, Inc., Austin). The mineral particles were stirred in the flotation cell and kept interacting with the platinum mesh to attain a desired potential.

All the process water used in the experiment was pretreated before used. The water need to be purged with high purity nitrogen (purity ≧ 99.999 %) for 1 hour. For the single pure mineral flotation, 1.5 g mineral particles were then transferred to the flotation cell by the de-oxygen process water. For the mixed mineral flotation, 0.75 g chalcopyrite and 0.75 g pyrite were mixed and quickly transferred to the flotation cell by the de-oxygen process water. The water was then added to approximately the same position with the upper nitrogen inlet. The upper nitrogen inlet was then purged with high purity nitrogen to exhaust the air trap in the cell and prevent the oxidation of the mineral in the pulp. The stir bar at the bottom of the cell was adjusted to make mineral particles efficiently contact with the platinum mesh. The mineral particles were conditioned at a set potential for 30 min. When the conditioning is completed, the upper nitrogen was shut down and the lower nitrogen was purged into the cell with the flow rate of 30 sccm. The speed of the stir bar was set at 700 rpm to make the flotation experiment effectively.

6.2.2 Voltammetry measurement

Chunk chalcopyrite sample was cut into an approximately 1 × 1 × 0.8 cm block. Copper wire was welded on the top of the block before it was mounted in epoxy resin.

A fresh surface was generated before each measurement by wet-polished by a series of polishing papers down to 1000 grade and rinsed with sufficient Milli-Q water. The chalcopyrite was transferred to the cell (Figure 6.1) immediately after the conditioning. Before each experiment, the solution used in the cell was purged by high purity nitrogen (purity ≧ 99.999 %) for 1 hour to remove most of the oxygen containing in the solution. During the voltammetry measurements, the needle that purged nitrogen was lifted up to the top of the solution to make the solution stay in a quiescent condition and prevent the oxygen in the air from dissolving in solutions at the same time.

Both cyclic voltammetry and linear sweep voltammetry techniques were used in the voltammetry measurement. The CHI600E electrochemical analyzer/workstation (CH Instruments, Inc., Austin) was used to do the analysis. The measurement of chalcopyrite sample was cycled between - 0.6 V and 0.8 V. The voltammograms were recorded at a rate of 4 mV/s in different solutions.

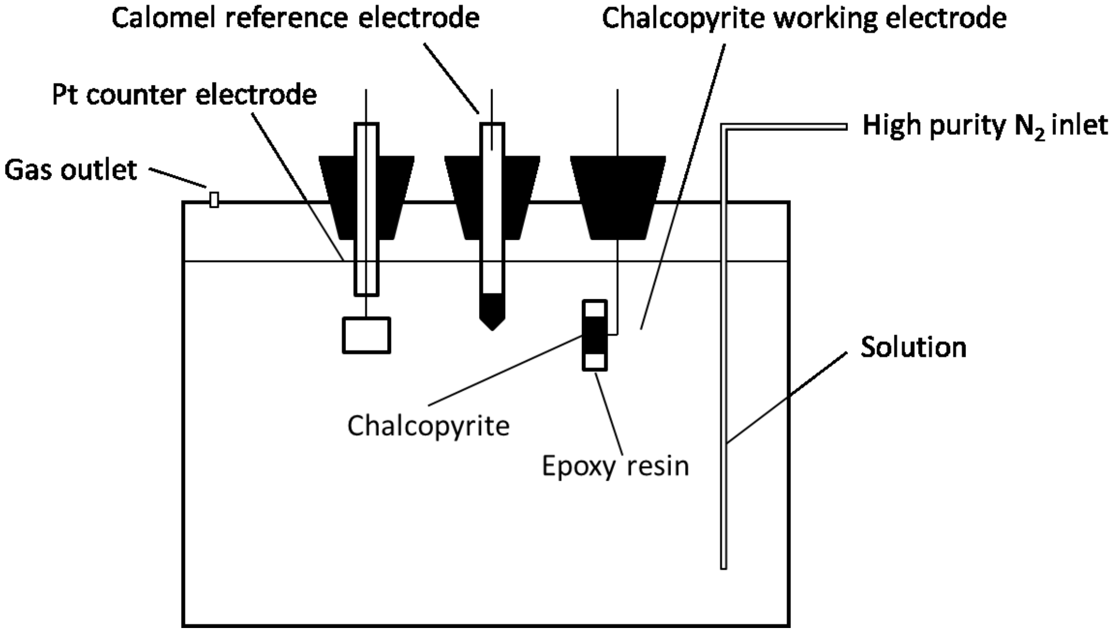

Figure 6.1 Schematics of voltammetry measurement cell

6.3 Results and discussion

6.3.1 Collectorless flotation of single mineral

Figure 6.2 shows the flotation response of chalcopyrite at different Eh in buffer solution, 0.4 M NaCl solution and sea water at pH 9.6, respectively. It can be seen from Figure 6.2 that chalcopyrite exhibits good collectorless flotation in oxidizing environment in the three different process water. The maximum flotation recovery of chalcopyrite is almost the same in the three different solutions, about 90 %. At reducing environment, chalcopyrite was found to be weakly floatable.

An interesting question is that what caused the sulfide minerals floatable without the addition of any collector. There is no doubt that elemental sulfur plays a significant role in acidic pH where it is thermodynamically stable at that region. However, there is no sufficient evidence to prove that elemental sulfur is the sole species responsible for the flotation in alkaline pH. According to equation 6.1 suggested by Gardner and Woods (1979), it shows that the product of elemental sulfur should be responsible for the flotation in alkaline solutions. From thermodynamic considerations, sulfate is easier to form than sulfur. However, the formation of sulfate from sulfides exhibits a considerable degree of irreversibility (Peters, 1977) and sulfur can exist as a metastable phase. Then the elemental sulfur was latterly detected by ESCA on oxidized chalcopyrite by Buckley and Woods (1982). However, Luttrell and Yoon (1983) showed that the elemental sulfur didn’t exceed 1.7 % of the monolayer capacity at pH 10. And at pH 12, it was less than 1 %. As a result, Luttrell and Yoon (1983) suggested that it may be polysulfides rather than elemental sulfur that responsible for the collectorless flotation at alkaline environment, and the formation of polysulfides is favored at oxidizing environments. For the two possible hydrophobic species of elemental sulfur and polysulfides, the former one is likely to be more hydrophobic.

$$CuFeS_2 + 3H_2O = CuS + Fe(OH)_3 + S^0 + 3H^+ + 3e \qquad 6.1$$

Figure 6.3 shows the flotation response of pyrite at different Eh at pH 9.6 in buffer solution, 0.4 M NaCl solution and sea water, respectively. It can be seen from Figure 6.4 that the flotation recoveries of pyrite are very low throughout the whole Eh range in the three different solutions. Heyes and Trahar (1984) also found that pulp potential (Eh) have a significant role in the collectorless flotation of sulfide minerals, but pyrite doesn’t exist a critical pulp potential for collectorless flotation and shows no sign of collectorless flotation with the flotation recovery around 20 % in the whole Eh range. Shuiyu et. al (1993) found that there is no any area of collectorless flotation for pyrite at pH higher than 6. Some investigators claimed the collectorless flotation of pyrite, particularly from coal sources (Fuerstenau & Sabacky, 1981; Esposito, Chander, & Aplan, 1987; Yoon et al., 1991). The results shown in Figure 6.3 are greatly consistent with the results shown in Figure 3.2 at pH 9.6, which is also the result of collectorless flotation of pyrite. There are two reasons for the improvement of pyrite flotation in NaCl solution and sea water compared to buffer solution. First, the increased ion concentration greatly reduced the bubble size and subsequently improved the probability of bubble to collect pyrite particles and improved the flotation recovery. Second, the removal of iron hydroxides/oxides from the surface by chloride ions prevents the oxidation process and inhibits the buildup of hydrophilic passive iron hydroxide/oxide coatings, which also improve the hydrophobicity and flotation recovery.

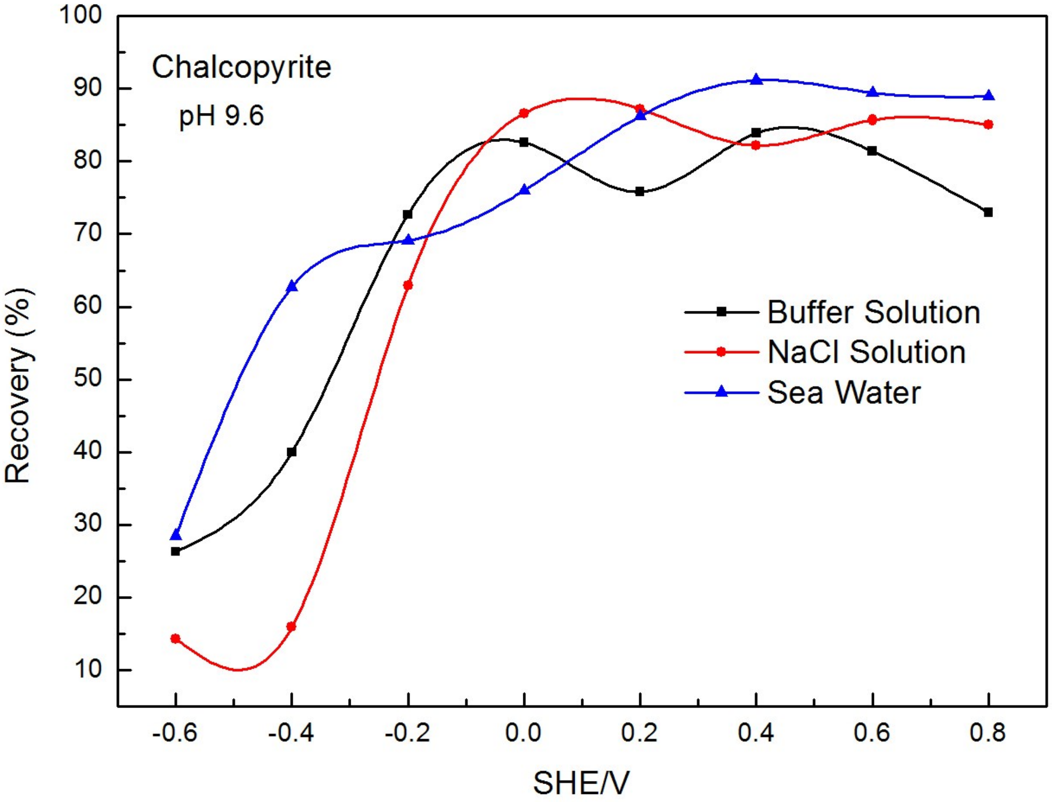

Figure 6.2 Flotation response of chalcopyrite at different Eh in different process water at pH 9.6

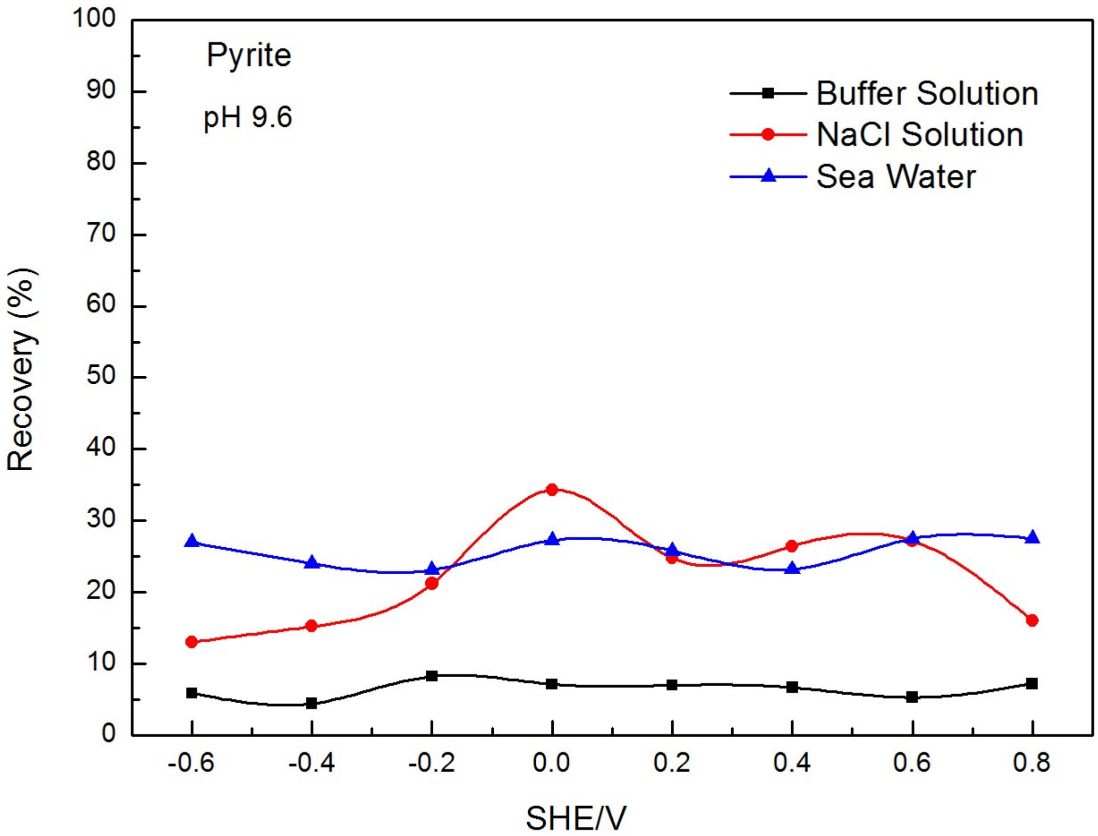

Figure 6.3 Flotation response of pyrite at different Eh in different process water at pH 9.6

6.3.2 Voltammetry measurement

Figure 6.4, Figure 6.5 and Figure 6.6 show the comparison of the potential dependence of chalcopyrite floatability with the cyclic voltammograms in different process water under oxygen-free environment. It can be seen from the comparison of the flotation recovery and cyclic voltammograms that there are good correlation between the potential of onset of the flotation and the onset of the anodic current.

According to Gardner and Woods (1979), the second anodic peak in

Figure 6.4 which commences from 0.1 V corresponds to the reaction as shown in equation 6.1. The first anodic peak in Figure 6.4 which commences from –0.2 V corresponds to the reaction as shown in equation 6.2 (Gardner & Woods, 1979). For the cathodic peak in Figure 6.4, it appears at the same potential as that for iron oxide/hydroxide on a gold electrode in solution as shown in equation 6.3 (Janetski, Woodburn & Woods, 1977; Jiang et al., 2000).

$$H_2S = S + 2H^+ + 2e \qquad 6.2$$

$$Fe(OH)_3 + e = Fe(OH)_2 + OH^- \qquad 6.3$$

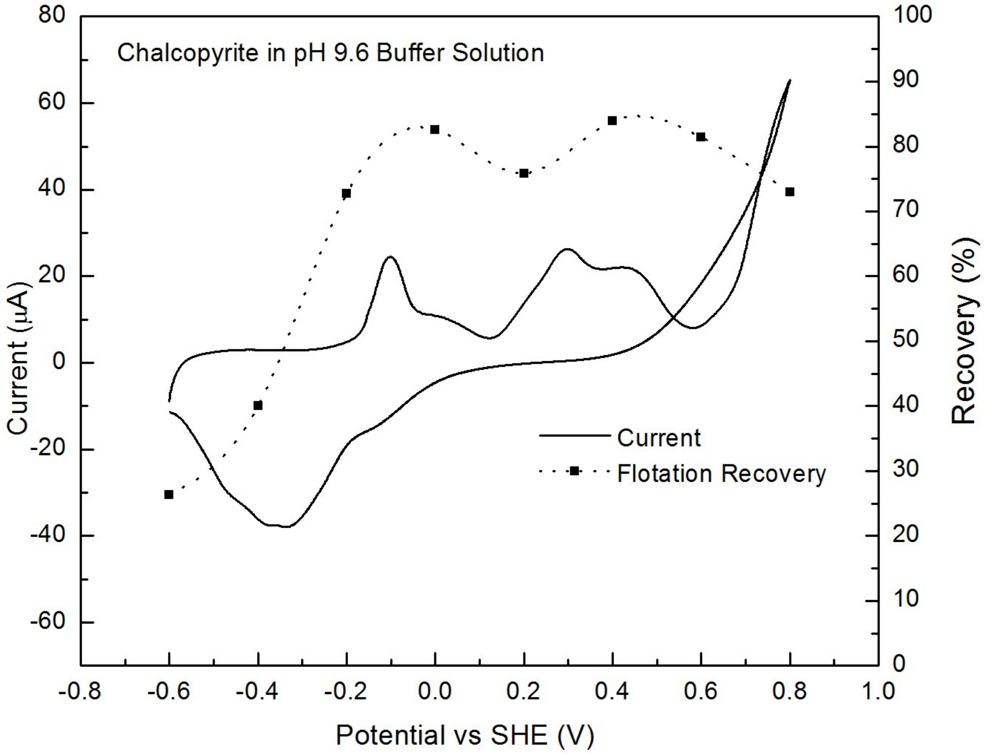

Figure 6.4 Cyclic voltammograms and flotation response of chalcopyrite in pH 9.6 buffer solution at different Eh

Figure 6.5 and Figure 6.6 show that the anodic peak in NaCl solution and sea water is weak compared to that in buffer solution. And the onset of the anodic peak also corresponds to the commencement of the flotation. For the cathodic peak at about −0.5 V in the cathodic sweep, it is attributed to the reaction as shown in equation 6.4 (Jiang et al., 2000).

$$S^0 + H_2O + 3e = HS^- + OH \qquad 6.4$$

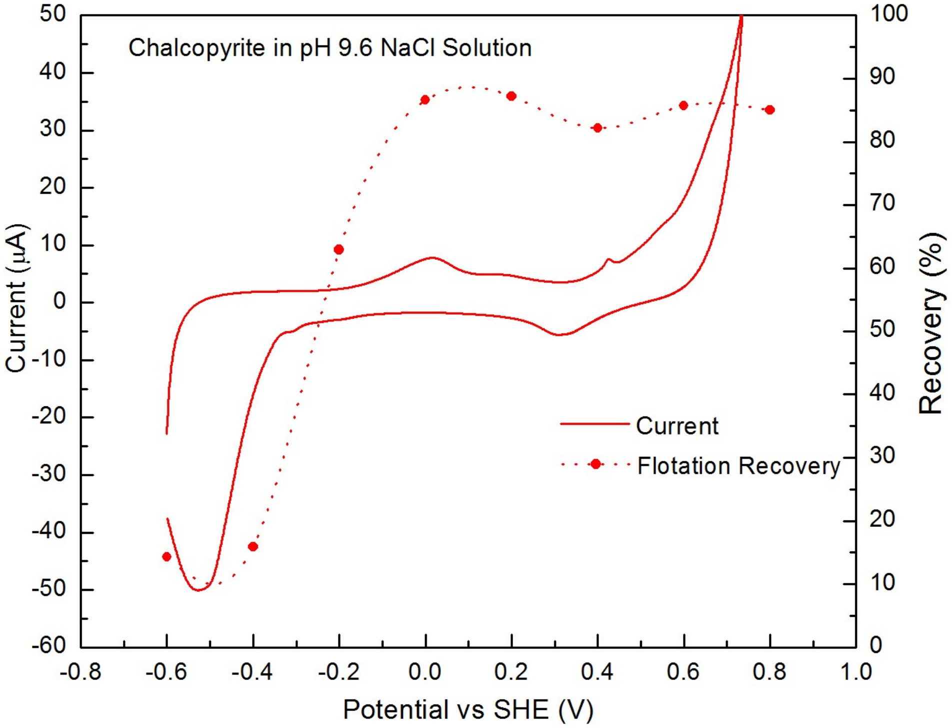

Figure 6.5 Cyclic voltammograms and flotation response of chalcopyrite in pH 9.6 NaCl solution at different Eh

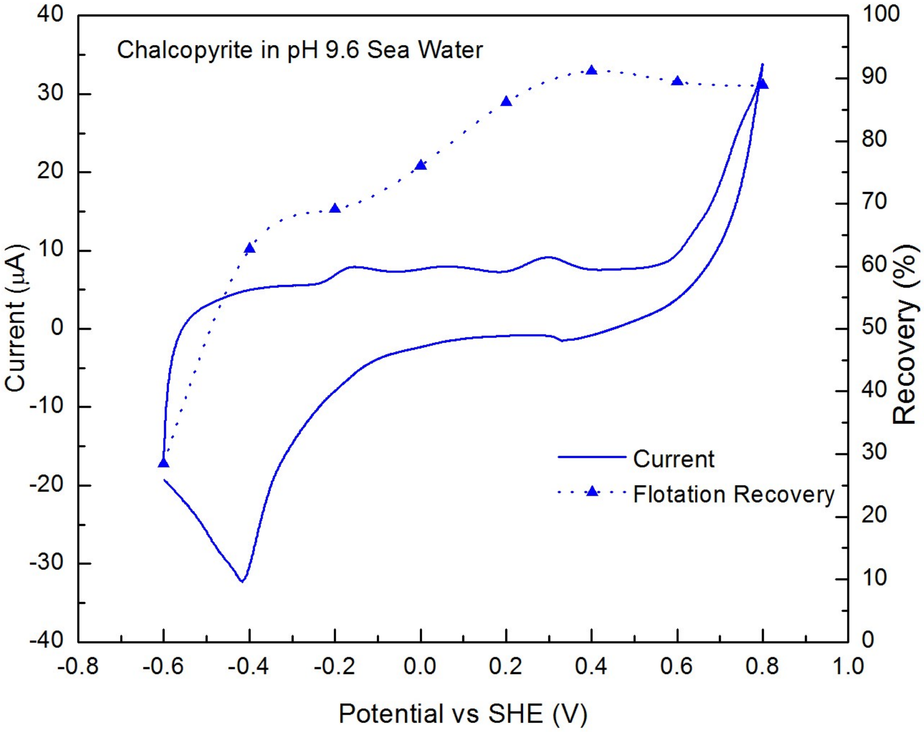

Figure 6.6 Cyclic voltammograms and flotation response of chalcopyrite in pH 9.6 sea water at different Eh

From the comparison of anodic and cathodic current shown in Figure 6.7 and 6.8, it could be found that the intensity of anodic peak in NaCl solution and sea water is much lower than that in buffer solution. Besides, the position of cathodic peak is quite different. In buffer solution, it is the reduction of iron oxide/hydroxide. However, in NaCl solution and sea water, the cathodic peak shift to more reduction potential which corresponds to the reduction of sulfur. Since chloride ion behaves as aggressive anions and is able to destroy passive films on minerals surface, study by Lehmann et al. (2000) has suggested a role of chloride ions in preventing the deposition of S^0 and

S_n^{2-} on pyrite surfaces and also inhibiting the buildup of passive iron hydroxyl/oxide coatings. For that reason, chalcopyrite surface doesn't form the hydrophilic iron hydroxide/oxide coatings, but the formation of hydrophobic elemental sulfur on the surface is also undermined which can be seen from the reduced intensity of anodic current. In NaCl solution and sea water, the removal of hydrophilic iron hydroxide/oxide and the much smaller bubble compared to that in buffer solution should greatly improve the flotation recovery of chalcopyrite, but the flotation recovery is almost the same with that in buffer solution, which further indicates that the formation of hydrophobic elemental sulfur on the surface is impaired in NaCl solution and sea water.

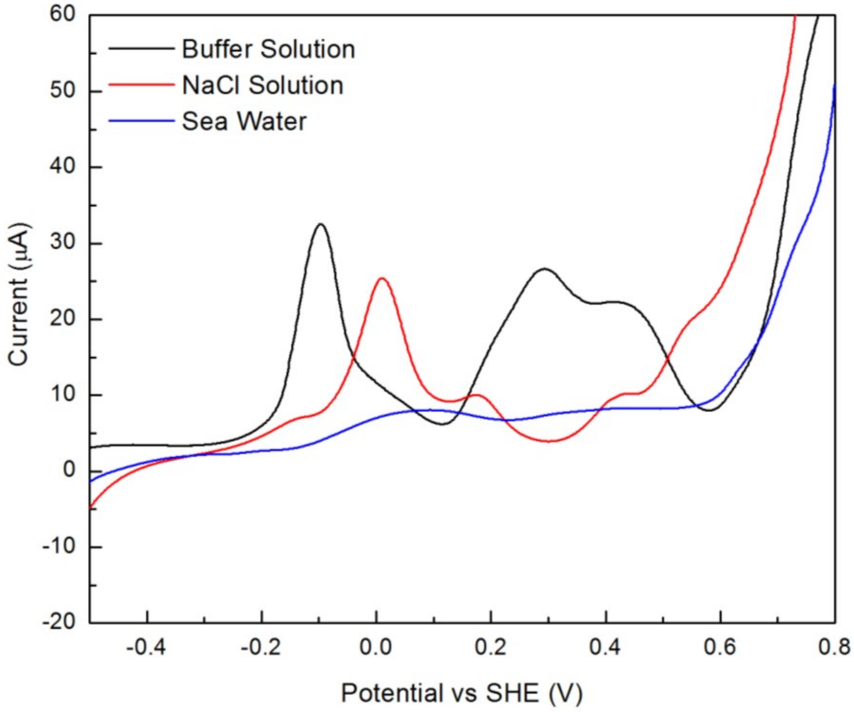

Figure 6.7 Anodic current of chalcopyrite at different Eh in different process

water at pH 9.6

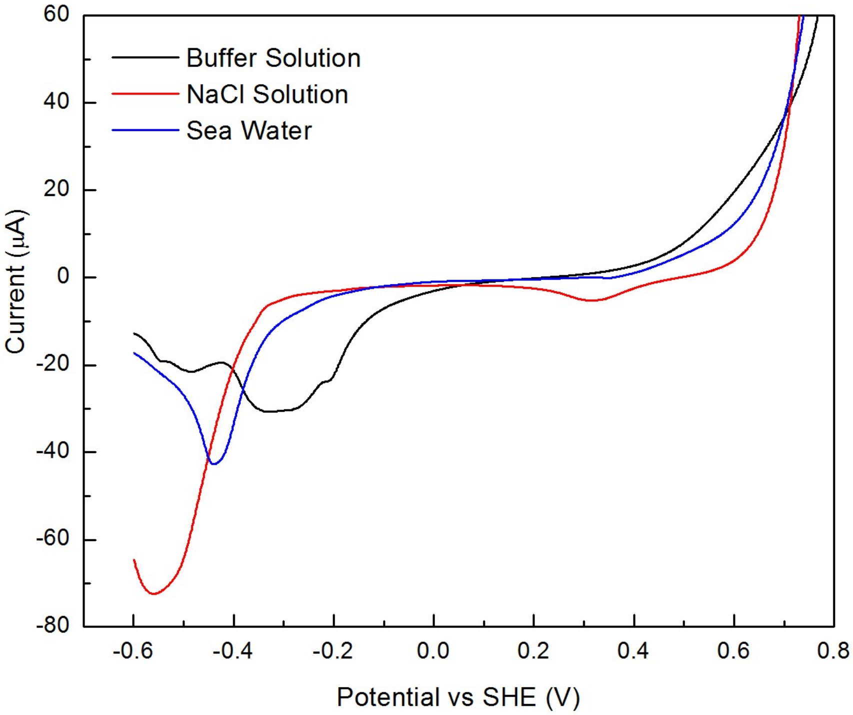

Figure 6.8 Cathodic current of chalcopyrite at different Eh in different process water at pH 9.6

6.3.3 Collectorless flotation of mixed mineral

Figure 6.9, 6.10 and 6.11 show the flotation response of chalcopyrite and pyrite in the mixed mineral system as compared to single mineral system in pH 9.6 buffer solution, NaCl solution and sea water respectively. Comparison of the results of single pure mineral with mixed mineral shows that the flotation of chalcopyrite is depressed in mixed mineral system and the flotation of pyrite is also depressed slightly in NaCl solution and sea water. In the galvanic cell which contains both chalcopyrite and pyrite, pyrite with higher rest potential will act as a cathode and chalcopyrite with lower rest potential will act as an anode. The electrons will flow from chalcopyrite to pyrite forming a galvanic cell and this electrons transfer will be enhanced by the very small amount of oxygen in solution which serves as an electron acceptor. The current is called galvanic current. The increase in the rate of anodic actions at the chalcopyrite surface may speed up the oxidation of elemental sulfur to hydrophilic sulfate or sulphoxy compounds on the chalcopyrite surface and depress the collectorless flotation. Besides, the dissolved iron ions were diffused into the solution. And the oxidation to hydrophilic ferric hydroxide/oxide is also enhanced (Ekmekçi & Demirel, 1997). Since self-induced flotation is very sensitive to the inhibition effect from hydroxides (Senior & Trahar, 1991; Grano et al., 1997), the formation of iron oxides/hydroxides on the surface of chalcopyrite will greatly reduce the collectorless floatability.

Even though the flotation of chalcopyrite is depressed in contact with pyrite, it still has a large Eh range which can potentially separate chalcopyrite from pyrite. The collectorless flotation of chalcopyrite and pyrite mixed mineral provide a great opportunity for the separation of chalcopyrite from pyrite.

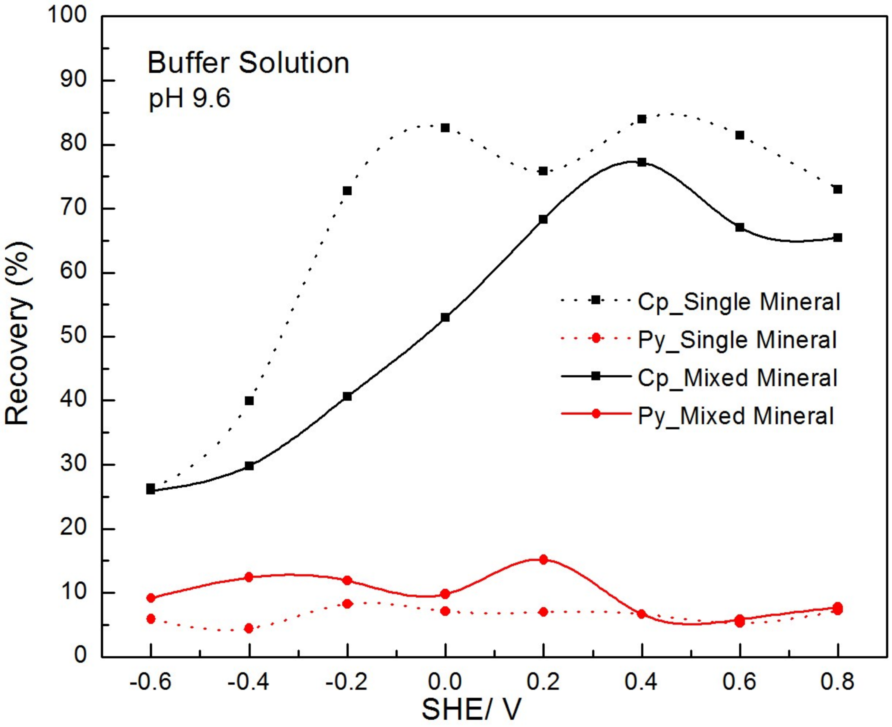

Figure 6.9 Flotation response of chalcopyrite and pyrite mixture (weight ratio 1:1) at different Eh in buffer solution at pH 9.6

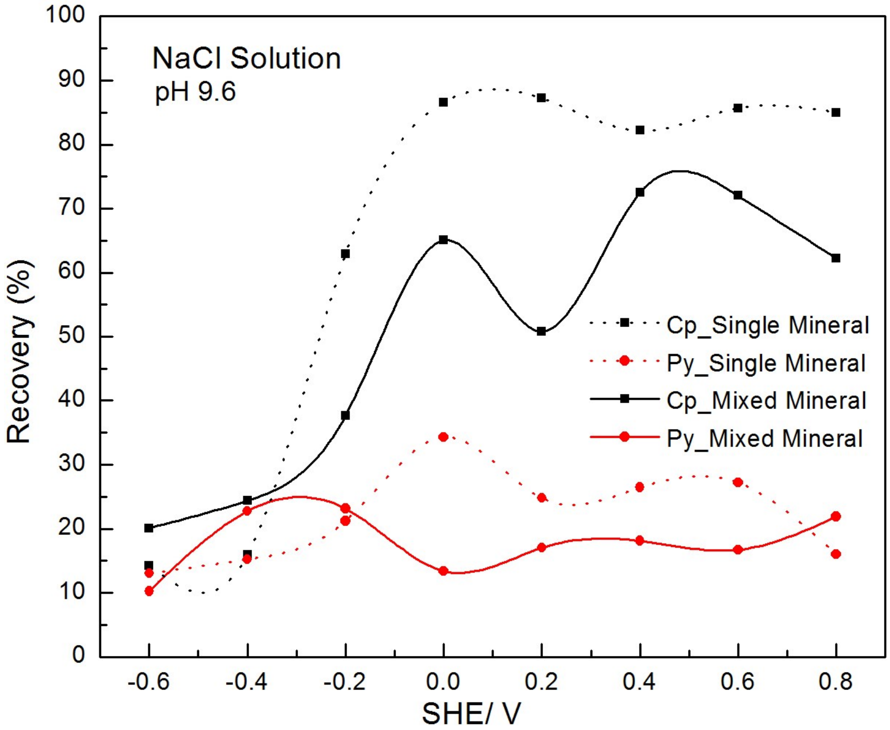

Figure 6.10 Flotation response of chalcopyrite and pyrite mixture (weight

ratio 1:1) at different Eh in NaCl solution at pH 9.6

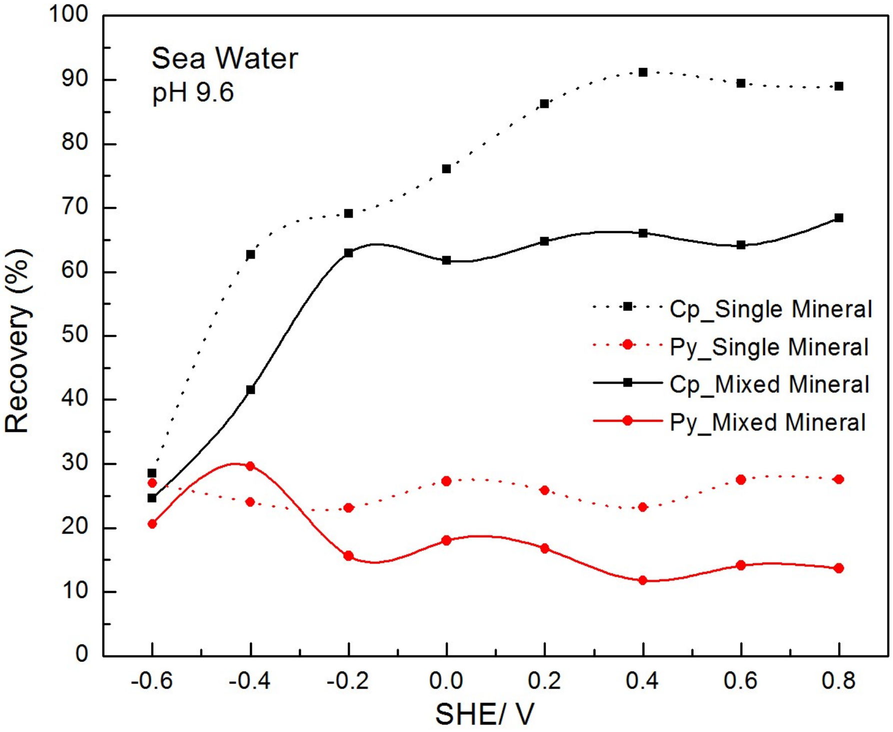

Figure 6.11 Flotation response of chalcopyrite and pyrite mixture (weight ratio 1:1) at different Eh in sea water at pH 9.6

6.4 References

Arbiter, N., Fujii, Y., Raja, A., & Hansen, B. (1964). *Surface properties of hydrophobic solids*. Society of Mining Engineers of AIME.

Buckley, A., & Woods, R. (1982). Investigation of the surface oxidation of sulfide minerals via ESCA and electrochemical techniques. *Interfacial Phenomena in Mineral Processing, Engineering Foundation, New York, NY*, 3-17.

Cheng, X., & IWASAKI, I. (1992). Pulp potential and its implications to sulfide flotation. *Mineral Processing and Extractive Metallurgy Review*, *11*(4), 187-210.

Esposito, M. C., Chander, S., & Aplan, F. F. (1987). Characterization of pyrite from coal sources. *Process Mineralogy VII, TMS, Warrendale, PA*, 475-493.

Ekmekçi, Z., & Demirel, H. (1997). Effects of galvanic interaction on collectorless flotation behaviour of chalcopyrite and pyrite. *International journal of mineral processing*, *52*(1), 31-48.

Finkelstein, N. P., Allison, S. A., Lovell, V. M., & Stewart, B. V. (1975). Natural and induced hydrophobicity in sulfide mineral systems. In *Advances in Interfacial Phenomena of Particulate/Solution/Gas Systems* (Vol. 71, pp. 165-175). Am Inst Chem Eng, Symp Ser New York.

Fuerstenau, M. C., & Sabacky, B. J. (1981). On the natural floatability of sulfides. *International Journal of Mineral Processing*, *8*(1), 79-84.

Gaudin, A. M. (1974). The role of oxygen in flotation. *Journal of Colloid and Interface Science*, *47*(2), 309-314.

Grano, S. R., Sollaart, M., Skinner, W., Prestidge, C. A., & Ralston, J. (1997). Surface modifications in the chalcopyrite-sulphite ion system. I. collectorless flotation, XPS and dissolution study. *International journal of mineral processing*,*50*(1), 1-26.

Guy, P. J., & Trahar, W. J. (1985). The effects of oxidation and mineral interaction on sulfide flotation. In *Flotation of sulfide minerals* (Vol. 6, pp.

91-110). Elsevier Amsterdam.

Gardner, J. R., & Woods, R. (1979). An electrochemical investigation of the natural flotability of chalcopyrite. *International Journal of Mineral Processing*, *6*(1), 1-16.

Hayes, R. A., Price, D. M., Ralston, J., & Smith, R. W. (1987). Collectorless flotation of sulfide minerals. *Mineral Processing and Extractive Metallurgy Review*, *2*(3), 203-234.

Heyes, G. W., & Trahar, W. J. (1979). Oxidation-reduction effects in the flotation of chalcocite and cuprite. *International Journal of Mineral Processing*,*6*(3), 229-252.

Janetski, N. D., Woodburn, S. I., & Woods, R. (1977). An electrochemical investigation of pyrite flotation and depression. *International Journal of Mineral Processing*, *4*(3), 227-239.

Jiang, Y. R., Zhou, L. H., Xue, Y. L., & Zhang, Q. X. (2000). Electrochemical flotation separation of chalcopyrite from molybdenite by CM Eh control. *TRANSACTIONS OF NONFERROUS METALS SOCIETY OF CHINA*, *10*, 110-113.

Lepetic, V. M. (1974). Flotation of chalcopyrite without collector after dry, autogenous grinding. *CIM BULLETIN*, *67*(746), 71-77.

Lehmann, M. N., Stichnoth, M., Walton, D., & Bailey, S. I. (2000). The effect of chloride ions on the ambient electrochemistry of pyrite oxidation in acid media. *Journal of the Electrochemical Society*, *147*(9), 3263-3271.

Luttrell, G. H., & Yoon, R. H. (1983). ESCA and mass spectrometric studies of the collectorless flotation of chalcopyrite. In *111th AIME Annual Meeting, March* (pp. 6-10).

Majima, H. (1969). How oxidation affects selective flotation of complex sulphide ores. *Canadian Metallurgical Quarterly*, *8*(3), 269-273.

Nakazawa, H., & Iwasaki, I. (1985). Effect of pyrite-pyrrhotite contact on their floatabilities. *Miner. Metall. Process.*, *2*(4), 206-220.

Plaksin, I. N. (1959). Interaction of minerals with gases and reagents in flotation. *Trans. AIME*, *214*, 319-324.

Peters, E. (1977). The electrochemistry of sulphide minerals. In *Trends in Electrochemistry* (pp. 167-290). Springer US.

Rao, M. Y., & Natarajan, K. A. (1989a). Effect of electrochemical interactions among sulfide minerals and grinding medium on chalcopyrite flotation. *Minerals and Metallurgical Processing*, *6*(3), 146-151.

Rao, M. Y., & Natarajan, K. A. (1989b). Electrochemical effects of mineral-mineral interactions on the flotation of chalcopyrite and sphalerite. *International Journal of Mineral Processing*, *27*(3), 279-293.

Ravitz, S. F., & Porter, R. R. (1933). Oxygen Free Flotation I: Flotation of Galena in Absence of Oxygen. *Amer. Inst. Min. Metall. Engrs, Tech. Publ*, *513*, 17.

Smart, R. S. C. (1991). Surface layers in base metal sulfide flotation. *Minerals Engineering*, *4*(7), 891-909.

Senior, G. D., & Trahar, W. J. (1991). The influence of metal hydroxides and collector on the flotation of chalcopyrite. *International journal of mineral processing*, *33*(1), 321-341.

Sun, S. Y., Wang, D. Z., & Li, B. D. (1993). The collectorless flotation and separation of chalcopyrite and pyrite by potential control. *Journal of Central-South Institute of Mining and Metallurgy (China)(People's Republic of China)*, *24*(4), 466-471.

Yoon, R. H., Lagno, M. L., Luttrell, G. H., & Mielczarski, J. A. (1991, August). On the hydrophobicity of coal pyrite. In *Proceedings of the IV International Conference on Processing and Utilization of High Sulfur Coals* (pp. 241-253). Elsevier, Amsterdam

Chapter 7 Conclusions and Contributions and Future Work

7.1 Conclusions

In this thesis work, the flotation behaviors of chalcopyrite and pyrite were investigated in different process water at different pHs with different electrolytes by adding various collectors to explore the potential of flotation in high salinity water. Both regular flotation and collectorless flotation are investigated to explore the flotation behavior and related mechanisms. The major conclusions of this thesis work are summarized as follows:

1) The flotation recovery of pyrite is greatly improved in NaCl solution and sea water as compared to that in Milli-Q water. The flotation of pyrite at high pH in Mill-Q water and sea water is greatly depressed, which is caused by the coatings of hydrophilic iron hydroxide and magnesium and calcium hydroxide on pyrite surface. The flotation recovery is the highest with the addition of PAX and the lowest with thionocarbamate among the three collectors. The contact angle results are consistent with the flotation results, which indicate that thionocarbamate has the lowest affinity with pyrite and PAX has the highest affinity with pyrite.

2) The flotation recovery of chalcopyrite is improved in NaCl solution and

sea water with and without collectors as compared to that in Milli-Q water. The performance of thionocarbamate is the best at pH less than 6 and pH 10 in sea water, which provides a potential chance to float chalcopyrite at high pH in sea water.

3) The galvanic interaction plays an important role in the mixed mineral flotation of chalcopyrite and pyrite, which makes the flotation behaviors quite different with single mineral flotation. The flotation of chalcopyrite was depressed and the flotation of pyrite is greatly improved. Even though there are galvanic interaction, pyrite activation and heterocoagulate for the mixed mineral system, the selectivity of thionocarbamate is better than PAX and iPOPECTU for the mixed mineral flotation in all three different solutions.

4) Magnesium and calcium ions in sea water can generate colloidal precipitates forming slime coating on the surface of minerals, which depress the flotation in alkaline condition. The slime coating was confirmed by SEM measurements, ToF-SIMS measurements and in-situ zeta potential distribution measurements. The research provides substantial evidence that slime coating happens on chalcopyrite and pyrite surfaces in sea water at high pH.

5) The concentration of solubilized iron leaching to the solution after 5 min

conditioning of pyrite in different solutions are proportional to the chloride ion concentration in solutions. This results in the removal of iron hydroxides/oxides from the surface by chloride ions, which prevents the oxidation process and inhibits the buildup of hydrophilic passive iron hydroxides/oxides coatings, forming a clean reacting surface.

6) In Milli-Q water, the flotation recoveries of pyrite greatly dropped at near neutral pH. But this low recovery disappeared when the flotation was conducted in NaCl solution and sea water. The consumption of PAX is the lowest in Milli-Q water and much higher in NaCl solution and sea water after 5 min conditioning in 1×10^{-5} M PAX at pH 6, which improve the surface hydrophobicity of pyrite in salt water. The mean value of the bubble size is more than three times smaller in NaCl solution than that in Milli-Q water, which greatly improves the collision probability between bubbles and particles.

7) The electrochemical impedance spectroscopy measurements and ToF-SIMS analysis indicate much less formation of iron hydroxides/oxides and higher porosity on the surface of pyrite in NaCl solution and sea water than that in Milli-Q water. It also indicates the adsorption of xanthate on pyrite surface forming a passivation layer in all the three solutions and this adsorption creates porosity on the surface of

pyrite in salt water but not in Milli-Q water.

8) Negative ions ToF-SIMS spectra of pyrite indicate the formation of amyl monothiocarbonate and amyl carbonate disulphide in NaCl solution and sea water, which may indicate the formation of iron hydroxide xanthate complexes in NaCl solution and sea water and introduce additional collecting power for pyrite flotation at pH 6.

9) The XPS analysis shows that dixanthogen and xanthate are adsorbed on the surface of pyrite conditioned in the three solutions with pyrite conditioned in NaCl solution adsorbs the largest amount. The larger amount of iron hydroxides/oxides on the surface of pyrite conditioned in Milli-Q water indicates more surface oxidation as compared to that conditioned in NaCl solution and sea water, which is consistent with the ToF-SIMS results and EIS results.

10) Collectorless flotation by potentiostatic control shows that chalcopyrite exhibits good collectorless flotation in oxidizing but not reducing environment. There are good correlation between the potential of onset of the flotation and the onset of the anodic current in the cyclic voltammograms. The flotation recoveries of pyrite are very low throughout the whole Eh range at the three different solutions without any sign of collectorless flotation. The flotation recovery of pyrite is

improved in NaCl solution and sea water as compared to buffer solution, which is attributed to reduced bubble size and the removal of hydrophilic iron hydroxides/oxides from pyrite surface by chloride ions. The flotation of the mixed mineral shows that there is still a large Eh range which can potentially separate chalcopyrite from pyrite.

7.2 Contributions to original knowledge

In this study, the flotation behaviors of single pure mineral and mixed mineral of chalcopyrite and pyrite in Milli-Q water, NaCl solution, and sea water are investigated. The performance of different collectors was also evaluated. Previous studies in sea water flotation mainly focused on the flotation of real mineral in industrial scale experiments and the flotation behavior of pyrite itself was rarely studied. The mechanism of pyrite flotation was investigated comprehensively by a range of different techniques and the results are consistent with the flotation results. The research provides substantial evidence of slime coatings on chalcopyrite and pyrite surface in sea water at high pH even with the presence of collector which is quite valuable for further exploration of ways to avoid this slime coating. In conclusion, this study improves our fundamental understanding of mineral flotation in sea water and gains basic knowledge on development of new technology for the depression of pyrite to produce high-grade concentrates of some valuable minerals.

7.3 Future work

Based on the study, there are still some areas for further investigations.

1) The flotation behavior of chalcopyrite and pyrite in NaCl solution with different NaCl concentration is necessary to be explored to figure out the effect of salt concentration to the flotation response.
2) The cyclic voltammograms of chalcopyrite and pyrite in different solutions with the addition of different collectors needs to be done to study the reaction on the mineral surface.
3) An effective method needs to be developed to depress the slime coating on the surface of mineral especially on the surface of chalcopyrite. Adsorption of multivalent cations, hydroxyl complexes and iron hydroxides by quartz is very well documented in the literature. The flotation of valuable mineral with quartz together may be provide a new way to prevent the slime coating forming on the mineral surface. Adding soda ash (Na_2CO_3) to form $CaCO_3$ or $MgCO_3$ should be investigated.
4) The potentiostatic control flotation can combine with the addition of different collectors to explore the combined effect of potentiostatic control and collectors.

5) Mixed collectors system and different flotation gases could be studied to explore the potential application in the sea water flotation to obtain both high recovery and high selectivity.

Bibliography

Antonijević, M. M., Dimitrijević, M., & Janković, Z. (1997). Leaching of pyrite with hydrogen peroxide in sulphuric acid. *Hydrometallurgy*, *46*(1), 71-83.

Antonijević, M. M., Dimitrijević, M. D., Šerbula, S. M., Dimitrijević, V. L. J., Bogdanović, G. D., & Milić, S. M. (2005). Influence of inorganic anions on electrochemical behaviour of pyrite. *Electrochimica acta*, *50*(20), 4160-4167.

Allison, S. A., Goold, L. A., Nicol, M. J., & Granville, A. (1972). A determination of the products of reaction betweer various sulfide minerals and aqueous xanthate solution, and a correlation of the products with electrode rest potentials. *Metallurgical Transactions*, *3*(10), 2613-2618.

Arbiter, N., Fujii, Y., Raja, A., & Hansen, B. (1964). *Surface properties of hydrophobic solids*. Society of Mining Engineers of AIME.

Bulut, G., & Atak, S. (2002). Role of dixanthogen on pyrite flotation: solubility, adsorption studies and Eh, FTIR measurements. *Minerals & metallurgical processing*, *19*(2), 81-86.

Bushell, C. H. G. (1962). Copper activation of pyrite. *Can Min Metall Bull*, *55*(601), 314-318.

Buckley, A., & Woods, R. (1982). Investigation of the surface oxidation of sulfide minerals via ESCA and electrochemical techniques. *Interfacial Phenomena in Mineral Processing, Engineering Foundation, New York, NY*, 3-17.

Buckley, A. N., & Woods, R. (1987). The surface oxidation of pyrite. *Applied Surface Science*, *27*(4), 437-452.

Buckley, A. N., & Woods, R. (1990). X-ray photoelectron spectroscopic and electrochemical studies of the interaction of xanthate with galena in relation to the mechanism proposed by Page and Hazell. *International Journal of Mineral Processing*, *28*(3), 301-311.

Boström, M., Williams, D. R., & Ninham, B. W. (2001). Surface tension of electrolytes: specific ion effects explained by dispersion forces. *Langmuir*, *17*(15), 4475-4478.

Craig, V. S. (2004). Bubble coalescence and specific-ion effects. *Current opinion in colloid & interface science*, *9*(1), 178-184.

Craig, V. S. J., Ninham, B. W., & Pashley, R. M. (1993a). Effect of electrolytes on bubble coalescence. *Nature*, *364*(6435), 317-319.

Craig, V. S. J., Ninham, B. W., & Pashley, R. M. (1993b). The effect of electrolytes on bubble coalescence in water. *The Journal of Physical Chemistry*, *97*(39), 10192-10197.

Chander, S. (1991). Electrochemistry of sulfide flotation: growth characteristics of surface coatings and their properties, with special reference to chalcopyrite and pyrite. *International journal of mineral processing*, *33*(1), 121-134.

Chander, S., & Briceno, A. (1987). Kinetics of pyrite oxidation. *Minerals and Metallurgical Processing*, *4*(3), 170-176.

Chandra, A. P., & Gerson, A. R. (2010). The mechanisms of pyrite oxidation and leaching: a fundamental perspective. *Surface Science Reports*, *65*(9), 293-315.

Cheng, X., & IWASAKI, I. (1992). Pulp potential and its implications to sulfide flotation. *Mineral Processing and Extractive Metullargy Review*, *11*(4), 187-210.

Critchley, J. K., & Hunter, C. J. (1986). Solubility products of ferric xanthates. *TRANSACTIONS OF THE INSTITUTION OF MINING AND METALLURGY SECTION C-MINERAL PROCESSING AND EXTRACTIVE METALLURGY*, *95*, C173-C175.

Cases, J. M., Kongolo, M., De Donato, P., Michot, L. J., & Erre, R. (1993). Interaction between finely ground pyrite and potassium amylxanthate in flotation: 1. Influence of alkaline grinding. *International journal of mineral processing*, *38*(3), 267-299.

Castro, S., & Laskowski, J. S. (2011). Froth flotation in saline water. *KONA Powder and Particle Journal*, *29*(4).

Castro, S. (2012). Challenges in flotation of Cu-Mo sulfide ores in sea water. In*Water in Mineral Processing–Proc. of the First International Symposium (J. Drelich, Ed.), SME* (pp. 29-40).

Castro, S., Rioseco, P., & Laskowski, J. S. (2012). Depression of molybdenite in seawater. In *Proc. 26th Int. Mineral Processing Congress, New Delhi* (pp. 739-752).

Dunne, R. (2012). Water Water Everywhere and not a Drop to Drink, Nor do I Know its Whereabouts. *SME Annual Meeting*, 1.

Du, H., & Miller, J. D. (2007). Interfacial water structure and surface charge of selected alkali chloride salt crystals in saturated solutions: A molecular dynamics modeling study. *The Journal of Physical Chemistry C*, *111*(27), 10013-10022.

Dimitrijevic, M., Antonijevic, M. M., & Jankovic, Z. (1996). Kinetics of pyrite dissolution by hydrogen peroxide in perchloric acid. *Hydrometallurgy*, *42*(3), 377-386.

Dimitrijević, M., Antonijević, M. M., & Dimitrijević, V. (1999). Investigation of the kinetics of pyrite oxidation by hydrogen peroxide in hydrochloric acid solutions. *Minerals Engineering*, *12*(2), 165-174.

Deng, M., Karpuzov, D., Liu, Q., & Xu, Z. (2013). Cryo-XPS study of xanthate adsorption on pyrite. *Surface and Interface Analysis*, *45*(4), 805-810.

Demoisson, F., Mullet, M., & Humbert, B. (2007). Investigation of pyrite oxidation by hexavalent chromium: Solution species and surface chemistry. *Journal of colloid and interface science*, *316*(2), 531-540.

De Donato, P., Mustin, C., Benoit, R., & Erre, R. (1993). Spatial distribution of iron and sulphur species on the surface of pyrite. *Applied Surface Science*, *68*(1), 81-93.

Descostes, M., Mercier, F., Thromat, N., Beaucaire, C., & Gautier-Soyer, M. (2000). Use of XPS in the determination of chemical environment and oxidation state of iron and sulfur samples: constitution of a data basis in binding energies for Fe and S reference compounds and applications to the evidence of surface species of an oxidized pyrite in a carbonate medium. *Applied Surface Science*, *165*(4), 288-302.

Eggleston, C. M., Ehrhardt, J. J., & Stumm, W. (1996). Surface structural controls on pyrite oxidation kinetics: An XPS-UPS, STM, and modeling study. *American Mineralogist*, *81*(9), 1036-1056.

Ekmekçi, Z., & Demirel, H. (1997). Effects of galvanic interaction on collectorless flotation behaviour of chalcopyrite and pyrite. *International journal of mineral processing*, *52*(1), 31-48.

Esposito, M. C., Chander, S., & Aplan, F. F. (1987). Characterization of pyrite from coal sources. *Process Mineralogy VII, TMS, Warrendale, PA*, 475-493.

Finkelstein, N. P. (1967). Kinetic and thermodynamic aspects of the interaction between potassium ethyl xanthate and oxygen in aqueous solution. *Trans. Inst. Min. Metall.*, *76*, C51-C59.

Finkelstein, N. P. (1970). Quantitative aspects of the role of oxygen in the interaction between xanthate and galena. *Separation Science*, *5*(3), 227-256.

Finkelstein, N. P., Allison, S. A., Lovell, V. M., & Stewart, B. V. (1975). Natural and induced hydrophobicity in sulfide mineral systems. In *Advances in Interfacial Phenomena of Particulate/Solution/Gas Systems* (Vol. 71, pp. 165-175). Am Inst Chem Eng, Symp Ser New York.

Fleming, M. G. (1952). Effects of alkalinity on the flotation of lead minerals. *Min. Eng*, *4*(12), 1231-1236.

Flint, L. R., & Howarth, W. J. (1971). The collision efficiency of small particles with spherical air bubbles. *Chemical Engineering Science*, *26*(8), 1155-1168.

Fairthorne, G., Fornasiero, D., & Ralston, J. (1997). Interaction of thionocarbamate and thiourea collectors with sulphide minerals: a flotation and adsorption study. *International journal of mineral processing*, *50*(4), 227-242.

Fuerstenau, M. C., Chander, S., & Woods, R. (2007). Sulfide mineral flotation. *Froth flotation a century of Innovation. Society for Mining, Metallurgy, and Exploration, Inc. (SME), Littleton, Colorado*, 425-464.

Fuerstenau, M. C., & Palmer, B. R. (1976). Anionic flotation of oxides and silicates. *Flotation--A. M. Gaudin Memorial*.

Fuerstenau, D. W., Gaudin, A. M., & Miaw, H. L. (1958). The influence of alumina slimes on galena flotation. *Amer. Inst. Min. Eng. Trans*, *211*, 792-795.

Fuerstenau, D. W., Rosenbaum, J. M., & Laskowski, J. (1983). Effect of surface functional groups on the flotation of coal. *Colloids and Surfaces*, *8*(2), 153-173.

Fuerstenau, M. C., & Sabacky, B. J. (1981). On the natural floatability of sulfides. *International Journal of Mineral Processing*, *8*(1), 79-84.

Fuerstenau, M. C., Kuhn, M. C., & Elgillani, D. A. (1968). The role of dixanthogen in xanthate flotation of pyrite. *Trans. AIME*, *241*, 148-156.

Fielding, L. J., Porter, Q. N., & Winter, G. (1980). Sigmatropic rearrangements of unsaturated dixanthogens. *Australian Journal of Chemistry*, *33*(12), 2615-2619.

Fornasiero, D., & Ralston, J. (1992). Iron hydroxide complexes and their influence on the interaction between ethyl xanthate and pyrite. *Journal of* *colloid and interface science*, *151*(1), 225-235.

Gaudin, A. M. (1957). Flotation. *McGraw Hill Book Co., Inc, New York (1957).*

Gaudin, A. M., Fuerstenau, D. W., & Miaw, H. L. (1960). Slime coatings in galena flotation. *CIM Bulletin*, *53*, 960-963.

Gaudin, A. M. (1974). The role of oxygen in flotation. *Journal of Colloid and Interface Science*, *47*(2), 309-314.

Goldhaber, M. B. (1983). Experimental study of metastable sulfur oxyanion formation during pyrite oxidation at pH 6-9 and 30oC. *American Journal of Science*, *283*(3), 193-217.

Giannetti, B. F., Bonilla, S. H., Zinola, C. F., & Rabóczkay, T. (2001). A study of the main oxidation products of natural pyrite by voltammetric and photoelectrochemical responses. *Hydrometallurgy*, *60*(1), 41-53.

Gonzalez-Elipe, A. R., Espinos, J. P., Fernandez, A., & Munuera, G. (1990). XPS study of the surface carbonation/hydroxylation state of metal oxides.*Applied Surface Science*, *45*(2), 103-108.

Granville, A., Finkelstein, N. P., & Allison, S. A. (1972). Review of reactions in the flotation system galena-xanthate-oxygen. *Trans. IMM*, *81*, C1-C30.

Greenlee, L. F., Lawler, D. F., Freeman, B. D., Marrot, B., & Moulin, P. (2009). Reverse osmosis desalination: water sources, technology, and today's challenges. *Water research*, *43*(9), 2317-2348.

Guy, P. J., & Trahar, W. J. (1985). The effects of oxidation and mineral interaction on sulfide flotation. In *Flotation of sulfide minerals* (Vol. 6, pp. 91-110). Elsevier Amsterdam.

Gardner, J. R., & Woods, R. (1979). An electrochemical investigation of the natural flotability of chalcopyrite. *International Journal of Mineral Processing*, *6*(1), 1-16.

Gardner, J. R., & Woods, R. (1977). Electrochemical investigation of contact angle and of flotation in the presence of alkylxanthates. II. Galena and pyrite surfaces. *Australian Journal of Chemistry*, *30*(5), 981-991.

Grano, S. R., Sollaart, M., Skinner, W., Prestidge, C. A., & Ralston, J. (1997). Surface modifications in the chalcopyrite-sulphite ion system. I. collectorless flotation, XPS and dissolution study. *International journal of mineral processing*,*50*(1), 1-26.

Hayes, R. A., Price, D. M., Ralston, J., & Smith, R. W. (1987). Collectorless flotation of sulfide minerals. *Mineral Processing and Extractive Metallurgy Review*, *2*(3), 203-234.

Heyes, G. W., & Trahar, W. J. (1979). Oxidation-reduction effects in the flotation of chalcocite and cuprite. *International Journal of Mineral Processing*,*6*(3), 229-252.

Hernandez-Aguilar, J. R., Coleman, R. G., Gomez, C. O., & Finch, J. A. (2004). A comparison between capillary and imaging techniques for sizing bubbles in flotation systems. *Minerals Engineering*, *17*(1), 53-61.

Horn, R. G., Del Castillo, L. A., & Ohnishi, S. (2011). Coalescence map for bubbles in surfactant-free aqueous electrolyte solutions. *Advances in colloid and interface science*, *168*(1), 85-92.

Hancer, M., Celik, M. S., & Miller, J. D. (2001). The significance of interfacial water structure in soluble salt flotation systems. *Journal of Colloid and Interface Science*, *235*(1), 150-161.

Harris, P. J., & Finkelstein, N. P. (1975). Interactions between sulphide minerals and xanthates, I. The formation of monothiocarbonate at galena and pyrite surfaces. *International Journal of Mineral Processing*, *2*(1), 77-100.

Hung, C. C., Lee, W. H., Hu, S. Y., Chang, S. C., Chen, K. W., & Wang, Y. L. (2008). Investigation of Bis-(3-sodiumsulfopropyl disulfide) (SPS) decomposition in a copper-electroplating bath using mass spectroscopy. *Journal of The Electrochemical Society*, *155*(5), H329-H333.

Huminicki, D. M., & Rimstidt, J. D. (2009). Iron oxyhydroxide coating of pyrite for acid mine drainage control. *Applied Geochemistry*, *24*(9), 1626-1634.

Ikumapayi, F., Sis, H., Johansson, B., & Rao, K. H. (2012). Recycling process water in sulfide flotation, Part B: Effect of H. *Minerals & Metallurgical*

Processing, *29*(4), 192-198.

Ihs, A., Uvdal, K., & Liedberg, B. (1993). Infrared and photoelectron spectroscopic studies of ethyl and octyl xanthate ions adsorbed on metallic and sulfidized gold surfaces. *Langmuir*, *9*(3), 733-739.

Jovancicevic, V., Bockris, J. M., Carbajal, J. L., Zelenay, P., & Mizuno, T. (1986). Adsorption and absorption of chloride ions on passive iron systems. *Journal of The Electrochemical Society*, *133*(11), 2219-2226.

Janetski, N. D., Woodburn, S. I., & Woods, R. (1977). An electrochemical investigation of pyrite flotation and depression. *International Journal of Mineral Processing*, *4*(3), 227-239.

Jiang, Y. R., Zhou, L. H., Xue, Y. L., & Zhang, Q. X. (2000). Electrochemical flotation separation of chalcopyrite from molybdenite by CM Eh control. *TRANSACTIONS OF NONFERROUS METALS SOCIETY OF CHINA*, *10*, 110-113.

Khan, S. U. M., Baltrus, J. P., Lai, R. W., & Richardson, A. G. (1991). X-ray photoelectron spectroscopic study of the interaction of xanthate with coal pyrite and mineral pyrite surfaces. *Applied surface science*, *47*(4), 355-363.

Khmeleva, T. N., Georgiev, T. V., Jasieniak, M., Skinner, W. M., & Beattie, D. A. (2005). XPS and ToF-SIMS study of a chalcopyrite–pyrite–sphalerite mixture treated with xanthate and sodium bisulphite. *Surface and interface analysis*, *37*(8), 699-709.

Kartio, I., Laajalehto, K., Suoninen, E., Karthe, S., & Szargan, R. (1992). Technique for XPS measurements of volatile adsorbed layers: application to studies of sulphide flotation. *Surface and interface analysis*, *18*(12), 807-810.

Klassen, V. I., & Mokrousov, V. A. (1963). *An introduction to the theory of flotation*. Butterworths.

Knipe, S. W., Mycroft, J. R., Pratt, A. R., Nesbitt, H. W., & Bancroff, G. M. (1995). X-ray photoelectron spectroscopic study of water adsorption on iron sulphide minerals. *Geochimica et Cosmochimica Acta*, *59*(6), 1079-1090.

Lowson, R. T. (1982). Aqueous oxidation of pyrite by molecular oxygen.*Chemical Reviews*, *82*(5), 461-497.

Laajalehto, K., Leppinen, J., Kartio, I., & Laiho, T. (1999). XPS and FTIR study of the influence of electrode potential on activation of pyrite by copper or lead. *Colloids and Surfaces A: Physicochemical and Engineering Aspects*, *154*(1), 193-199.

Lehmann, M. N., Stichnoth, M., Walton, D., & Bailey, S. I. (2000). The effect of chloride ions on the ambient electrochemistry of pyrite oxidation in acid media.*Journal of the Electrochemical Society*, *147*(9), 3263-3271.

Leppinen, J. O., Basilio, C. I., & Yoon, R. H. (1989). In-situ FTIR study of ethyl xanthate adsorption on sulfide minerals under conditions of controlled potential. *International Journal of Mineral Processing*, *26*(3), 259-274.

Learmont, M. E., & Iwasaki, I. (1984). Effect of grinding media on galena flotation. *Minerals and Metallurgical Processing*, *1*(2), 136.

Lepetic, V. M. (1974). Flotation of chalcopyrite without collector after dry, autogenous grinding. *CIM BULLETIN*, *67*(746), 71-77.

Luttrell, G. H., & Yoon, R. H. (1983). ESCA and mass spectrometric studies of the collectorless flotation of chalcopyrite. In *111th AIME Annual Meeting, March* (pp. 6-10).

Levay, G., Smart, R. S. C., & Skinner, W. M. (2001). The impact of water quality on flotation performance. *Journal of the South African Institute of Mining and Metallurgy (South Africa)*, *101*(2), 69-75.

Liu, J., Xu, Z., & Masliyah, J. (2004). Interaction between bitumen and fines in oil sands extraction system: Implication to bitumen recovery. *The Canadian Journal of Chemical Engineering*, *82*(4), 655-666.

Liu, J., Xu, Z., & Masliyah, J. (2004). Role of fine clays in bitumen extraction from oil sands. *AIChE journal*, *50*(8), 1917-1927.

Liu, J., Xu, Z., & Masliyah, J. (2005). Interaction forces in bitumen extraction from oil sands. *Journal of colloid and interface science*, *287*(2), 507-520.

Liu, J., Zhou, Z., Xu, Z., & Masliyah, J. (2002). Bitumen–clay interactions in aqueous media studied by zeta potential distribution measurement. *Journal of colloid and interface science*, *252*(2), 409-418.

Liu, G., Qiu, Z., Wang, J., Liu, Q., Xiao, J., Zeng, H., Zhong, H., & Xu, Z. (2015). Study of N-isopropoxypropyl-N'-ethoxycarbonyl thiourea adsorption on chalcopyrite using in situ SECM, ToF-SIMS and XPS. *Journal of colloid and interface science*, *437*, 42-49.

Liu, Q., & Zhang, Y. (2000). Effect of calcium ions and citric acid on the flotation separation of chalcopyrite from galena using dextrin. *Minerals Engineering*, *13*(13), 1405-1416.

Majima, H. (1969). How oxidation affects selective flotation of complex sulphide ores. *Canadian Metallurgical Quarterly*, *8*(3), 269-273.

Mehta, A. P., & Murr, L. E. (1983). Fundamental studies of the contribution of galvanic interaction to acid-bacterial leaching of mixed metal sulfides.*Hydrometallurgy*, *9*(3), 235-256.

Mielczarski, J. A., & Yoon, R. H. (1989). Spectroscopic studies of the structure of the adsorption layer of thionocarbamate: I. On copper and activated zinc sulfide. *Journal of colloid and interface science*, *131*(2), 423-432.

Miller, D. J., Biesinger, M. C., & McIntyre, N. S. (2002). Interactions of CO_2 and CO at fractional atmosphere pressures with iron and iron oxide surfaces:

one possible mechanism for surface contamination?. *Surface and interface analysis*, *33*(4), 299-305.

Murphy, C. N., & Winter, G. (1973). Monothiocarbonates and their oxidation to disulphides. *Australian Journal of Chemistry*, *26*(4), 755-760.

Mielczarski, J., Werfel, F., & Suoninen, E. (1983). XPS studies of interaction of xanthate with copper surfaces. *Applications of surface science*, *17*(2), 160-174.

Nesbitt, H. W., & Muir, I. J. (1998). Oxidation states and speciation of secondary products on pyrite and arsenopyrite reacted with mine waste waters and air. *Mineralogy and Petrology*, *62*(1-2), 123-144.

Nagaraj, D. R., Basilio, C., & Yoon, R. H. (1989). The chemistry and structure-activity relationships for new sulphide collectors. In *Processing of Complex Ores: Proceedings of the International Symposium on Processing of Complex Ores, Halifax, August 20-24, 1989* (p. 157). Elsevier.

Nakazawa, H., & Iwasaki, I. (1985). Effect of pyrite-pyrrhotite contact on their floatabilities. *Miner. Metall. Process.*, *2*(4), 206-220.

Pang, J., Briceno, A., & Chander, S. (1990). A study of pyrite/solution interface by impedance spectroscopy. *Journal of The Electrochemical Society*, *137*(11), 3447-3455.

Pang, J., & Chander, S. (1990). Oxidation and wetting behavior of chalcopyrite in the absence and presence of xanthates. *Minerals and Metallurgical Processing*, *7*, 149-155.

Parsonage, P. G. (1984). Effects of slime and colloidal particles on the flotation of galena. *Flotation of sulphide minerals*, 111-139.

Phillip, B., & Fichte, C. (1960). Kinetische Untersuchungen zur Zersetzung von Xanthogenaten. *Faserforsch. Tex. Tech.*, *11*, 118-124.

Pou, T. E., Murphy, O. J., Young, V., Bockris, J. O. M., & Tongson, L. L. (1984). Passive films on iron: the mechanism of breakdown in chloride containing solutions. *Journal of the Electrochemical Society*, *131*(6), 1243-1251.

Palagi, C. G., & Stillar, S. S. (1976). Anaconda C. E. Weed Concentrator. *Flotation--A. M. Gaudin Memorial* (pp. 1029-1042). AIME New York, NY.

Pillai, K. C., Young, V. Y., & Bockris, J. M. (1985). X-ray photoelectron spectroscopy studies of xanthate adsorption on pyrite mineral surfaces.*Journal of colloid and interface science*, *103*(1), 145-153.

Plaksin, I. N. (1959). Interaction of minerals with gases and reagents in flotation. *Trans. AIME*, *214*, 319-324.

Peters, E. (1977). The electrochemistry of sulphide minerals. In *Trends in Electrochemistry* (pp. 167-290). Springer US.

Pietrobon, M. C., Grano, S. R., Sobieraj, S., & Ralston, J. (1997). Recovery mechanisms for pentlandite and MgO-bearing gangue minerals in nickel ores from Western Australia. *Minerals Engineering*, *10*(8), 775-786.

Rao, M. Y., & Natarajan, K. A. (1989a). Effect of electrochemical interactions among sulfide minerals and grinding medium on chalcopyrite flotation. *Minerals and Metallurgical Processing*, *6*(3), 146-151.

Rao, M. Y., & Natarajan, K. A. (1989b). Electrochemical effects of mineral-mineral interactions on the flotation of chalcopyrite and sphalerite. *International Journal of Mineral Processing*, *27*(3), 279-293.

Ravitz, S. F., & Porter, R. R. (1933). Oxygen Free Flotation I: Flotation of Galena in Absence of Oxygen. *Amer. Inst. Min. Metall. Engrs, Tech. Publ*, *513*, 17.

Reid, E. E. (1958). *Organic chemistry of bivalent sulfur* (Vol. 1). Chemical Publishing Company.

Rogers, J. (1962). Principles of sulfide mineral flotation. In *Froth Flotation* (pp. 139-169). AIME New York, NY.

Ranta, L., Minni, E., Suoninen, E., Heimala, S., Hintikka, V., Saari, M., & Rastas, J. (1981). XPS studies of adsorption of xanthate on sulfide surfaces. *Applications of surface science*, *7*(4), 393-401.

Senior, G. D., & Trahar, W. J. (1991). The influence of metal hydroxides and collector on the flotation of chalcopyrite. *International journal of mineral processing*, *33*(1), 321-341.

Smart, R. S. C. (1991). Surface layers in base metal sulfide flotation. *Minerals Engineering*, *4*(7), 891-909.

Smart, R. S., Amarantidis, J., Skinner, W. M., Prestidge, C. A., La Vanier, L., & Grano, S. R. (2003). *Surface analytical studies of oxidation and collector adsorption in sulfide mineral flotation* (pp. 3-62). Springer Berlin Heidelberg.

Szargan, R., Karthe, S., & Suoninen, E. (1992). XPS studies of xanthate adsorption on pyrite. *Applied surface science*, *55*(4), 227-232.

Sheikh, N., & Leja, J. (1977). Mössbauer spectroscopy of Fe xanthates. *Separation Science*, *12*(5), 529-540.

Sheikh, N., & Leja, J. (1973). Evaluation of iron xanthates by mossbauer spectroscopy. *Can. Min. Metall. Bull.*, *66*(8), 31.

Sutherland, K. L. (1948). Physical chemistry of flotation. XI. Kinetics of the flotation process. *The Journal of Physical Chemistry*, *52*(2), 394-425.

Sutherland, K. L., & Wark, I. W. (1955). Principles of Flotation, Australasian Institute of Mining and Metallurgy. *Inc., Melbourne*, *164*.

Sun, S. Y., Wang, D. Z., & Li, B. D. (1993). The collectorless flotation and separation of chalcopyrite and pyrite by potential control. *Journal of Central-South Institute of Mining and Metallurgy (China)(People's Republic of China)*, *24*(4), 466-471.

Tolley, W., Kotlyar, D., & Van Wagoner, R. (1996). Fundamental electrochemical studies of sulfide mineral flotation. *Minerals Engineering*,*9*(6), 603-637.

Todd, E. C., Sherman, D. M., & Purton, J. A. (2003). Surface oxidation of pyrite under ambient atmospheric and aqueous (pH= 2 to 10) conditions: electronic structure and mineralogy from X-ray absorption spectroscopy. *Geochimica et Cosmochimica Acta*, *67*(5), 881-893.

Valdivieso, A. L., López, A. S., & Song, S. (2005). On the cathodic reaction coupled with the oxidation of xanthates at the pyrite/aqueous solution interface. *International Journal of Mineral Processing*, *77*(3), 154-164.

Velásquez, P., Leinen, D., Pascual, J., Ramos-Barrado, J. R., Cordova, R., Gómez, H., & Schrebler, R. (2001). XPS, SEM, EDX and EIS study of an electrochemically modified electrode surface of natural chalcocite (Cu 2 S).*Journal of Electroanalytical Chemistry*, *510*(1), 20-28.

Weber, M. E. (1981). Collision efficiencies for small particles with a spherical collector at intermediate Reynolds numbers. *J. Separation Process Tcchnol*, *2*, 29-33.

Wark, I. W. (1938). Principles of flotation. *Australasian Institute of Mining and Metallurgy*, (a), 187.

Wark, I. W., & Cox, A. B. (1934). Principles of flotation, II—an experimental study of the influence of cyanide, alkalis and copper sulfate on the effect of potassium ethyl xanthate at mineral surfaces. *Transactions AIME*, *112*, 245-266.

Wark, E. E., & Wark, I. W. (1933). The Physical Chemistry of Flotation. III. The Relationship between Contact Angle and the Constitution of the Collector. *The Journal of Physical Chemistry*, *37*(6), 805-814.

Wang, X. H., & Forssberg, K. E. (1991). Mechanisms of pyrite flotation with xanthates. *International journal of mineral processing*, *33*(1), 275-290.

Wang, X., Forssberg, K. E., & Bolin, N. J. (1989). Thermodynamic calculations on iron-containing sulphide mineral flotation systems, I. The stability of iron-xanthates. *International Journal of Mineral Processing*, *27*(1), 1-19.

Wang, J., Xie, L., Liu, Q., & Zeng, H. (2015). Effects of salinity on xanthate adsorption on sphalerite and bubble–sphalerite interactions. *Minerals Engineering*, *77*, 34-41.

Weber, M. E., & Paddock, D. (1983). Interceptional and gravitational collision efficiencies for single collectors at intermediate Reynolds numbers. *Journal of Colloid and Interface Science*, *94*(2), 328-335.

Weisener, C., & Gerson, A. (2000). An investigation of the Cu (II) adsorption mechanism on pyrite by ARXPS and SIMS. *Minerals Engineering*, *13*(13), 1329-1340.

Winter, G., & Woods, R. (1973). The relation of collector redox potential to flotation efficiency: monothiocarbonates. *Separation Science*, *8*(2), 261-267.

Xu, Z., Liu, J., Choung, J. W., & Zhou, Z. (2003). Electrokinetic study of clay interactions with coal in flotation. *International Journal of Mineral Processing*,*68*(1), 183-196.

Yoon, R. H., & Luttrell, G. H. (1989). The effect of bubble size on fine particle flotation. *Mineral Processing and Extractive Metallurgy Review*, *5*(1-4), 101-122.

Yoon, R. H., Lagno, M. L., Luttrell, G. H., & Mielczarski, J. A. (1991, August). On the hydrophobicity of coal pyrite. In *Proceedings of the IV International Conference on Processing and Utilization of High Sulfur Coals* (pp. 241-253). Elsevier, Amsterdam

Appendix

Selected original flotation data obtained by micro-flotation test are listed in the following tables.

Table 8.1 Flotation results of chalcopyrite in the absence of collector in Milli-Q water at different pHs

Test No.	pH value		Concentrate (g)			Tail (g)			Total	Recovery
	Initial	Final	Paper Mass	Paper + Conc.	Conc.	Paper Mass	Paper + Tail	Tail	(g)	(%)
1	2.00	1.74	1.2143	2.3690	1.1547	1.2527	1.4761	0.2234	1.3781	83.78928
2	4.00	4.07	1.2664	2.3608	1.0944	1.2674	1.5231	0.2557	1.3501	81.06066
3	6.00	6.28	1.2264	2.3227	1.0963	1.2820	1.5080	0.2260	1.3223	82.90857
4	8.06	7.16	1.2405	2.2890	1.0485	1.2360	1.5150	0.2790	1.3275	78.98305
5	9.98	9.41	1.2795	2.3647	1.0852	1.2378	1.5194	0.2816	1.3668	79.39713
6	10.99	10.99	1.2684	2.1387	0.8703	1.2775	1.7371	0.4596	1.3299	65.44101
7	11.98	12.14	1.2310	1.9112	0.6802	1.2407	1.8922	0.6515	1.3317	51.07757
8	13.00	13.16	1.2820	1.7297	0.4477	1.2586	2.1628	0.9042	1.3519	33.11635

Table 8.2 Flotation results of chalcopyrite in the absence of collector in NaCl solution at different pHs

Test No.	pH value		Concentrate (g)			Tail (g)			Total (g)	Recovery (%)
	Initial	Final	Paper Mass	Paper + Conc.	Conc.	Paper Mass	Paper + Tail	Tail		
1	2.01	1.77	1.2545	2.4759	1.2214	1.2794	1.4308	0.1514	1.3728	88.97145
2	4.01	4.22	1.2607	2.3387	1.0780	1.2910	1.4459	0.1549	1.2329	87.43613
3	5.99	6.32	1.2432	2.4125	1.1693	1.2658	1.4565	0.1907	1.3600	85.97794
4	8.04	7.36	1.2538	2.4233	1.1695	1.2930	1.4764	0.1834	1.3529	86.44394
5	10.00	10.02	1.2583	2.4917	1.2334	1.2781	1.4425	0.1644	1.3978	88.23866
6	11.00	11.07	1.2397	2.4124	1.1727	1.3012	1.4689	0.1677	1.3404	87.48881
7	12.02	12.11	1.2705	2.4959	1.2254	1.2800	1.4612	0.1812	1.4066	87.11787
8	12.99	13.18	1.2430	2.3426	1.0996	1.2952	1.5975	0.3023	1.4019	78.43641

Table 8.3 Flotation results of chalcopyrite in the absence of collector in sea water at different pHs

Test No.	pH value		Concentrate (g)			Tail (g)			Total (g)	Recovery (%)
	Initial	Final	Paper Mass	Paper + Conc.	Conc.	Paper Mass	Paper + Tail	Tail		
1	2.01	1.99	1.2309	2.3995	1.1686	1.2286	1.4118	0.1832	1.3518	86.4477
2	3.93	4.13	1.2690	2.5368	1.2678	1.2782	1.3938	0.1156	1.3834	91.64378
3	5.97	6.29	1.2768	2.4251	1.1483	1.2272	1.3992	0.1720	1.3203	86.97266
4	7.98	7.99	1.2895	2.5460	1.2565	1.2726	1.4159	0.1433	1.3998	89.76282
5	10.04	10.10	1.2417	1.9470	0.7053	1.2771	1.9222	0.6451	1.3504	52.22897
6	11.00	10.69	1.2312	1.3129	0.0817	1.2682	2.0524	0.7842	0.8659	9.43527
7	11.99	12.08	1.2276	1.3001	0.0725	1.2369	2.1266	0.8897	0.9622	7.534816
8	12.95	12.95	1.2447	1.3290	0.0843	1.2463	1.8849	0.6386	0.7229	11.66136

Table 8.4 Flotation results of chalcopyrite in Milli-Q water with 1×10^{-5} M PAX at different pHs

Test No.	pH value		Concentrate (g)			Tail (g)			Total	Recovery
	Initial	Final	Paper Mass	Paper + Conc.	Conc.	Paper Mass	Paper + Tail	Tail	(g)	(%)
1	2.03	2.05	1.2907	2.4404	1.1497	1.2540	1.3864	0.1324	1.2821	89.67319
2	4.05	4.06	1.2871	2.4347	1.1476	1.2678	1.4049	0.1371	1.2847	89.32825
3	6.05	6.46	1.2871	2.4511	1.1640	1.2598	1.4133	0.1535	1.3175	88.34915
4	8.07	7.77	1.2484	2.3284	1.0800	1.2989	1.4655	0.1666	1.2466	86.63565
5	10.05	9.89	1.2923	2.4757	1.1834	1.2477	1.4324	0.1847	1.3681	86.49952
6	11.09	11.00	1.2500	2.4257	1.1757	1.2896	1.5107	0.2211	1.3968	84.17096
7	12.09	12.03	1.2558	2.3400	1.0842	1.2742	1.4510	0.1768	1.2610	85.97938
8	13.00	12.98	1.3013	2.4231	1.1218	1.2416	1.4715	0.2299	1.3517	82.99179

Table 8.5 Flotation results of chalcopyrite in Milli-Q water with 1×10^{-5} M thionocarbamate at different pHs

Test No.	pH value		Concentrate (g)			Tail (g)			Total	Recovery
	Initial	Final	Paper Mass	Paper + Conc.	Conc.	Paper Mass	Paper + Tail	Tail	(g)	(%)
1	2.04	2.10	1.2618	2.2708	1.0090	1.2912	1.4814	0.1902	1.1992	84.13943
2	4.01	4.36	1.2692	2.3332	1.0640	1.2907	1.4837	0.1930	1.2570	84.64598
3	6.07	6.33	1.2812	2.3110	1.0298	1.3106	1.4873	0.1767	1.2065	85.35433
4	8.02	7.79	1.2988	2.3772	1.0784	1.2568	1.4573	0.2005	1.2789	84.32246
5	10.00	10.02	1.2643	2.2280	0.9637	1.3039	1.5024	0.1985	1.1622	82.92032
6	11.01	11.18	1.2525	2.2346	0.9821	1.2961	1.5100	0.2139	1.1960	82.11538
7	12.05	12.02	1.2624	2.1829	0.9205	1.2960	1.5460	0.2500	1.1705	78.64161
8	13.03	13.04	1.2575	2.3057	1.0482	1.2854	1.5020	0.2166	1.2648	82.87476

Table 8.6 Flotation results of chalcopyrite in Milli-Q water with 1×10^{-5} M iPOPECTU at different pHs

Test No.	pH value		Concentrate (g)			Tail (g)			Total	Recovery
	Initial	Final	Paper Mass	Paper + Conc.	Conc.	Paper Mass	Paper + Tail	Tail	(g)	(%)
1	2.03	2.09	1.3016	2.4008	1.0992	1.2772	1.4644	0.1872	1.2864	85.44776
2	4.00	4.28	1.2548	2.3024	1.0476	1.2686	1.4629	0.1943	1.2419	84.35462
3	6.04	6.50	1.3129	2.3716	1.0587	1.2667	1.4609	0.1942	1.2529	84.49996
4	8.03	7.30	1.2815	2.3346	1.0531	1.3048	1.5022	0.1974	1.2505	84.21431
5	10.01	9.86	1.3067	2.3960	1.0893	1.2765	1.4826	0.2061	1.2954	84.08986
6	11.02	11.08	1.2986	2.3504	1.0518	1.2752	1.4854	0.2102	1.2620	83.3439
7	12.04	12.23	1.3084	2.3974	1.0890	1.2753	1.5222	0.2469	1.3359	81.51808
8	13.07	12.99	1.3164	2.4341	1.1177	1.2753	1.4438	0.1685	1.2862	86.89939

Table 8.7 Flotation results of chalcopyrite in NaCl solution with 1×10^{-5} M PAX at different pHs

Test No.	pH value		Concentrate (g)			Tail (g)			Total	Recovery
	Initial	Final	Paper Mass	Paper + Conc.	Conc.	Paper Mass	Paper + Tail	Tail	(g)	(%)
1	2.00	1.94	1.2527	2.3389	1.0862	1.2160	1.3514	0.1354	1.2216	88.9162
2	4.03	4.56	1.2458	2.4031	1.1573	1.2203	1.3455	0.1252	1.2825	90.2378
3	6.04	7.05	1.2454	2.3616	1.1162	1.2377	1.3460	0.1083	1.2245	91.1556
4	8.04	7.31	1.2426	2.5425	1.2999	1.2190	1.2682	0.0492	1.3491	96.3531
5	9.99	9.66	1.2504	2.5483	1.2979	1.2309	1.2911	0.0602	1.3581	95.5673
6	11.06	11.10	1.2426	2.4874	1.2448	1.2181	1.3280	0.1099	1.3547	91.8875
7	11.98	11.99	1.2484	2.5019	1.2535	1.2086	1.3464	0.1378	1.3913	90.0956
8	12.99	13.06	1.2357	2.4141	1.1784	1.2248	1.3879	0.1631	1.3415	87.8420

Table 8.8 Flotation results of chalcopyrite in NaCl solution with 1×10^{-5} M thionocarbamate at different pHs

Test No.	pH value		Concentrate (g)			Tail (g)			Total	Recovery
	Initial	Final	Paper Mass	Paper + Conc.	Conc.	Paper Mass	Paper + Tail	Tail	(g)	(%)
1	2.04	2.05	1.2239	2.4054	1.1815	1.2550	1.3400	0.0850	1.2665	93.2886
2	4.01	4.68	1.2387	2.4669	1.2282	1.2603	1.3324	0.0721	1.3003	94.4551
3	6.03	6.57	1.2189	2.4336	1.2147	1.2426	1.3368	0.0942	1.3089	92.8031
4	8.04	7.61	1.2169	2.4219	1.2050	1.2479	1.3580	0.1101	1.3151	91.6280
5	10.04	9.64	1.2203	2.3643	1.1440	1.2457	1.3635	0.1178	1.2618	90.6641
6	11.03	10.96	1.2153	2.4133	1.1980	1.2483	1.3560	0.1077	1.3057	91.7516
7	11.98	11.96	1.2185	2.4171	1.1986	1.2427	1.4064	0.1637	1.3623	87.9836
8	13.02	13.05	1.2115	2.1900	0.9785	1.2316	1.4053	0.1737	1.1522	84.9245

Table 8.9 Flotation results of chalcopyrite in NaCl solution with 1×10^{-5} M iPOPECTU at different pHs

Test No.	pH value		Concentrate (g)			Tail (g)			Total	Recovery
	Initial	Final	Paper Mass	Paper + Conc.	Conc.	Paper Mass	Paper + Tail	Tail	(g)	(%)
1	2.02	2.01	1.2327	2.4111	1.1784	1.2579	1.4033	0.1454	1.3238	89.0165
2	4.01	4.53	1.2344	2.4606	1.2262	1.2369	1.3642	0.1273	1.3535	90.5948
3	6.07	6.79	1.2671	2.4939	1.2268	1.2397	1.3702	0.1305	1.3573	90.3853
4	8.02	7.55	1.2577	2.5162	1.2585	1.2274	1.3807	0.1533	1.4118	89.1415
5	10.01	9.88	1.2441	2.4815	1.2374	1.2286	1.3525	0.1239	1.3613	90.8984
6	11.03	11.22	1.2718	2.4836	1.2118	1.2358	1.3699	0.1341	1.3459	90.0364
7	12.05	12.09	1.2647	2.5208	1.2561	1.2398	1.4155	0.1757	1.4318	87.7287
8	12.99	13.09	1.2764	2.5023	1.2259	1.2328	1.4179	0.1851	1.4110	86.8816

Table 8.10 Flotation results of chalcopyrite in sea water with 1×10^{-5} M PAX at different pHs

Test No.	pH value		Concentrate (g)			Tail (g)			Total	Recovery
	Initial	Final	Paper Mass	Paper + Conc.	Conc.	Paper Mass	Paper + Tail	Tail	(g)	(%)
1	2.04	2.05	1.2777	2.4310	1.1533	1.3049	1.4650	0.1601	1.3134	87.81026
2	4.04	4.68	1.2673	2.4609	1.1936	1.2785	1.4438	0.1653	1.3589	87.83575
3	6.04	7.29	1.2663	2.4479	1.1816	1.3091	1.4593	0.1502	1.3318	88.72203
4	8.03	8.13	1.2582	2.4281	1.1699	1.2784	1.4501	0.1717	1.3416	87.20185
5	10.04	9.92	1.2520	2.0722	0.8202	1.2779	1.8562	0.5783	1.3985	58.64855
6	10.97	10.72	1.2539	1.4183	0.1644	1.2782	2.2266	0.9484	1.1128	14.77354
7	12.13	12.06	1.2976	1.4390	0.1414	1.2501	2.1359	0.8858	1.0272	13.76558
8	13.04	12.93	1.2460	1.4076	0.1616	1.2899	2.2532	0.9633	1.1249	14.36572

Table 8.11 Flotation results of chalcopyrite in sea water with 1×10^{-5} M thionocarbamate at different pHs

Test No.	pH value		Concentrate (g)			Tail (g)			Total	Recovery
	Initial	Final	Paper Mass	Paper + Conc.	Conc.	Paper Mass	Paper + Tail	Tail	(g)	(%)
1	2.03	2.07	1.2984	2.4087	1.1103	1.2798	1.3917	0.1119	1.2222	90.84438
2	4.03	4.39	1.2938	2.4581	1.1643	1.2751	1.3469	0.0718	1.2361	94.19141
3	6.01	7.52	1.3000	2.3962	1.0962	1.2565	1.4003	0.1438	1.2400	88.40323
4	8.04	8.07	1.3151	2.5036	1.1885	1.2597	1.3618	0.1021	1.2906	92.08895
5	10.02	10.11	1.2366	2.3579	1.1213	1.2399	1.3875	0.1476	1.2689	88.36788
6	11.10	10.80	1.3001	1.4454	0.1453	1.2561	2.1555	0.8994	1.0447	13.9083
7	12.07	12.01	1.3034	1.4327	0.1293	1.2722	2.0216	0.7494	0.8787	14.71492
8	13.03	12.97	1.3212	1.4603	0.1391	1.2670	1.9534	0.6864	0.8255	16.85039

Table 8.12 Flotation results of chalcopyrite in sea water with 1×10^{-5} M iPOPECTU at different pHs

Test No.	pH value		Concentrate (g)			Tail (g)			Total	Recovery
	Initial	Final	Paper Mass	Paper + Conc.	Conc.	Paper Mass	Paper + Tail	Tail	(g)	(%)
1	1.96	1.98	1.2368	2.2106	0.9738	1.2903	1.3768	0.0865	1.0603	91.84193
2	4.07	4.47	1.2919	2.4118	1.1199	1.2594	1.3601	0.1007	1.2206	91.74996
3	6.03	7.20	1.2414	2.3884	1.1470	1.2905	1.3819	0.0914	1.2384	92.61951
4	8.00	8.02	1.2455	2.3409	1.0954	1.2714	1.3701	0.0987	1.1941	91.73436
5	10.01	10.00	1.3041	1.9863	0.6822	1.3143	1.9503	0.6360	1.3182	51.75239
6	11.03	10.78	1.2457	1.3595	0.1138	1.2941	2.1557	0.8616	0.9754	11.66701
7	12.04	12.03	1.2406	1.3638	0.1232	1.2763	1.8813	0.6050	0.7282	16.91843
8	13.02	13.07	1.2459	1.3563	0.1104	1.2884	1.8468	0.5584	0.6688	16.50718

Table 8.13 Flotation results of pyrite in the absence of collector in Milli-Q water at different pHs

Test No.	pH value		Concentrate (g)			Tail (g)			Total	Recovery
	Initial	Final	Paper Mass	Paper + Conc.	Conc.	Paper Mass	Paper + Tail	Tail	(g)	(%)
1	2.03	1.91	1.3089	1.7262	0.4173	1.3103	1.9970	0.6867	1.1040	37.7989
2	4.04	4.03	1.2761	1.4465	0.1704	1.3073	2.2797	0.9724	1.1428	14.9107
3	6.03	5.81	1.2550	1.2790	0.0240	1.2678	2.2296	0.9618	0.9858	2.4346
4	8.00	7.27	1.2701	1.3173	0.0472	1.3085	2.3516	1.0431	1.0903	4.3291
5	10.04	10.22	1.2610	1.3741	0.1131	1.2951	2.1911	0.8960	1.0091	11.2080
6	11.05	11.20	1.2488	1.3495	0.1007	1.3166	2.1707	0.8541	0.9548	10.5467
7	12.06	12.30	1.2641	1.3441	0.0800	1.2950	2.2289	0.9339	1.0139	7.8903
8	13.00	13.12	1.2723	1.3395	0.0672	1.2954	2.1336	0.8382	0.9054	7.4221

Table 8.14 Flotation results of pyrite in the absence of collector in NaCl solution at different pHs

Test No.	pH value		Concentrate (g)			Tail (g)			Total	Recovery
	Initial	Final	Paper Mass	Paper + Conc.	Conc.	Paper Mass	Paper + Tail	Tail	(g)	(%)
1	2.00	1.96	1.2237	2.4064	1.1827	1.2544	1.4461	0.1917	1.3744	86.0521
2	4.02	4.04	1.2132	2.2754	1.0622	1.2551	1.5793	0.3242	1.3864	76.6157
3	6.05	6.03	1.2251	1.9887	0.7636	1.2566	1.9028	0.6462	1.4098	54.1637
4	8.05	7.04	1.2171	2.0514	0.8343	1.2582	1.7930	0.5348	1.3691	60.9378
5	10.03	9.95	1.2021	1.6396	0.4375	1.2432	2.1741	0.9309	1.3684	31.9716
6	11.01	11.00	1.2187	1.5345	0.3158	1.2599	2.2962	1.0363	1.3521	23.3563
7	12.02	12.04	1.2194	1.4915	0.2721	1.2620	2.3804	1.1184	1.3905	19.5685
8	13.01	13.01	1.2254	1.3850	0.1596	1.2624	2.5261	1.2637	1.4233	11.2134

Table 8.15 Flotation results of pyrite in the absence of collector in sea water at different pHs

Test No.	pH value		Concentrate (g)			Tail (g)			Total	Recovery
	Initial	Final	Paper Mass	Paper + Conc.	Conc.	Paper Mass	Paper + Tail	Tail	(g)	(%)
1	2.06	2.00	1.2172	2.4314	1.2142	1.2501	1.4373	0.1872	1.4014	86.6419
2	4.03	4.02	1.2054	2.1063	0.9009	1.2345	1.7376	0.5031	1.4040	64.1667
3	5.96	6.49	1.2181	1.8067	0.5886	1.2607	2.0258	0.7651	1.3537	43.4808
4	8.08	8.06	1.2120	1.8514	0.6394	1.2378	1.9675	0.7297	1.3691	46.7022
5	10.03	10.05	1.2077	1.3730	0.1653	1.2441	2.4916	1.2475	1.4128	11.7002
6	11.06	11.06	1.1985	1.3038	0.1053	1.2540	2.3562	1.1022	1.2075	8.7205
7	11.99	11.99	1.2000	1.2963	0.0963	1.2721	2.3083	1.0362	1.1325	8.5033
8	13.02	13.03	1.2036	1.2901	0.0865	1.2433	2.0137	0.7704	0.8569	10.0945

Table 8.16 Flotation results of pyrite in Milli-Q water with 1×10^{-5} M PAX at different pHs

Test No.	pH value		Concentrate (g)			Tail (g)			Total	Recovery
	Initial	Final	Paper Mass	Paper + Conc.	Conc.	Paper Mass	Paper + Tail	Tail	(g)	(%)
1	2.02	2.02	1.2751	2.2822	1.0071	1.2929	1.3078	0.0149	1.0220	98.5421
2	4.07	4.20	1.2607	2.3883	1.1276	1.2994	1.3152	0.0158	1.1434	98.6182
3	6.04	7.11	1.2758	1.5930	0.3172	1.3002	2.0542	0.7540	1.0712	29.6117
4	7.98	7.35	1.2421	2.1959	0.9538	1.2965	1.5432	0.2467	1.2005	79.4502
5	10.04	10.06	1.2648	2.3005	1.0357	1.3116	1.3407	0.0291	1.0648	97.2671
6	11.04	11.09	1.2638	1.8072	0.5434	1.2861	1.7833	0.4972	1.0406	52.2199
7	12.03	12.24	1.2607	1.4740	0.2133	1.3105	2.1627	0.8522	1.0655	20.0188
8	13.00	13.12	1.2504	1.3612	0.1108	1.3109	2.2195	0.9086	1.0194	10.8691

Table 8.17 Flotation results of pyrite in Milli-Q water with 1×10^{-5} M thionocarbamate at different pHs

Test No.	pH value		Concentrate (g)			Tail (g)			Total	Recovery
	Initial	Final	Paper Mass	Paper + Conc.	Conc.	Paper Mass	Paper + Tail	Tail	(g)	(%)
1	2.02	1.94	1.3040	2.0304	0.7264	1.2557	1.6602	0.4045	1.1309	64.2320
2	4.00	4.00	1.3175	1.6605	0.3430	1.2650	2.0017	0.7367	1.0797	31.7681
3	6.07	5.91	1.3117	1.3972	0.0855	1.2550	2.3272	1.0722	1.1577	7.3853
4	8.04	7.98	1.3096	1.4240	0.1144	1.2559	2.3287	1.0728	1.1872	9.6361
5	10.07	10.08	1.3125	1.6608	0.3483	1.2660	2.0086	0.7426	1.0909	31.9278
6	11.07	11.19	1.3126	1.5214	0.2088	1.2576	2.1490	0.8914	1.1002	18.9784
7	12.02	12.11	1.2924	1.4236	0.1312	1.2692	2.4382	1.1690	1.3002	10.0908
8	13.04	13.01	1.3026	1.4704	0.1678	1.2508	2.2472	0.9964	1.1642	14.4133

Table 8.18 Flotation results of pyrite in Milli-Q water with 1×10^{-5} M iPOPECTU at different pHs

Test No.	pH value		Concentrate (g)			Tail (g)			Total	Recovery
	Initial	Final	Paper Mass	Paper + Conc.	Conc.	Paper Mass	Paper + Tail	Tail	(g)	(%)
1	2.02	1.97	1.2688	2.2629	0.9941	1.2386	1.4404	0.2018	1.1959	83.12568
2	4.03	4.16	1.2373	1.5958	0.3585	1.2377	2.0119	0.7742	1.1327	31.65004
3	5.97	5.69	1.2651	1.3686	0.1035	1.2276	2.2285	1.0009	1.1044	9.37160
4	7.97	7.89	1.2609	1.4025	0.1416	1.2307	2.1707	0.9400	1.0816	13.09172
5	10.02	9.70	1.2767	1.5751	0.2984	1.2491	2.0808	0.8317	1.1301	26.4047
6	11.03	11.09	1.2383	1.3906	0.1523	1.2268	2.1447	0.9179	1.0702	14.23098
7	12.00	12.13	1.2545	1.3451	0.0906	1.2495	2.2446	0.9951	1.0857	8.34485
8	12.97	12.85	1.2624	1.4045	0.1421	1.2563	2.3087	1.0524	1.1945	11.8962

Table 8.19 Flotation results of pyrite in NaCl solution with 1×10^{-5} M PAX at different pHs

Test No.	pH value		Concentrate (g)			Tail (g)			Total	Recovery
	Initial	Final	Paper Mass	Paper + Conc.	Conc.	Paper Mass	Paper + Tail	Tail	(g)	(%)
1	2.00	1.99	1.2454	2.5740	1.3286	1.2596	1.2744	0.0148	1.3434	98.8983
2	4.01	4.09	1.2678	2.6115	1.3437	1.2726	1.2897	0.0171	1.3608	98.7434
3	6.06	6.26	1.2717	2.6339	1.3622	1.2341	1.2384	0.0043	1.3665	99.6853
4	8.10	7.22	1.2693	2.5120	1.2427	1.2722	1.2953	0.0231	1.2658	98.1751
5	10.02	10.08	1.2585	2.5022	1.2437	1.2576	1.2694	0.0118	1.2555	99.0601
6	11.01	11.07	1.2295	2.5685	1.3390	1.2694	1.2781	0.0087	1.3477	99.3545
7	11.99	12.02	1.2202	1.6264	0.4062	1.2399	2.0483	0.8084	1.2146	33.4431
8	13.00	13.09	1.2547	1.3924	0.1377	1.2719	2.4722	1.2003	1.3380	10.2915

Table 8.20 Flotation results of pyrite in NaCl solution with 1×10^{-5} M thionocarbamate at different pHs

Test No.	pH value		Concentrate (g)			Tail (g)			Total	Recovery
	Initial	Final	Paper Mass	Paper + Conc.	Conc.	Paper Mass	Paper + Tail	Tail	(g)	(%)
1	1.99	1.92	1.2778	2.5838	1.3060	1.2826	1.3314	0.0488	1.3548	96.3980
2	4.02	4.02	1.2214	2.5499	1.3285	1.2345	1.2533	0.0188	1.3473	98.6046
3	6.08	6.06	1.2768	2.5090	1.2322	1.2422	1.2882	0.0460	1.2782	96.4012
4	8.10	7.12	1.2658	2.0509	0.7851	1.2508	1.8127	0.5619	1.3470	58.2851
5	10.04	9.90	1.2875	1.8508	0.5633	1.2325	2.0569	0.8244	1.3877	40.5923
6	11.04	11.07	1.2859	1.4844	0.1985	1.2615	2.4658	1.2043	1.4028	14.1503
7	12.03	12.12	1.2634	1.4388	0.1754	1.2278	2.4114	1.1836	1.3590	12.9065
8	12.99	13.09	1.2371	1.3626	0.1255	1.2889	2.6070	1.3181	1.4436	8.6935

Table 8.21 Flotation results of pyrite in NaCl solution with 1×10^{-5} M iPOPECTU at different pHs

Test No.	pH value		Concentrate (g)			Tail (g)			Total	Recovery
	Initial	Final	Paper Mass	Paper + Conc.	Conc.	Paper Mass	Paper + Tail	Tail	(g)	(%)
1	2.01	2.00	1.2717	2.5697	1.2980	1.2337	1.2398	0.0061	1.3041	99.5322
2	4.01	4.02	1.2723	2.6355	1.3632	1.2451	1.2523	0.0072	1.3704	99.4746
3	6.04	6.06	1.2892	2.6061	1.3169	1.2297	1.2307	0.0010	1.3179	99.9241
4	8.03	6.80	1.2600	2.5307	1.2707	1.2218	1.3555	0.1337	1.4044	90.4799
5	9.99	10.03	1.2311	2.0537	0.8226	1.2847	1.7800	0.4953	1.3179	62.4175
6	11.05	11.01	1.2177	1.5535	0.3358	1.2666	2.2580	0.9914	1.3272	25.3014
7	12.03	12.13	1.2703	1.4477	0.1774	1.2461	2.4265	1.1804	1.3578	13.0653
8	12.99	13.07	1.2965	1.4098	0.1133	1.2383	2.4628	1.2245	1.3378	8.4691

Table 8.22 Flotation results of pyrite in sea water with 1×10^{-5} M PAX at different pHs

Test No.	pH value		Concentrate (g)			Tail (g)			Total	Recovery
	Initial	Final	Paper Mass	Paper + Conc.	Conc.	Paper Mass	Paper + Tail	Tail	(g)	(%)
1	1.97	1.98	1.2345	2.5629	1.3284	1.2416	1.2492	0.0076	1.3360	99.4311
2	4.02	4.04	1.2766	2.5696	1.2930	1.2388	1.2588	0.0200	1.3130	98.4768
3	6.06	6.94	1.2698	2.5619	1.2921	1.2757	1.2855	0.0098	1.3019	99.2473
4	8.00	8.06	1.2358	2.5738	1.3380	1.2838	1.3143	0.0305	1.3685	97.7713
5	10.00	10.11	1.2554	1.7477	0.4923	1.2784	2.0883	0.8099	1.3022	37.8053
6	10.95	10.79	1.2348	1.3112	0.0764	1.2667	2.3022	1.0355	1.1119	6.8711
7	12.02	12.05	1.2582	1.3563	0.0981	1.2761	2.1296	0.8535	0.9516	10.3090
8	12.98	13.08	1.2386	1.3190	0.0804	1.2817	1.9436	0.6619	0.7423	10.8312

Table 8.23 Flotation results of pyrite in sea water with 1×10^{-5} M thionocarbamate at different pHs

Test No.	pH value		Concentrate (g)			Tail (g)			Total	Recovery
	Initial	Final	Paper Mass	Paper + Conc.	Conc.	Paper Mass	Paper + Tail	Tail	(g)	(%)
1	2.01	2.04	1.2407	2.4749	1.2342	1.2499	1.2517	0.0018	1.2360	99.8544
2	3.94	4.22	1.2496	1.8746	0.6250	1.2679	1.7307	0.4628	1.0878	57.4554
3	5.95	6.59	1.2383	1.7435	0.5052	1.2686	1.7946	0.5260	1.0312	48.9915
4	8.04	7.75	1.2505	1.6817	0.4312	1.2621	1.8671	0.6050	1.0362	41.6136
5	10.06	9.94	1.2688	1.4522	0.1834	1.2622	2.2737	1.0115	1.1949	15.3486
6	10.98	10.79	1.2394	1.3474	0.1080	1.2637	2.0695	0.8058	0.9138	11.8188
7	11.98	11.92	1.2315	1.3287	0.0972	1.2548	1.9721	0.7173	0.8145	11.9337
8	13.00	12.96	1.2354	1.3025	0.0671	1.2515	1.9089	0.6574	0.7245	9.2616

Table 8.24 Flotation results of pyrite in sea water with 1×10^{-5} M iPOPECTU at different pHs

Test No.	pH value		Concentrate (g)			Tail (g)			Total	Recovery
	Initial	Final	Paper Mass	Paper + Conc.	Conc.	Paper Mass	Paper + Tail	Tail	(g)	(%)
1	1.99	1.98	1.2565	2.3781	1.1216	1.2370	1.2822	0.0452	1.1668	96.1262
2	3.96	4.09	1.2116	2.4987	1.2871	1.2130	1.2244	0.0114	1.2985	99.1221
3	6.01	7.12	1.2555	2.5189	1.2634	1.2575	1.3266	0.0691	1.3325	94.8143
4	8.03	8.11	1.2258	2.3252	1.0994	1.2435	1.4875	0.2440	1.3434	81.8371
5	10.05	10.05	1.2233	1.3643	0.1410	1.2131	2.3649	1.1518	1.2928	10.9066
6	11.02	10.72	1.2141	1.3341	0.1200	1.2506	2.0535	0.8029	0.9229	13.0025
7	12.05	12.09	1.2546	1.3405	0.0859	1.2507	2.0418	0.7911	0.8770	9.7948
8	13.04	13.16	1.2247	1.2951	0.0704	1.2132	1.8730	0.6598	0.7302	9.6412